CS/AR-2/2006-07

# STREAMFLOW MODELLING OF BHAGIRATHI RIVER : HYDROGRAPH SEPARATION USING ISOTOPIC AND GEOCHEMICAL TECHNIQUES


NATIONAL INSTITUTE OF HYDROLOGY
JALVIGYAN BHAWAN
ROORKEE -247 667
2004-2007

# PREFACE

The three important river systems originating from the Himalayan region are: the Indus, the Ganges and the Brahamaputra. Excluding Brahamaputra and Indus, which flow parallel to northern range of Greater Himalayas, towards west and east respectively, all other remaining rivers including few tributaries of Brahamaputra and Indus cut across the Himalayas and flow from north to south. The River Ganga, one of the major rivers of Himalayas originates from the Gangotri Glacier. Importance of the River Ganga in the Indian context is better understood from the fact that it continues to play a major role in the socio-economic development of the entire northern part of the country. The dependency of Uttaranchal, Uttar Pradesh, and other lower riparian states on the water resources of Ganga River for the sustenance and growth of agricultural and hydroelectric power sector is ever growing. River Ganga receives significant contribution from snow and glacier melt through Bhagirathi and Alaknanda rivers, main tributaries of river Ganga, originates in Higher Himalayas. During the lean flow period in summer, the snow and glacier melt remains important for drinking and irrigation purpose and for the sustenance of hydroelectric projects. It is therefore required to carry out the scientific studies to estimate the contribution of snow and glacier melt, subsurface and surface - runoff component of Ganga River in upper reaches (i.e., Bhagiathi River and Alaknanda).

BRNS, DAE, Govt. of India, Mumbai funded the present project to NIH for hydrograph separation in order to understand the contribution of different component in Bhagirathi river using isotopic and geochemical techniques and flow modeling. Isotopic signatures of different component such as precipitation, snow/ glacier melt, subsurface flow, surface runoff were developed by collecting representative water sample of each category. NIH collected the hydrological and meteorological data from CWC and other field agencies. Along with the isotopic models, SNOWMOD and ANN modelling were applied to cross check the results of isotopic investigations.

The project activities were planned under the guidance of Dr. Bhishm Kumar Scientist F and Head, Hydrological Investigations Division and executed by Dr S. P.Rai, Scientist E1 Hydrological Investigations Division at NIH. Dr. Noble Jacob Isotope Hydrology Section, Isotope Applications Division, Bhabha Atomic Research Center, Trombay, Mumbai played the role of Principal Coordinator of the project. Dr Sanjay Jain Scientist E II, Surface Water Hydrology Division carried out stream flow modeling using SNOWMOD model and Shri Senthil Kumar Scientist E1 Surface Water Hydrology Division developed ANN model. The other scientists of the Institute who have been actively involved during the project include Shri S. K. Verma, Scientist C and Shri Pankaj Garg Scientist B and extended their help in sample collection. The laboratory analysis stable isotopes were carried out by Shri Jamil Ahmad SRA, Shri Vipin Agrawal, SRA and Vishal Gupta, RA. In addition to this, Sh. Y. S. Rawat, Project Officer appointed under the project, also assisted in the field work and preparation of the report. I hope that the results of the project would be very much useful for the sustainable development and management of the water resources projects in the Himalayan region in general and for the Bhagirathi/Ganga River Basin in particular. However, there is a need to carry out the long-term studies which will enhance the knowledge about the melting pattern of the Himalayan glaciers and provide the capabilities of the hydrological models for simulating the runoff within the desirable accuracy.

Raj Deva Singh

**March 31, 2009**
**Roorkee**

**(R. D. Singh)**
**Director**

# Acknowledgement

The investigators are deeply grateful to the Department of BRNS, DAE, Govt. of India, Mumbai very generous funding for carrying out this hydrological study using the isotopic techniques.

We indeed grateful to Dr. S. V. Navada, Scientist G, then Head Isotope Hydrology Section, Isotope Applications Division, Bhabha Atomic Research Centre, Trombay for inspiration and encouragement to carryout this study. His critical comments and suggestion during analysis and preparation of report help us in improving the final project report. Authors are also thankful to Dr. Saravan Kumar Scientist 'H' of Isotope Hydrology Section, Isotope Applications Division, Bhabha Atomic Research Centre Trombay for helping in analysis of data.

Dr. K. D. Sharma, then Director NIH, provided necessary official support and guidance without which it was not possible for me to complete this project. Present Director, Shri R. D. Singh encouraged to complete this project successfully. I express my sincere thanks to Director's NIH for their great support and guidance.

We are thankful to Shri Rm. P. Nachiappan, then scientist 'B' helped in great way in preparing the project proposal and framework of the project. My thanks are due to Project Officer, Dr. Atul Kohli, who contributed lot in the field work and data preparation/analyses including other laboratory works. My thanks are due to laboratory staff, Shri Mohar Singh and Shri Suresh Kumar for analyzing the isotope samples.

At last but not least, we express my sincere thanks to the field and other staff who helped in various ways in completion of this project.

(Bhishm Kumar)

# CONTENT

Page No.

Page No.

# LIST OF FIGURES

# LIST OF TABLES

# LIST OF PLATES

# CHAPTER 1

## 1.0 Introduction

The three important river systems originating from the Himalayan region are: the Indus, the Ganges and the Brahamaputra. Excluding Brahamaputra and Indus, which flow parallel to northern range of Greater Himalayas, towards west and east respectively, all other remaining rivers including few tributaries of Brahamaputra and Indus cut across the Himalayas and flow from north to south. The River Ganga, one of the major rivers of Himalayas originates from the Gangotri Glacier. Bhagirathi and Alaknanda rivers are the main tributaries of river Ganga, which originate from the higher Himalyas. These two tributaries confluence at Devprayag and form the River Ganga. Importance of the River Ganga in the Indian context is better understood from the fact that it continues to play a major role in the socio-economic development of the entire northern part of the country. The dependency of Uttarakhand, Uttar Pradesh, and other lower riparian states on the water resources of Ganga River for the sustenance and growth of agricultural and hydroelectric power sector is ever growing. River Ganga receive significant contribution from snow and glacier melt water. During the lean flow period in summer, the snow and glacier melt water remains important for drinking and irrigation purpose and for the sustenance of hydroelectric projects. Therefore, correct information of snow and glacier melt water contribution to the Ganga River is of utmost importance for the water resources development and management of this region.

Despite its importance, very less hydrological information is available on the Bhagirathi and Alaknanda River, mainly due to the inaccessible and difficult terrains. A few attempts have been made to develop reliable hydrological models for runoff forecasting in the Bhagirathi basin. The water balance/modelling aspects of the stream flow in the Bhagirathi River at Devprayag have been attempted by Singh et al. (1994) and Tangri (2000). However, a number of fundamental issues remain unresolved, such as: (a) role of groundwater in the stream-flow and its spatial and temporal variability, (b) role of snowmelt and its temporal variability, (c) rainfall – runoff relationship and ( l) relative significance of the tributaries to the stream flow in the main river. These issues are very much important because the assessment of runoff, snow/ice melt and groundwater contribution of Bhagirathi River are required for the planning and management of water resources and design and operation of engineering schemes such as hydropower projects. The water availability and suitable hydraulic head in the mountainous area provide enormous potential for hydropower generation. There are many countries like Switzerland and Norway, where most of the national energy demand is met by the hydropower generated in the mountainous areas (Bandopadhya et al. 1977).

The collection of hydrometeorological data in the Himalayan regions is a difficult task. Therefore, previous researchers could not segregate the contribution of different components in Bhagirathi and Alaknanda River. Bhagirathi River basin has spatially and temporally varied contribution from different constituents of the hydrologic system such as rainfall, runoff, subsurface inflow in the form of groundwater and snow/glacial melt. In order to separate the various components of stream flow of Bhagirathi river, the only reliable alternative method is to adopt a advance technology such as isotopic techniques. In the present project, stable and radioactive isotope techniques along with geochemical tracers have been used for the hydrograph separation of Bhagirathi River. Isotopic results have been compared with those obtained by conventional techniques. This is the first study of its kind in India where in isotope techniques have been employed to understand the contribution of various hydrological components to the stream flow of Bhagirathi River.

## 1.1 Objectives

The project area was investigated with the following main objectives as follows:

a) Isotopic characterization of rainfall, snowmelt, runoff and groundwater in the Bhagirathi River Basin

b) Hydrograph separation using isotopic and hydrochemical techniques to evaluate the surface water and groundwater interaction along the Bhagirathi River

c) Development of a stream flow model for the Bhagirathi River

## 1.2 Study Area

Bhagirathi River basin extending an area of 7660 km$^2$, from Gangotri glacier (Gaumukh) to Devprayag was considered for the present study (Fig. 1.1). The present study area falls within the administrative boundaries of Uttarakhand state. The Bhagirathi River basin is the part of headwater catchment of the river Ganga. It is characterized by an altitudinal variation of about 440 m a.m.s.l at Devprayag to 7138 m a.m.s.l. at Chakhamba peaks and forms a part of the Central Himalayas. The higher reaches of the study area are glaciated with snow.

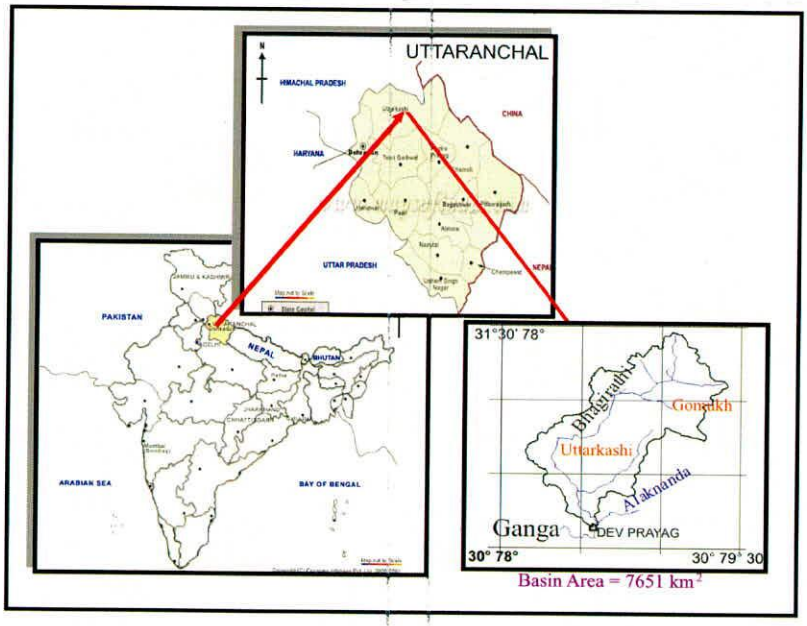


Fig.1.1 Study area of Bhagirathi River basin.

### 1.2.1 Geomorphic features

The Bhagirathi river basin is characterized by the young immature mountains of the Central Himalaya with glacial valleys (Plate-1.1) in the higher reaches and deep river gorges in the lower parts. The Gangotri glacier does not occupy the entire section of its valley but has longitudinal valleys along its sides - between its lateral moraine and the valley walls. At some places, the SLOPE wash and/or the alluvial deposits have covered the glacial deposits and even affected their shapes. There are large depressions, now partially or fully filled up between the oldest preserved moraines and the valley walls at the confluence of large tributaries with the main glacier, such as Tapoban, at the confluence of Meru glacier and Brahmpuri, at the confluence of Kirti Bamak, etc. Besides these, there are a number of small and large lakes over the glacier. These lakes are being filled up by debris from surface moraines and some of the dried ones contain varve like accumulations of clay-sand association (Tangri 2000).

The river Bhagirathi originates from Gangotri glacier snout, named as Gaumukh (Plate 1.2). It is a six$^{th}$ order stream. It has a broad U shaped valley (Plate 1.3) upstream of Jhala in the upper reaches, but cuts across the Great and Lesser Himalaya in a narrow V shaped gorge. Near Bhatwari, the Bhagirathi river has an open valley with wide river terrace and overlapping spurs. Between Bhatwari and Suki, the river flows through a narrow and deep gorge. Upstream of Jangla, the Bhagirathi river has cut almost a vertical gorge through an old glacial pavement made up of granite. It swings to west near Uttarkashi and further downstream takes a U turn to assume an easterly flow. At Tehri, it joins another glacier fed river - the Bhilangana, and flows southwards cutting gorge (Fig. 1.2).

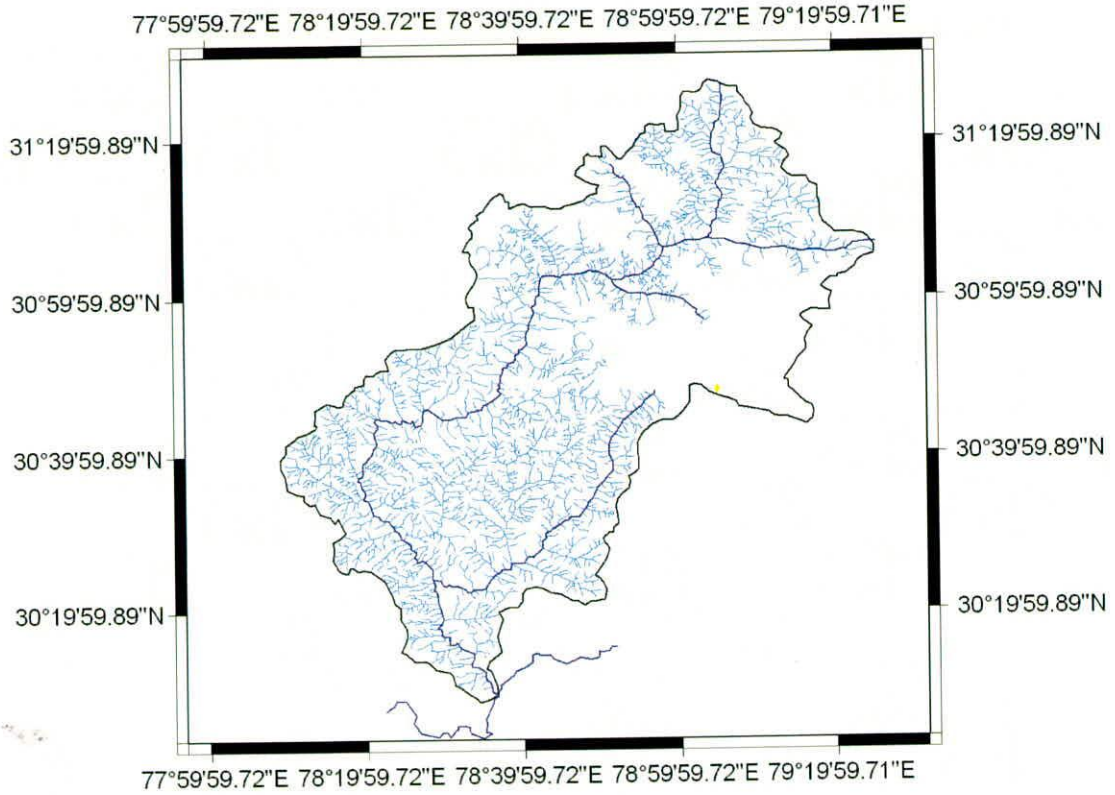


Fig. 1.2: Drainage map of Bhagirathi River Basin.

The Bhagirathi River basin is sub-divided into 75 macro and micro watersheds of which the Bhagirathi, Bhilangana, Alaknanda, Asi Ganga, Jadh Ganga (Plate 1.4), Khurmala Gad, Pilang Gad, Jalkur Nadi etc. are relatively larger in size (Tangri, 2000). The detailed morphometric details of the Bhagirathi River basin are presented in table 1.1 and 1.2.

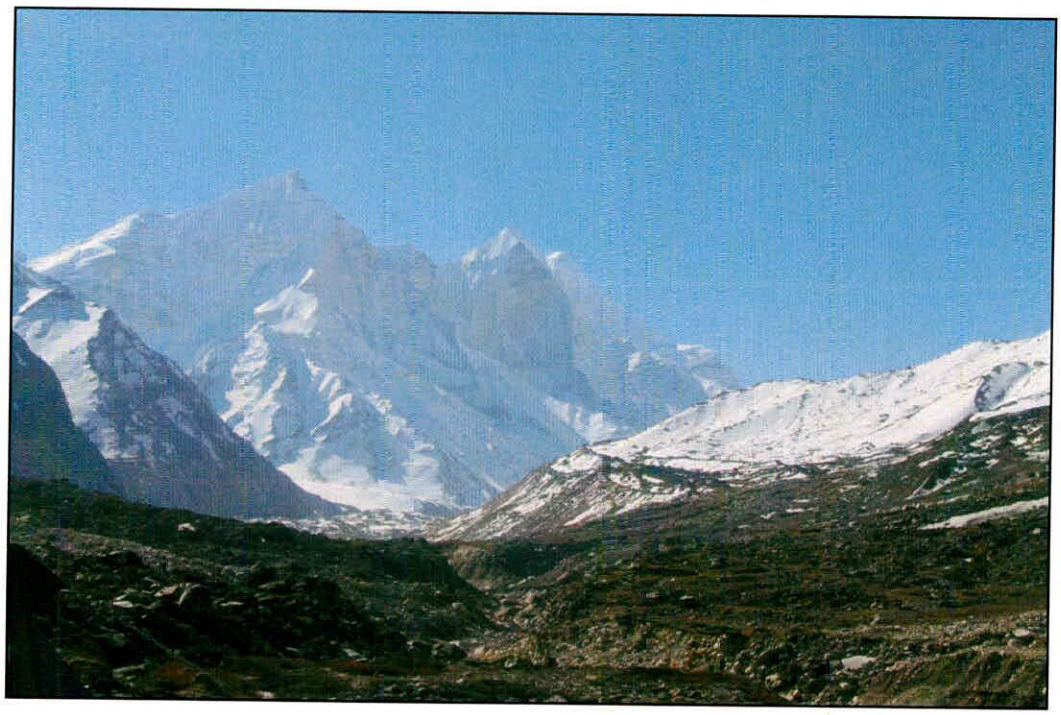

Plate 1.1: Snow-clad Bhagirathi peaks: a view from Bhojwasa.


Plate 1.2: View of Gangotri snout (i.e.,Gaumukh) during the study period of 2005.

Plate 1.3: A view of the U shaped Bhagirathi valley as seen from the top of snout of Gangotri Glacier.

Plate 1.4: A view of deep Bhagirathi River gorges

Table 1.1: Linear Parameters of Bhagirathi River Basin

| S.No | Parameters | Value |
|---|---|---|
| 1 | Basin Perimeter | 552.60 (km) |
| 2 | Basin length or Valley length | 153.8 (km) |
| 3 | Total stream length of all orders (km) | 3321.60 (L1) |
| | | 864.10 (L2) |
| | | 387.64 (L3) |
| | | 266.30 (L4) |
| | | 190.44 (L5) |
| | | 75.44 (L6) |
| 4 | Mean stream length of each order (km) | 5105.52 |
| 5 | Mean stream length of each order (km) | 1.90 |
| | | 2.15 |
| | | 4.41 |
| | | 13.32 |
| | | 63.48 |
| | | 75.44 |
| 6 | Total number of streams of all order | 1747 |
| | | 401 |
| | | 88 |
| | | 20 |
| | | 3 |
| | | 1 |
| | Total number of streams of all order | 2260 |
| 7 | Bifurcation ratio (Horton, 1945) | Av. 4.60 |
| 8 | Stream-length ratio (Horton, 1945) | Av. 2.43 |
| 9 | Length of overland flow (Horton, 1945) (km) | 0.75 |

Table 1.2: Areal parameters of the Bhagirathi basin

| S.No. | Parameters | Value |
|---|---|---|
| 1 | Total Drainage Area ($km^2$) | 7651.06 |
| 2 | Drainage Denisty (per $km^2$) | 0.67 |
| 3 | Constant of Stream Maintenance (Schumm, 1956) (km) | ~1.5 |
| 4 | Circularity Ratio (Miller, 1953) | 0.31 |
| 5 | Elongation Ratio (Schumn, 1956) | 0.64 |
| 6 | Form Factor (Horton, 1932) | 0.32 |

Mojor tributaries of Bhagirathi River with in the study area are Bhilangana, Assi Ganga, and Kedar Ganga. In addition to these tributaries, large number of flowing nalas and springs also exist in different parts of the study area. The digital elevation map (DEM) of the study area has been developed using the contour and spot height of the basin. It is seen that the minimum altitude of the catchment is 467 m a.m.s.l. and maximum is 6904 m a.m.s.l. (Fig. 1.3). On the basis of the DEM, the Bhagirathi basin can be divided into six altitudinal zones. The area under different elevation zones are presented in Table 1.3.

Table 1.3: Area of Bhagirathi River basin under different elevation zones

| Elevation Range | Area ($Km^2$) | Elevation Range | Area ($Km^2$) |
|---|---|---|---|
| >6600 | 3.40 | 3000-3600 | 584.49 |
| 6000-6600 | 108.43 | 2400-3000 | 653.29 |
| 5400-6000 | 840.90 | 1800-2400 | 1070.54 |
| 4800-5400 | 1397.20 | 1200-1800 | 1091.11 |
| 4200-4800 | 890.23 | 600-1200 | 429.15 |
| 3600-4200 | 590.75 | <600 | 4.12 |

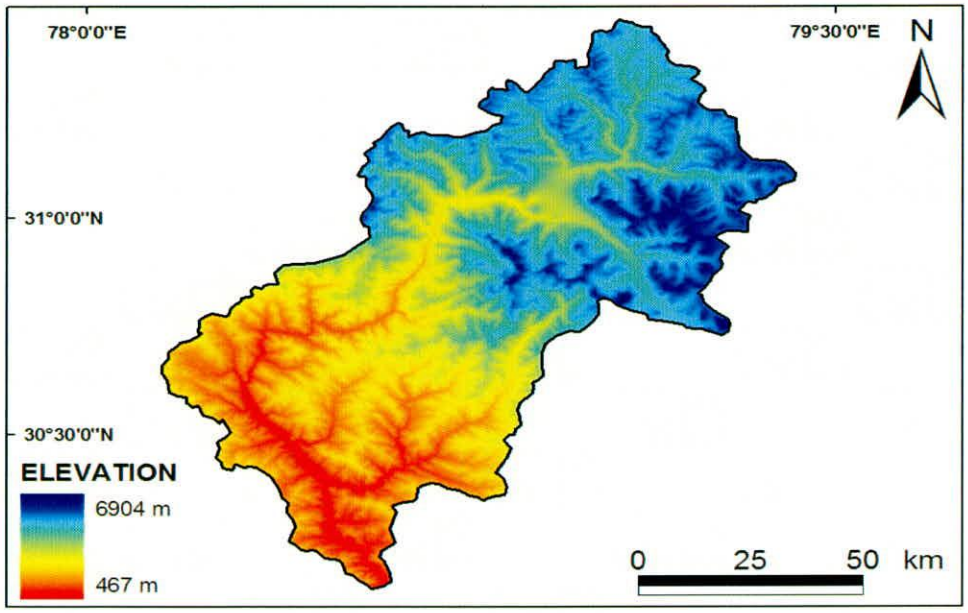


Fig. 1.3 : Digital Elevation Map of Bhagirathi River catchment.

### 1.2.2 Hydrology

The study area experiences a severe winter (December to March) characterized by the occurrence of heavy snowfall at higher altitudes. The important source of moisture for winter precipitation is from western disturbances originating from the Caspian sea. The winter season is followed by pre-monsoon season (April to June) characterized by hailstorms and thunderstorms that get more severe towards the end of the season. The monsoon season sets usually by July and extends up to September. The Bay of Bengal is the major source of moisture for precipitation during monsoon season in which 75 % of the annual rainfall is received. The post-monsoon season (October-November) is generally dry with scanty rainfall. Bhagirathi River receives meltwater from

Gangotri glacier in summer season (May to September). In addition to Gangotri glacier, the river Bhagirathi also receives water from other lateral glaciers like Matri Bamak, Chirbas Bamak, Deo Gan Bamak, etc.

Upper reaches of the Bhagirathi basin remain under snow cover throughout the year. The popularly known as Gangotri Glacier is a cluster of many glaciers and the main Gangotri Glacier (length: 20-30 km; width: 0.2-2.35 km; area: 86.32 $km^2$) forms the trunk part of the system. This is known as Gangotri Glacier system. The major glacier tributaries of the Gangotri Glacier system are Raktvarn Glacier (area: 5530$km^2$) Chaturangi Glacier (area: 67.70 $km^2$), Kirti Glacier (area: 33.14 $km^2$), Swachand Glacier (area: 1671 $km^2$), Ghanohim Glacier (area: 12.97 $km^2$), Meru Glacier (area:

6.11 $km^2$), Maindi Glacier (area: 4.76 $km^2$) and a few others having a total glacierized area of about 3.08 $km^2$. This is a valley-type glacier system with glacierized area of about 286 $km^2$ (Singh et al., 2005). Snow and glacier melt runoff play a vital role in making all the north Indian rivers perennial. Depending upon the prevailing climatic conditions, the runoff contribution from the snow/glaciers starts in May, after depletion of accumulated seasonal snow. Usually, the melt contribution from these glaciers continues till October.

### 1.2.3 Geological setup

Bhagirathi River basin comprises of rocks belonging to the Central Crystalline Group, Garhwal Group, Vaikrita Group, Baliana Krol and Tal Group, Sumana Groups and Kanwar Group (Fig. 1.4). The detailed geology is described below:

***Central Crystalline Group* (CCG) :** It possibly forms the oldest crystalline basement of the Himalaya. Although, it has witnessed different Precambrian orogenies prior to the strong Himalayan orogeny, much of the original character is preserved. CCG consist of gneisses, migmatites, crystalline schist, thick quartzite with a conspicuous horizons of calc-silicates with psammite gneisses in the upper part form bulk of the metasediments, which may be compared with the Bundelkhand Gneissic Complex of the Peninsular part. It also contains other younger granites. Its southern contact with the Garhwal Group is a tectonic plane referred to as the Main Central Thrust.

***Garhwal Group* :** It forms a major part of the Lesser Himalaya and is represented by thick sequence of low grade metasediments consisting of quartzite with penecontemporaneous mafic metavolcanics and carbonate rocks extending from Nepal through Kali valley in the east to the Tons Valley in the west and continues into Himachal Pradesh and beyond. It is limited in the north by the Main Central Thrust and in the south by the Main Boundary Fault (MBF 2). In Lesser Himalayas, it is exposed in two tectonic linear zones separated by rocks of Vaikrita Group.

The Garhwal group of rocks is divided into five formations, viz. Uttarkashi, Khattukhal, Rautgara, Tejam and Berinag formations in an ascending order. Uttarkashi Formation is the oldest group of rocks exposed in anticlinal cores in the Bhagirathi valley around Uttarkashi. Jain (1971) proposed this name for quartizite, limestone, and slate/phyllite and divided into five members- Netala Quartizite, Lower Uttarkashi Limestone, Pokhri Slate, Upper Uttarkashi Limestone and Bareti Quartzite. At 500 m downstream from the Dabrani bridge on the Uttarkashi-Gangotri road, a thick zone of dolomitic marble and calcsilicate is intercalated with bands of psammite, pelite and greenschist/amphibolite. An intercalated sequence of mica-schist and gneiss occurs along the road. On the upstream side towards Lohari Nag, the Bhagirathi River has cut a steep gorge through the metamorphics.

***Rautgara Formation* :** It is a sequence of massive, cream coloured, purplish and brownish fine grained quartzite interbedded with purple green mottled slate and calcareous phyllite as the Saryu valley Quartzite (Valdiya 1962).

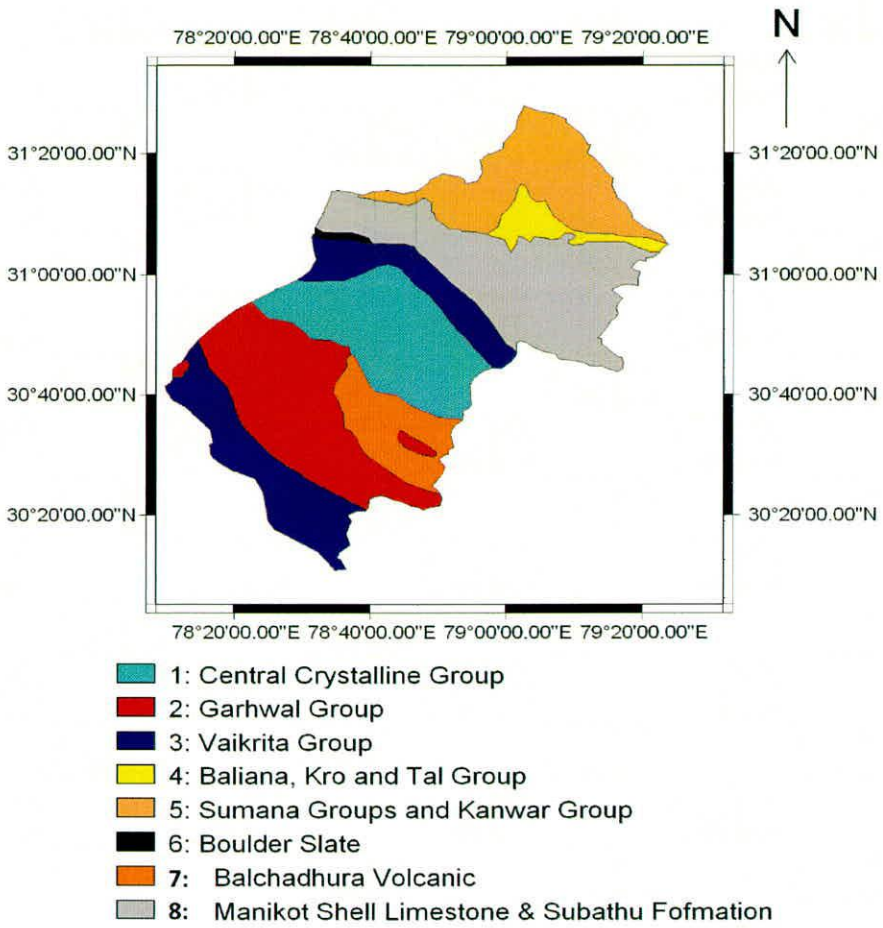


Figure 1.4 : Geological map of the study area (after Kumar, 2005)

***Deoban Formation :*** It represents the second carbonate facies of the Garhwal Group conformably overlies the Rautgara Formation and is overlain by Berinag Formation.

***Berinag Formation :*** Berinag formation is similar to the Rautgara Formation. It comprises of a thick succession of quartzite with penecontemporaneous mafic metavolcanic.

***Vaikrita Group :*** Vaikrita group is redefined to include the metasedimentaries exposed between the granite gneisses constituting the Central Crystlline and the overlying Martoli Group and its equivalents. In Bhagirathi valley, it is exposed between Sukhi and Harsil. The Gangotri Granitoid intrusive into Vaikrita and the overlying Martoli Grroups, it includes biotite granite, tourmaline granodiorite, tourmaline aplite and pegmatite. In the upper part of the basin, granodiorite occurs in the form of laccolithic body intrusive into the black slates (referred to as Haimanta) in the Bhagirathi peak region and form the 'Shivling massif'.

A hot spring exists at Gangnani in the Bhagirathi Valley, which emanates through highly deformed, contorted and sheared phyllonite and mylonitized schist on the footwall of the Vaikrita Thrust.

***Martoli Group :*** A thick sequence of unmetamorphosed to feebly metamorphosed rocks has been mapped from Kali valley in the east to Jadh Ganga in the west. In Lesser Himalaya, it forms a narrow linear zone constituting the Krol Belt comprising the Baliana, Krol and Tal Groups. The Martoli fault separate it from the Central Crystallines.

***Sumana and Kanwar Group*** : In the Tethys Himalaya, the supersequence comprises the Sumana and Kanwar Groups which rest unconformably over the Martoli Group. The Sumana group include Garbyang, Shiala, Variegated and Muth formations. A thick succession of purple conlomerate, purple to greenish grey quartzite that unconformably overlies the Martoli Group. The quartzite of Ralam formation passes gradationally to the overlying thick sequence of alternating bands of calcilutite, calc-siltstone and brown dolomitic limestone with chloritic layers is called as Garbyang formation. The Garbyang formation is conformably overlain by about 500 m thick shale with bands of grey nodular limestone, sandy shale and dolomite which is named as Shiala Series. The Shiala formation is conformably overlain by Variegated formation which is made up of dolomite and siliceous limestone. The Variegated formation is overlain by Muth formation which is made up of quartzite and dolomitic limestone.

The sequence of limestone and black shale unconformably overlying the Sumana Group constitute the Kanwar Group.

### 1.2.4 Hydrogeology

The Bhagirathi basin is cut by numerous faults trending N-S and NE-SW. Fractures and joints are conspicuous in all rock formations. Not only do these structures control the drainage pattern, but they also play an important role in promoting groundwater recharge and the emergence of springs. There is a strong relationship between the tectonic linears and high discharge of springs, the major springs are lying on them because the fault and thrust plane act as barriers due to the development of clay layer along the fault plane (fault gouge) (Valdiya, 1989).

Fracture zones, related to the faults and other lineaments, are characterized by sheared and crushed rocks; They are understandably good locations for the occurence of springs, even in rocks that are otherwise impermeable. The hard rocks of the Central crystalline, Garhwal and Vaikrita have very low intergranular porosity, but they are characterized by fissures, fractures, and joints developed due to the recurrent tectonic activities. The zones of the Garhwal Thrust, the Main Boundary Thrust and the Central Crystalline Thrust show pockets of high secondary porosity. Clusters of springs are found in this zone with high yield which is attributed to these lineaments. In general, five sets of fractures and joints are recognizable in Lesser Himalayan rocks. Among these, NNE-SSE trending ones are very prominent, followed by the N E-SW and NW-SE oriented joints and the gentle dip planes that strike ESE-WNW and ENE-WSW.

In the study area, rainfall infiltrates through the intergranular pore spaces, openings, fissures, fractures, joints, bedding planes etc and re-appears downslope as seepages and springs. Thus, ground water occurs in the secondary porosity of the formation and flows under unconfined condition. Development of water is posible on a local scale depending on the land forms. Both hot and cold spring occur in this region. The hot springs (eg. Gangani Spring) are generally found in crystallines and are structurally controlled. Therefore, the geomorphological features and the local geology of the area play an important role in the groundwater recharge and controls the occurrence and distribution of springs.

The terraces comprising of assorted material such as boulder, cobble, gravel, sand and clays are the most significant repository of groundwater. The terraces are tapped in many places in the form of open and bore wells.

### 1.2.5 Hydro power potential

Uttarakhand has a vast hydroelectric potential and preliminary hydrological, geographical investigations estimated about 19000 MW potential in this state of which, only 7% has so far been tapped. At present the 7% potential is generated through 12 hydropower projects with an installed generation capacity of 1280 MW (Plate 1.5 and Plate 1.6). In Bhagirathi and Alaknanda basins four-hydel projects are in various stages with an installed capacity of about 2104 MW (Table 1.4).

Table 1.4: Hydropower operations in the Bhagirathi and Alaknanda basins (Source Nawani et al., 2002)

| S.No. | Name of scheme | River | District | Installed capacity | | Annual energy (MU) | Yr of comm |
|---|---|---|---|---|---|---|---|
| | | | | Unit | Total MW | | |
| **Project Already Running** | | | | | | | |
| 1 | Maneri Bhali Stage-I | Bhagirathi | Uttarkashi | 3 | 90 | | 84-85 |
| 2 | Ramganga | Ramganga | Pauri | 3 | 198 | 431 | 75-76 |
| 3 | Tehri | Bhagirathi | Tehri | 4HPP | 1000 | 3568 | |
| **Project Under Construction** | | | | | | | |
| 4 | Maneri Bhali Stage-II | Bhagirathi | Uttarkashi | 4 | 304 | 1566 | Govt. |
| 5 | Koteshwar 100 1225 THDC | Bhagirathi | Tehri | 4 | 400 | 125 | THDC |
| 6 | Vishnuprayag | Alaknanda | Chamoli | 4 | 400 | 2005 | M/s JP |
| **Scheme I.P. in advance/completed** | | | | | | | |
| 7 | Pala Maneri | Bhagirathi | Uttarkashi | 4 | 416 | 1575 | |
| 8 | Lohar Nag Pali | Bhagirathi | Uttarkashi | 4 | 520 | 1900 | |
| 9 | Tapovan | Dhauli Ganga | Chamoli | 3 | 360 | 1618 | |


**Plate 1.5 A View of Tehri Dam**


**Plate 1.6 A view of Maneribhali Dam**

### 1.2.6 Flora and fauna

The study area is characterized by appreciable flora and fauna. Thick vegetation ranges from Pine (between 900 m to 2000 m altitudes a.m.s.l.), Deodar forests (between 2000 m to 3000 m altitudes above a.m.s.l), Fir and Spruce forest (only in northern part above 3000 m), Kharshu Birch and Juniperus forest upto altitude of 4000 m including Semru trees and Alpine forests (between 3500 m to 4877 m altitudes above a.m.s.l) in almost every where in the study area.

The chief faunas found in the study area are leopard, snow leopard, Himalayan bear and brown bear. The snow leopard is a rare species found only in alpine forests. Other important faunas are musk deer, the Kakar (barking deer), the Sambar (the Jardo) and Varau (deer). Numerous varieties of birds such as pigeons, doves, etc. are found in the Uttarkashi district, as well as in the other parts of study area. Black dvargo (Chaina ki Maina – local name) is found at an altitude of about 3700 m. Sparrow, Phakta and other small birds are also found at the same altitude (Kumar, 2005).

## 1.3 Previous Work

In the recent past, many studies covering different aspects of geology, geomorphology and glaciology have been carried out on Bhagirathi River and its origin i.e., Gangotri glacier. The Himalayan rivers such as Ganga and Brahamputra together account for 3% of the total global flux of dissolved load to the world ocean (Sarin et al. 1989). It has been estimated that the non Himalayan rivers of Peninsular India carry less than 5% of the total mass transport as compared to Himalayan rivers (Subramanian, 1979).

Sediment transport by the glacier melt water has been studied by a number of investigators (Hasnain et al., 1989; Hasnain, 1992, 1996; Hasnain & Renoj 1996; Chauhan & Hasnain 1993; Sarin et al 1992, Pandey et al. 1999) in the last two decades. The chemistry of head waters of River Ganga has been investigated by Singh and Hasnain (1999, 2002); Pandey et al. (1999) and Chakrapani (2005).

Tangri (2000) has made an attempt to study the basic drainage network and associated geomorphological aspects of the Bhagirathi River basin. The water balance/modelling aspects of the stream-flow in the Bhagirathi River at Devprayag have been attempted by Singh et al. (1994) and Tangri (2000). The Dokriani glacier melt runoff pattern and suspended flow have been studied by Singh and Shastri (1999) and Singh et al., (2003). Singh et al., (2005) have made an attempt to study the diurnal variations of discharge and suspended sediment concentration in Gagotri glacier melt water at Gaumukh. The average snowmelt contribution to the total streamflow of Ganga River at Devprayag was found to be 28.7 % by adopting a simplified water balance approach considering the role of groundwater as negligible.

The stable isotopic characteristics of Himalayan River namely, Ganga, Yamuna and Indus River have been studied by Ramesh and Sarin, (1992), Dalai et al., (2002) and Pande et al., (2000), respectively. Chakrapani and Veizer (2005) have studied carbon isotopic compositions to understand the source of Dissolved Inorganic Carbon in the Bhagirathi River. The correlation of conductivity and stable isotope $\delta^{18}O$ in Ganga River at Patna (lower reaches) has been studied to understand the groundwater interaction with the river (Lambs, 2004). However, these studies were carried out for gaining general information and do not focus on flow modeling due to which many crucial information are masked or subdues.

# CHAPTER 2

## METHODOLOGY AND WATER SAMPLING

### 2.0 Isotope Technique

Isotopes are the atoms of an element having same atomic number (Z) but different atomic weight (A). In other words, the atoms of an element having different number of neutrons (N) but same number of protons or electrons are called isotopes. For example, hydrogen has three isotopes having the same atomic number of 1 but different atomic masses or weights of 1, 2 and 3 respectively i.e., ${}_1^1H_0$, ${}_1^2H_1$ and ${}_2^3H_2$.

Similarly oxygen has eleven isotopes, $^{12}O$,$^{13}O$, $^{14}O$, $^{15}O$, $^{16}O$, $^{17}O$, $^{18}O$, $^{19}O$, $^{20}O$, $^{21}O$ and $^{22}O$, but except $^{16}O$, $^{17}O$, and $^{18}O$ all other isotopes are radioactive and their existance in nature is very small (half life vary from 150 seconds to few femo seconds - of the order $10^{-15}$ seconds) therefore, we normally talk about only three isotopes of oxygen i.e., $^{16}O$, $^{17}O$, and $^{18}O$. The carbon also has three isotopes $^{12}C$, $^{13}C$ and $^{14}C$.

### 2.1 Classification of Isotopes

Isotopes can be classified into two important categories, (i) stable isotopes and (ii) radioactive isotopes. Stable isotopes are the atoms of an element, which are satisfied with the present arrangement of proton, neutron and electron. On the other hand, radioactive isotopes are the atoms of an element which do not satisfy with the present arrangement of atomic particles and disintegrate by giving out alpha ( $\alpha$ ), beta ( $\beta$ ) particles and/or gamma ($\gamma$) radiation etc. and transform into an another type of atom. This process continued till the stable nuclide (element) is formed. For example, $^1H$ and $^2H$ are stable isotopes while $^3H$ is adioactive. Similarly $^{12}C$ and $^{13}C$ are stable isotopes while $^{14}C$ is radioactive. On the other hand, isotopes of oxygen ($^{16}O$, $^{17}O$ and $^{18}O$) are stable.

Isotopes can also be classified as natural and artificial isotopes, i.e., the isotopes that occurs naturally are called natural isotopes while those produced in a reactor or laboratory under controlled conditions are known as artificial isotopes. Normally the artificially produced isotopes are radioactive while both stable and radioactive, isotopes occur naturally.

Another category of isotopes, called as environmental isotopes,are naturally occurring stable and radioactive isotopes and radioisotopes introduced into the atmosphere due to anthropogenic activities etc. The environmental radioisotopes, whether naturally occurring due to cosmic ray interaction with various gaseous molecules or anthropogenically produced and become the part of hydrological cycle are safe in normal conditions and do not pose any threat to the human health.

The following diagram gives a clear picture about the classification of various isotopes.

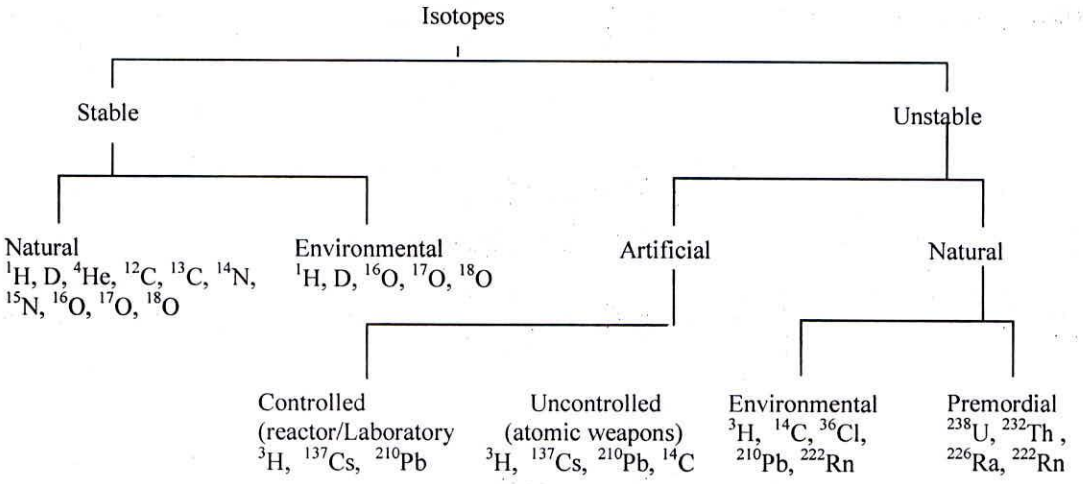

### 2.1.1 Stable isotopes

As described earlier, the atoms of an element which do not decay with time are called stable isotopes of that element. Over 2000 isotopes of 92 naturally occuring elements have been identified out of which several hundred are stable isotopes. But for hydrological investigations, we talk much about hydrogen and oxygen stable isotopes. As we know that water molecule is made up of two hydrogen atoms and one oxygen atom therefore, many combinations (18) are possible out of which $^{1}H^{1}H^{16}O$, $^{1}H^{1}H^{18}O$, $^{1}HD^{16}O$, $^{1}HD^{18}O$, $^{1}H^{1}H^{17}O$ and $^{1}HD^{17}O$ are important. The natural occurrence of few very important types of water molecules is given below:

$H_2{}^{16}O$ ~ 997640 ppm (99.7640 %)
$H_2{}^{18}O$ ~ 2040 ppm (0.204 %)
$HD^{16}O$ ~ 320 ppm (0.032 %)

There are a few other stable isotopes ($^{4}He$, $^{7}Li$, $^{11}B$, $^{13}C$, $^{15}N$, $^{34}S$, $^{37}Cl$, and $^{87}Sr$) which have been found useful in many hydrological studies. These stable isotopes are popularly called environmental stable isotopes as they are available in the environment and introduced in the hydrological cycle naturally. Thus the investigator does not require them to or inject into the system for carrying out hydrological studies.

Measurements of stable isotopes are done in terms of abundance ratios i.e. atomic mass of heavy atom to the atomic mass of light atom. For example, heavy water $^{2}H_2{}^{16}O$ ($D_2{}^{16}O$ ) has a mass of 20 compared to normal water $^{1}H_2{}^{16}O$ which has a mass of 18. Similarly heavier stable molecule of water $D_2{}^{18}O$ has a mass of 22. This is because of the variation in the number of neutrons in the nucleus. However, the absolute abundance ratio of isotopes is not usually measured in natural waters and in other components. Only the relative difference in the ratio of the heavy isotopes to the more abundant light isotope of the sample with respect to a reference is determined. The difference is designated as $\delta$ and is defined as follows:

$$\delta = (R_{sample} - R_{reference}) / R_{reference} \quad (1.1)$$

where R's are the ratios of the $^{18}O/ {}^{16}O$ and D/H isotopes, in the case of water.

The difference between the sample and the reference is usually quite small, $\delta$ values are therefore, expressed in per mille differences (‰) i.e. per thousand, $\delta$ (‰ ) = $\delta$ x 1000.

$$\delta (‰) = [(R_{sample} - R_{referenc}) / R_{reference}] \times 10^{3}$$
$$= [(R_{sample} / R_{reference}) - 1] \times 10^{3} \quad (1.2)$$

If the $\delta$ value is positive, it refers to the enrichment of the sample in the heavy-isotope species with respect to the reference and negative value corresponds to the sample depleted in the heavy-isotope species.

The reference standard normally considered is VSMOW (Vienna Standard Mean Ocean Water) Craig (1963) evaluated the isotopic ratios of SMOW as;

$$^{18}O/ {}^{16}O = (1993.4 \pm 2.5) \times 10^{-6} \text{ and } D/H = (158 \pm 2) \times 10^{-6} \quad (1.3)$$

### 2.1.2 Isotopic fractionation

The variation in the global distribution of different isotopes in various hydrologic systems are mainly brought about by isotopic fractionation. The isotopic fractionation, which is proportional to the differences in the mass of the isotope water species, may be described as the partitioning of the isotopes by physical or chemical processes. The chemical and isotopic fractionation processes involve redistribution of isotopes of oxygen or hydrogen among various phases. These processes can be either equilibrium isotopic reactions with equal reaction rates for both forward and backward reactions or non-

equilibrium (kinetic) isotopic reactions with mass dependent reaction rates which are unidirectional.

The distribution of isotopes among various phases of water which are in equilibrium is not uniform. In other words, the water vapour in equilibrium with liquid water is slightly depleted in heavier isotopes, in comparison to the latter. This is because of the differences in the bond energy in the liquid phase between the isotopic molecules, resulting in the differences in the vapour pressure of the isotopic species of water. The difference in the ratio of heavier to lighter isotopes in one phase to that of the other is then, is defined by equilibrium fractionation factor $\alpha^+$:

$$\alpha^+ = \frac{(R_x)_{liquid}}{(R_x)_{vapour}}$$

where $R_x$ is the ratio of concentrations of heavier to lighter isotopes.

The equilibrium fractionation factor has been determined by several investigators through vapour pressure measurement of pure isotopic species (Szapiro & Steckel, 1967), through isotopic analyses of water and water vapour in equilibrium (Majoube, 1971; Bottinga and Craig, 1969; and Kakiuchi and Matsuo, 1979), or by dynamic distillation methods (Borowitz, 1962). However, the results presented by Majoube (1971) is widely used in isotope hydrology studies. Majoube (1971) proposed the equation for $\alpha^+$ as:

$$\ln \alpha^+ = AT^{-2} + BT^{-1} + C$$

Where T is the absolute air temperature in Kelvin, and A, B, and C are coefficients. The values of the coefficients proposed by Majoube (1971) for $^{18}O/^{16}O$ are 1137, -0.4156 and -0.00207, respectively; for D/H are 24844, -76.248 and 0.05261, respectively.

To study the effect of evaporation in the surface water bodies such as lakes, the fractionation factor $\alpha^*$ is used in place of $\alpha^+$. $\alpha^*$ is inverse of $\alpha^+$. At the temperature of interest to a hydrologist, the value of $\alpha^*$ is always less than one. The equilibrium enrichment factor $\varepsilon^*$ is more convenient to express the relative changes in the isotopic ratios of liquid water and water vapour in equilibrium. $\varepsilon^*$ is equal to $(1 - \alpha^*) * 1000$ (Gonfiantini, 1986).

Under natural conditions, the actual isotopic composition of water vapour is significantly more depleted than the values predicted using equilibrium enrichment factors. The difference between the total enrichment factor ($\varepsilon$) and the equilibrium enrichment factor ($\varepsilon^*$) is called as excess separation factor or kinetic enrichment factor ($\Delta\varepsilon$). The kinetic enrichment factor is defined by Craig and Gordon (1965) as follows:

$$\Delta\varepsilon = (1 - h)\left(\frac{\rho_i}{\rho} - 1\right)$$

where h, is the relative humidity normalised to the liquid surface temperature, and $\rho_i$ and $\rho$ are the transport resistance of the rarer and common isotopic water species in air. Attempts to evaluate the kinetic enrichment factor has been made Gat (1970) through field evaporation pan experiments, by Merlivat (1978) through laboratory experiments and by Vogt (1976) through wind tunnel experiments. Gonfiantini (1986) proposed 14.2 and 12.5 as the values of $(\rho_i/\rho)$ for oxygen and hydrogen isotopes, respectively.

Zimmermann and Ehhalt (1970), Zimmermann (1979) and a few other investigators made use of deuterium isotopes in lake studies. They contended that in the case of deuterium, the kinetic enrichment effect is small and it facilitates in avoiding complications that arise due to estimation of mean relative humidity values. However, Zuber (1983) showed that the kinetic effects in the case of deuterium differs very much in field conditions from that of laboratory controlled experiments. His findings confirmed the earlier reports of Gat (1970) on the basis of evaporation pan experiments in Lake Tiberias study.

### 2.1.3 Isotopic composition

The isotopic composition of atmospheric moisture, and consequently precipitation, exhibits a broad spectrum of spatial and temporal variation. Several investigators (Dansgaard, 1953, 1954; Epstein and Mayeda, 1953; and Friedman, 1953) attempted to study the natural abundance of $\delta^{18}O$ and $\delta D$ in meteoric waters. The relationship between $\delta^{18}O$ and $\delta D$ in freshwaters was first noted by Friedman (1953). Using IAEA/WMO database (Global Network of Isotope in Precipitation) on monthly composite samples of precipitation developed Global Meteoric Water Line (GMWL) having the equation $\delta D = 8*\delta^{18}O + 10$. Where 8 is the slope and 10 is the y-intercept of $\delta D$ - $\delta^{18}O$ line of fresh global meteoric waters (Dansgaard, 1964 and Yurtsever and Gat, 1981).

Currently, the equation of the Global Meteoric Water Line (GMWL) constructed on the basis of the long-term weighted mean hydrogen and oxygen isotopic ratios collected through IAEA/WMO database is $\delta D = 8.2\ \delta^{18}O + 11.27$ (Rozanski et al., 1993).

The above equation is identical to the earlier equations of the GMWL proposed by Dansgaard (1964) and Yurtsever and Gat (1981) and also confirms that Craig's equation ($\delta^{2}H = 8\ \delta^{18}O + 10$ ‰ SMOW) is good approximation of the points representing average isotopic composition of global freshwaters. The reasons for the deviations in the $\delta^{18}O$ - $\delta D$ relationship at different stations is because of the differences in the initial vapour isotopic composition, initial dew point temperature, degree and way of cooling, and kinetic effects during the fall of rain drops (Dansgaard, 1964).

On the basis of extensive groundwater samples collected in the northern India, the slope of the MWL for the Indian monsoon, proposed by Bhattacharya et al. (1985) is 7.2 which is distinctly different from 8.4 proposed by Datta et al (1991) on the basis of long-term annual weighted mean values of isotope ratios in the precipitation samples collected at New Delhi. The variation in the slope of the MWL indicates that the relation between $\delta^{18}O$ and $\delta D$ is more complex in the case of Indian monsoon precipitation (Despande et al. 2003).

**'d' excess parameter**

The 'd' excess parameter or d-index means the surplus deuterium relative to the Craig's Line (Dansgaard, 1964). The characteristics of the d-index are a) equilibrium processes do not change the d-index of any of the phases, b) non-equilibrium evaporation from a limited amount of water reduces the d-index of the water as long as the exchange is not a dominating factor, c) d-index of the water will remain constant during a non-equilibrium evaporation from an infinitely large and well mixed reservoir, while d-index of vapour will be positive and increase with the rate of reaction, and d) The averaged d-index of precipitation at a given locality reflects the rate of evaporation in the source area.

### 2.1.4 Groundwater dating

Groundwater age corresponds to the travel time from the time of recharge of groundwater to the time of its sampling. At the time of its recharge, tritium ($^{3}H$) and $^{14}C$ concentration in the infiltrating water is generally highest due to its continuous interaction with the atmospheric activity, which is the source for the naturally produced $^{3}H$ and $^{14}C$. Once infiltrated, these isotopes become unsupported and start decaying and their concentration in water start decreasing. The travel time of groundwater is calculated from the rate of decay of these isotopes. The maximum tritium in groundwater is considered as a value close to that of the tritium content in the infiltrating water in the recharge area. While $^{14}C$ is expressed in term of percentage modern carbon with 100% as the concentration in the atmosphere (100pmc = 13.56 dpm per gram of carbon), $^{3}H$ is expressed in Tritium Units (1TU=0.118 Bq/kg of water). Although, $^{14}C$ in the infiltrating water, is expected to be close to atmospheric value but several times it is not the case. This is due to the dilution of modern carbon with $^{14}C$ free carbonates present in the soils. Similarly, tritium in the atmosphere varies in the order of 10 to $10^{3}$ TU. The high concentrations of the order $10^{3}$ TU were generated during early 1960's due to the thermonuclear bomb tests, the effect of which is diminishing after the moratorium of atmospheric tests.

## 2.2 Isotopic Technique for Hydrograph Separation

### 2.2.1 Two component mixing model

The flow in a river at any point is generally a mixture of two components viz., the base flow integrated upto the location of interest and the runoff generated in response to a precipitation event. If these two components are isotopically different, the isotopic composition of the stream water at the point of interest may be between these two values. The extent of change is a function of proportion of runoff to the baseflow. This can be expressed by the following equations which conform to the law of mass conservation:

$$m_r = m_1 + m_2 \tag{1}$$

$$m_r C_r = m_1 C_1 + m_2 C_2 \tag{2}$$

where m is the quantity of components expressed in fraction, C is the tracer concentration, the subscript r denote the stream admixture at the point of interest, and the subscripts 1 and 2 denote the two components that contribute to the stream. If the stream discharge data is available, then the actual quantity of components could be calculated. It expressed as a fraction, $m_r$ is equal to one and the $m_1$ and $m_2$ is a ratio to the total discharge at a any point of time. Therefore, rewriting the equation (1), we get:

$$m_1 = 1 - m_2 \tag{3}$$

Substituting equation (3) in (2) and rearranging, we get:

$$m_2 = \frac{C_1 - C_r}{C_1 - C_2} \tag{4}$$

Equations (1) and (4) could be used to compute the fraction of the two components of the stream flow at a given point in space and time. However, the two component mixing models can be successfully used for hydrograph separation only if the following assumptions are valid (Sklash and Farvolden, 1982):

a) the isotopic composition of the two end members be unique or the variations are known and well documented.
b) the isotopic composition of the end members are significantly different, and the difference larger than the analytical precision of the mass spectrometer, and
c) the contributions from the vadose water and from the surface detentions or storage are negligible during the investigation.

### 2.2.2 Three component model

The investigation by Kennedy et al. (1986) and De Walle et al. (1988) indicate that in certain cases the assumption that only two components exist may not be valid. In such cases, the isotopic value of the admixture may fall outside the mixing line defined by the two suspected end members. The third component in the above cases is often found to be soil water or in some cases channel precipitation. The effect of a summer rainfall event on the stream flow process was studied by Pionke et al.(1988) in a small Pennsylvania hill watershed. They found that during a single storm event, the near stream groundwater table raises without substantially affecting the regional water table. In this hydrologic process that affect streamflow volume and quality, three components viz. channel precipitation, surface runoff and groundwater are initiated sequentially. They suggested that the dominant component of the stream flow also changes during the storm event.

The separation of the hydrograph of the stream generated by three components can be carried out using the following equation of the type proposed by De Walle et al. (1988), provided if contribution of one of the components is known:

$$\frac{Q_1}{Q_r} = \left(\frac{C_r - C_3}{C_1 - C_3}\right) - \frac{Q_2}{Q_r}\left(\frac{C_2 - C_3}{C_1 - C_3}\right)$$

Where Q is the discharge (in $M^3$ or M), C is the tracer concentration and subscript r is the admixture or the stream at the sampling point, subscripts 1, 2 and 3 represent the three end members contributing to the flow.

In the absence of quantity information on the contribution of any of the components trilinear graphical technique could be adopted. Hinton et al. (1994) made use of $^{18}O$ and $SiO_2$ data pertaining to the three components viz. soil water, new water and till water, in a microwatershed located in the Harp lake catchment, Ontario, Canada. They proposed the following set of equations that can be solved to determine the relative contribution of the three components of the stream flow, if two tracers are used:

$$\frac{Q_1}{Q_r} = X_n = \frac{[(C_r^a - C_2^b)(C_3^a - C_2^a) - (C_r^a - C_2^a)(C_3^b - C_2^b)]}{[(C_1^b - C_2^b)(C_3^a - C_2^a) - (C_1^a - C_2^a)(C_3^b - C_2^b)]}$$

$$\frac{Q_2}{Q_r} = \left(\frac{C_r^a - C_3^a}{C_2^a - C_3^a}\right) - X_n\left(\frac{C_1^a - C_3^a}{C_2^a - C_3^a}\right)$$

$$\frac{Q_3}{Q_r} = \left(\frac{C_r^a - C_2^a}{C_3^a - C_2^a}\right) - X_n\left(\frac{C_1^a - C_2^a}{C_3^a - C_2^a}\right)$$

Where, Q is the discharge (in $M^3$ or M), C is the tracer concentration, superscripts a and b denote the two tracers used for the study, and subscripts 1,2,3, and r denote the three inflow components and the river, respectively. Further, Hinton et al. (1994) suggested that for a successful application of three component mixing model, the following assumptions should be valid:

a) there are only three sources that contribute to the streamflow,
b) isotopic and/or chemical concentration of the sources must be distinct,
c) the concentration of the three suspected sources should not be collinear for either of the tracers,
d) the concentration (or index) of each suspected source should be constant during the event being studied, and
e) the tracers mix conservatively.

### 2.3 Sample Collection

Although, the river Bhagirathi originates from the Gangotri glacier, other small stream are also feeding the river as it flows downstream. Therefore, to understand the spatial variability of different component of river discharge and isotopic variation in precipiataion the sampling sites were establised at various altitude from Gangotri to Devprayag (Fig 2.1, Table 2.1 and 2.2).

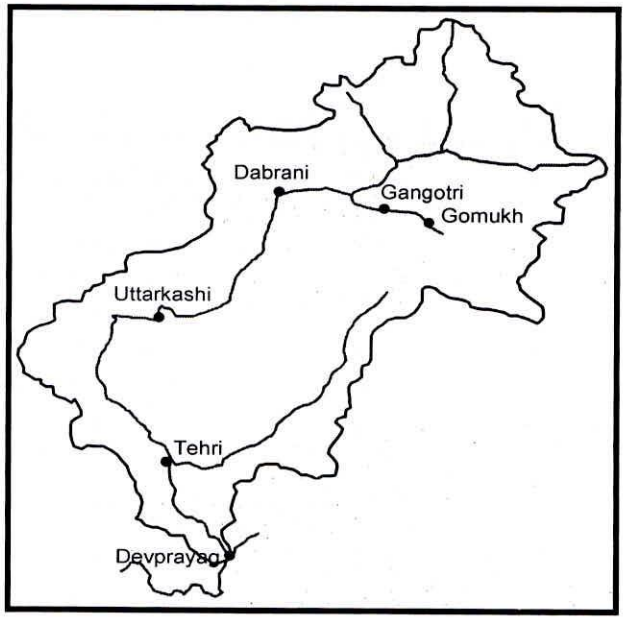


Fig. 2.1 Site of sampling along the Bhagirathi River.

Table 2.1 Rainfall station in the Bhagirathi River basin.

| Sites | Altitude(m) | Details of sites |
|---|---|---|
| Devprayag | 465 | Rain gauge installed by CWC at the outlet of the basin, monthly integrated sample and in rainy season daily samples were collected |
| Tehri | 640 | Rain gauge installed by CWC at the outlet of the Dam |
| Uttarkashi | 1140 | Rain gauge installed by NIH at PWD guest house |
| Maneri | 1170 | Rain gauge installed by Forest Department near the Maneri spring |
| Dabrani | 2050 | Rain gauge installed by NIH near the river bridge |
| Gangotri | 3053 | Rain gauge installed by NIH at PWD guest house |

Table 2.2: Location of river water sampling sites along the Bhagirathi River

| Site | Altitude (m) | Frequency of sampling |
|---|---|---|
| Devprayag | 465 | Fortnightly, weekly and daily river water samples collected |
| Tehri | 640 | Fortnightly and weekly river water samples collected |
| Sirayi | 646 | Fortnightly, weekly and daily river water samples collected during 2004-2005, site was closed due to submergence in the reservoir. |
| Simlasoo | 648 | Fortnightly, weekly and daily river water samples collected during 2004-2005, site was closed due to submergence in the reservoir. |
| Dharasu | 850 | Fortnightly, weekly and daily river water samples collected |
| Uttarkashi | 1140 | Fortnightly, weekly and daily river water samples collected |
| Dabrani | 2050 | Fortnightly, weekly and daily river water samples collected from April to October in each year. |
| Gangotri | 3053 | Fortnightly, weekly and daily river water samples collected |

The selection of river sampling site was made on the basis of altitude and availability of discharge measurement stations. From these sites, fortnightly sampling during non-monsoon months and weekly to daily sampling during monsoon months have been carried out for stable isotope ($\delta^{18}O$, $\delta D$) analysis in the case of river and precipitation. For the analysis of tritium, fortnightly sampling of river and monthly sampling of precipitation were coducted. 60 ml of water sample was collected fo $^{2}H$ and $^{18}O$. Samples were also collected from river, spring, shallow and deep bore wells for the analysis of major cations and anions.

Groundwater in the study area appears in the form of seepages and springs. Some of the existing India mark hand pumps were selected for the sampling of the groundwater from the deeper zones. To study the spatial and temporal variations of isotopes ($^{2}H$, $^{18}O$ and $^{3}H$) in ground water, groundwater samples were collected during premonsoon, monsoon and postmonsoon seasons from the handpumps and springs located at various altitudes. For understanding the temporal variations of isotopes in handpums at Uttarkasi, Devprayag and Tehri were selected for sampling on a monthly basis. A person was engaged for sampling work at each site and adequate training was provided on sample collection procedure.

### 2.3.1 Collection of rain water sample

Ordinary rain gauge was installed at each sites for the collection of rainwater (Plate 2.1). Rainwater sampling was carried out on the monthly basis by integrating daily rain samples for a period June 2004 to Oct 2006. A monthly sample represents the rain collected over the period beginning from the first day until the end of the month. The rainwater from the rain gauge was collected daily into a large capacity (~5 l) container having tight inner lid and a screw cap. At the end of the month, the integrated monthly rainwater sample was drawn from the total volume of water collected over the entire month. From the integrated sample, 60 ml of water was collected for stable isotopes and 500 ml for environmental tritium. Diffusive and evaporative losses from the rain gauges and storage containers were avoided by the use of liquid paraffin or silicon oil. For hydrograph separation purpose daily sampling of rainfall was also carried out.

### 2.3.2 River water sampling

River samples were collected from the mid-stream sections or flowing portions (Plate 2.2). Standing water was avoided. Sampling at the confluence of Bhagirathi and Alaknanda was done downstream of the confluence with great care due to the problems of incomplete mixing. River water samples were collected from each site on daily, weekly and fortnightly basis (Table 2.1).

### 2.3.3 Groundwater sampling

Groundwater samples were collected from springs, shallow and deep hand pumps for isotope and chemical analysis. Spring samples were collected as close as possible to the discharge point. Groundwater samples were collected from the hand pumps after purging the standing water column for about 15 minutes. 60 ml water samples for $^{2}H$, $^{18}O$ analysis and 500ml of the sample for $^{3}H$ were collected. In situ measurements like water temperature, pH, conductivity along with all other relevant site information were also recorded.

### 2.3.4 Snow and ice sampling

Under a DST project of NIH, Roorkee, snow and ice samples were collected from the Gangotri glacier. Snow samples were collected in sealable plastic bags or containers. The snow sampling is carried out shortly after every snowfall in order to avoid sublimation, re-crystallization, redistribution, melting or mixing with rainfall, which alter its isotopic composition. Once, the snow was melted in the containers, the water was transferred to plastic bottles for $^{2}H$, $^{18}O$ and $^{3}H$ analyses. Since Gaumukh is inaccessible during winter due to heavy snowfall, melt water during May to June was collected as the representative sample of snow for winter season. A few ice samples were collected using a hand auger from the upper part of the glacier.

## 2.4 Measurement of $\delta^{18}O$ and $\delta^{2}H$

Measurement of $\delta^{2}H$ in water requires preparation of a representative hydrogen gas from the water sample because normally a mass spectrometer cannot analyze water directly. At present, there are two basic procedures to prepare representative hydrogen gas: 1) reduction of water to hydrogen gas by reaction with hot metal, and 2) isotopic equilibration of tank hydrogen with the water sample. In the present study, equilibration method is adopted for the measurement of $^{2}H$ and $^{18}O$.

### 2.4.1 Equilibration with $H_2$ gas

In this method, a small amount of hydrogen gas is equilibrated with the water sample in a closed bottle, wherein isotopic exchange takes place and the D/H ratio of the hydrogen gas is changed to a value that of the water, but being off-set by a certain amount of fractionation which is determined by the temperature of equilibration. At 25 °C the fractionation is large – the hydrogen gas is depleted by about 737.5 ‰ relative to water.

The temperature coefficient is also large (about -6 ‰ per °C) and that makes it essential to keep precisely the temperature to be constant. This is one of the simple viable methods at present that allow for fully automatic determination of D/H ratio in water samples. In addition, commercial systems are available whereby large number of samples can be processed in a batch. It is also to be noted that the same extraction system can be used for both D/H ratio as well as $^{18}O/^{16}O$ ratio in water.

In the facility available at NIH, Roorkee, a set of 60 samples are loaded in small vials (~ 10 ml) provided with rubber septum to make the bottle airtight. In each bottle, a few beads of platinum catalyst (Hokko beads) are put which are light and being hydrophobic stay on top of the water surface. In principle, the catalyst is re-useable. The set is put in 60 holes in an aluminum block arranged in the form of x-y matrix with each hole having a set of precise x-y value addressable by the control program. Next, the bottles are flushed with pure tank hydrogen by an arrangement using Gilson hypodermic needle which is inserted into the rubber septum by computer control. 60 bottles are flushed one after another and filled with the gas at a pressure slightly above the atmosphere. The temperature of the aluminum block is accurately maintained (at 35 °C) since the fractionation is highly temperature sensitive (decreases by 6 ‰ for 1 °C rise). The flushing of the space above the water removes little amount of water along with the air but does not impact the analysis since standards are also treated exactly the same way. In general, several standards are placed in the array to take care of minor temperature variations across the block. For calibration, IAEA standards (VSMOW, VSLAP and GISP) are occasionally used against the internal water standards. The precision of the measurements can be optimized by choice of an appropriate sample size. Normally, laboratories use amounts between 1 to 5 ml. After a few hours the equilibration is complete and the gas can be extracted by expanding to the inlet of the mass spectrometer after scrubbing the moisture by –100 °C trap.


Plate 2.1 Rain gauge location at Gaumukh and Gangotri.

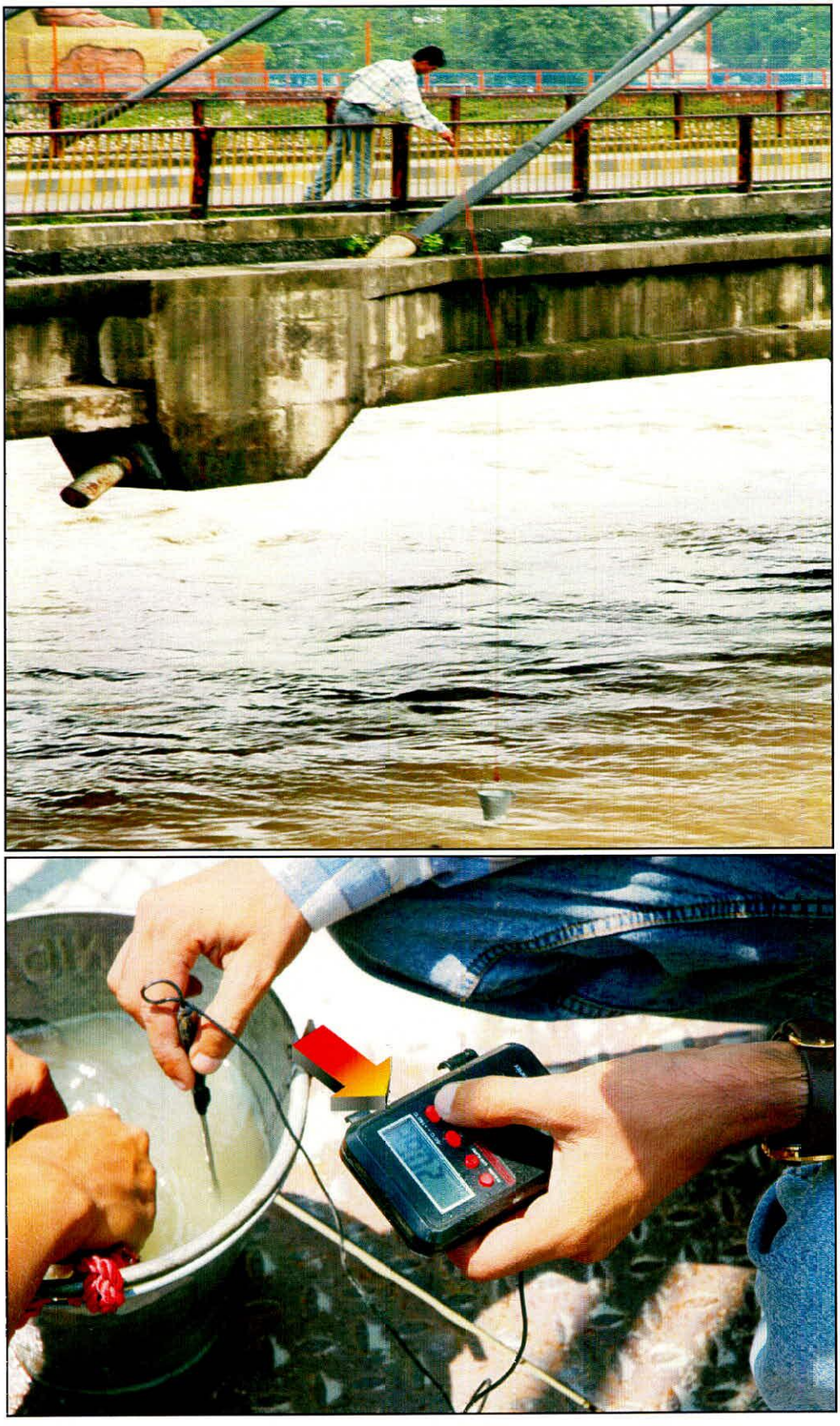

Plate 2.2 Sample collection from the middle of River and measurement of physical parameter.

### 2.4.2 Equilibration with $CO_2$

The most common method to measure the $^{18}O/^{16}O$ ratio in a water sample is to equilibrate carbon dioxide gas with the water sample at a 40°C temperature and to measure subsequently the isotopic composition of the carbon dioxide gas. In practice, a standard water whose isotopic ratio is known, is analyzed in parallel with the samples. The raw data are converted using the isotopic ratio of the standard

The principle of the method is similar to that of D/H ratio described earlier For calibration, IAEA standards (VSMOW, VSLAP and GISP) are occasionally used against the internal standards.

### 2.5 Tritium Measurement

500ml of the water sample was distilled (called primary distillation) in the laboratory to remove all dissolved salts. The various ions that are naturally found in water ($Cl^-$, $SO_4^{--}$, $CO_3^{--}$, $Mg^{++}$, $Na^+$, $K^+$, etc) could interfere the electrolysis process (i.e. produces gases at either the anode or cathode other than oxygen or hydrogen) and also corrode the mild steel electrodes used for tritium enrichment.

After primary distillation, samples were enriched by electrolysis. The electrolytic reduction was done to concentrate the tritium, since the samples contain mainly HHO and HTO molecules. By passing electric current through a conducting water solution, the bonds of the water molecules broke with the evolution of hydrogen and oxygen gases. The temperature of the sample was maintained between 0°C to 5°C in order to achieve maximum fractination or enrichment of HTO. After the electrolytic proces, 500ml samples was reduced to 25 ml. This enriched samples were again distilled and collected in 20ml glass vials. These samples were treated chemically as per standard manual of laboratory. The treated samples along with the standards were counted using an ultra low level Quantulus (Wallac model 1220) for the measurement of tritium activity. The measured tritium concentration were corrected and express in term of TU.

### 2.6 Measurement of Mojor Ions

More than 350 water samples including pre and post monsoon groundwater and river water samples from all the sampling locations were collected for major cations and anions measurements.

Weekly to fortnightly samples from the Bhagirathi river at Dabrani aand monthly groundwater and spring samples were also collected during 2004-2005 and analysed for the major ions. For anion analysis, 20ml of water samples were filtered and stored in polyethene bottles, where as another set of same samples were analysed to pH < 2 by adding ultra pure conc. $HNo_3$ for cation measurements. Anions viz. $Cl^-$, $So_4^{2-}$, $No_3^{2-}$ and $F^-$ and cations viz. $Na^+$, $Ca^{2+}$, $Mg^{2+}$ and $K^+$ were analysed in BARC, mumbai using Ion Chromotography (Dionx, DX-500) by employing elutrochemical detector (ED-40) in conductivity mode. The accuracy of the chemical ion data was calculated using change balance equation given below and the Change Balancing Error (CBE) calculated using equation (a) were within ±10%

$$CBE(\%) = \frac{meq(cations) - meq(anions)}{meq(cations) + meq(anions)} * 100$$

# CHAPTER 3

## ISOTOPIC CHARACTERIZATION OF PRECIPITATION

### 3.0 Isotopic Composition of Precipitation

Precipitation is the ultimate source of water in all the river basins and long term sampling of precipitation help to construct the local meteoric- water line (LMWL) on a $\delta^2H$ versus $\delta^{18}O$ graph, which is critical baseline against which the stable isotope ratios of water can be compared and the processes affecting them can be deduced.

Environmental isotope data of precipitation from 2004-2006 is shown in Table 3.1 and the monthly variation of $\delta^{18}O$ in precipitation collected at various station of Bhagirathi basin is shown in Figure 3.1. It is seen that the $\delta^{18}O$ of precipitation are enriched during pre monsoon (April to June) and post monsoon (October to November) while depleted values occur during the summer monsoon period (July to September) and winter monsoon period (December to March).

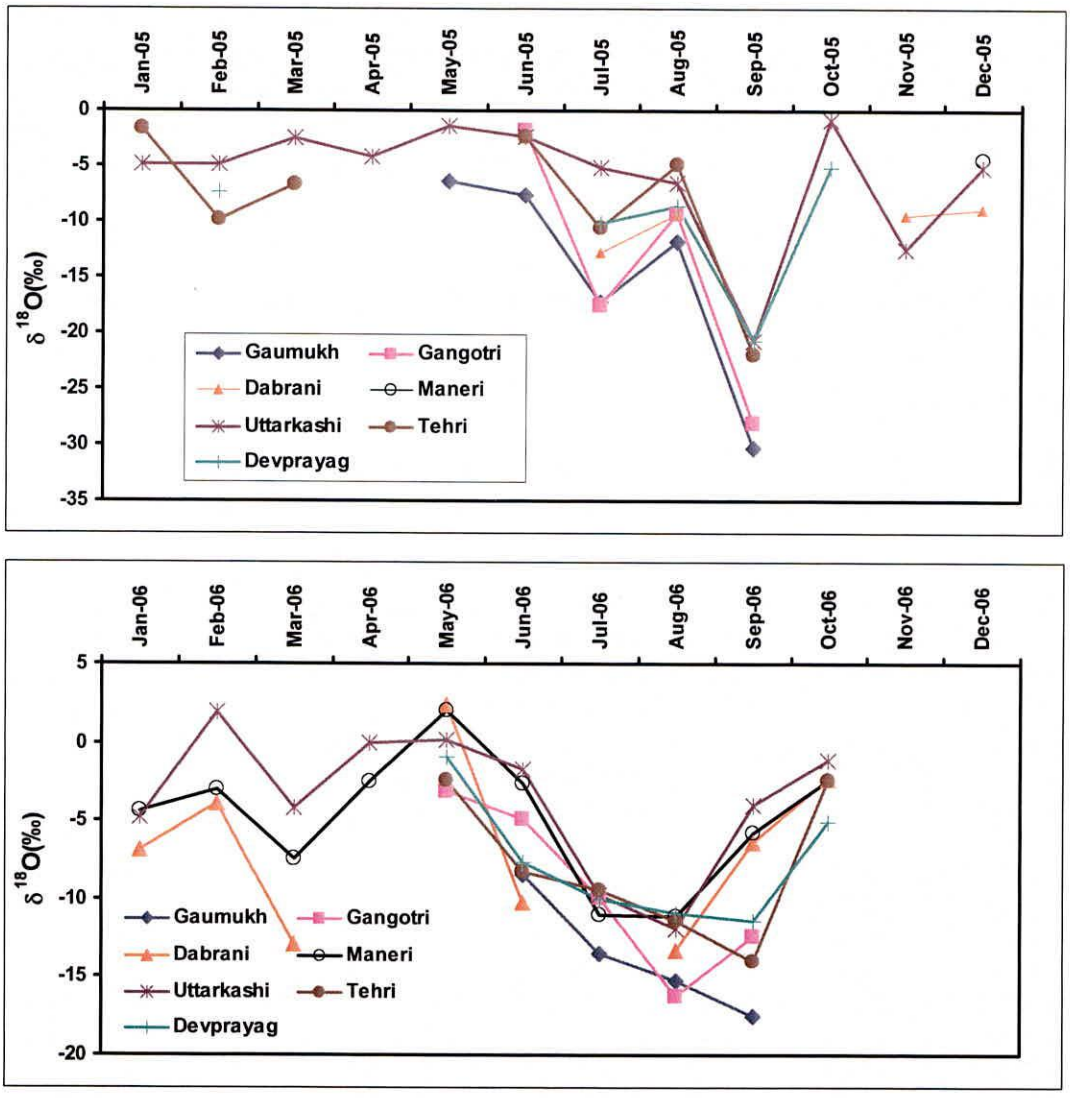


Fig 3.1 Variation of monthly $\delta^{18}O$ in precipitation at different stations of Bhagirathi basin (2004-2006).

Table 3.1: Average $\delta^{18}O$ and $\delta D$ of precipitation during the study period.

| Months | Gaumukh | | Gangotri | | Dabrani | | Maneri | | Uttarkashi | | Tehri | | Devprayag | |
|---|---|---|---|---|---|---|---|---|---|---|---|---|---|---|
| | $\delta^{18}O$ | $\delta D$ | $\delta^{18}O$ | $\delta D$ | $\delta^{18}O$ | $\delta D$ | $\delta^{18}O$ | $\delta D$ | $\delta^{18}O$ | $\delta D$ | $\delta^{18}O$ | $\delta D$ | $\delta^{18}O$ | $\delta D$ |
| May-04 | -2.6 | -6.2 | -6.2 | | | | | | | | | | | |
| Jun-04 | -6.7 | -40.4 | *-7.6* | -37.6 | | | | | -2.5 | -5.7 | | | -3.1 | -14.5 |
| Jul-04 | -5.5 | -26.0 | -6.7 | -40.7 | | | | | -2.4 | -6.5 | *-5.3* | -26.8 | -5.0 | -29.1 |
| Aug-04 | -17.5 | -128.5 | -14.6 | -109.8 | -11.2 | -79.6 | | | *-11.1* | -78.0 | | | *-10.7* | -79.8 |
| Sep-04 | -22.2 | -165.7 | -19.9 | -141.8 | | -39.1 | | | -1.5 | -2.8 | *-10.4* | -75.2 | -4.4 | -26.3 |
| Oct-04 | -16.5 | -123.3 | -17.4 | -119.6 | -13.6 | -96.7 | | | -6.4 | -36.3 | 0.5 | 5.0 | -3.0 | -12.3 |
| Nov-04 | | | | | | | | | | | | | | |
| Dec-04 | | | | | | | | | -4.1 | -13.0 | -1.3 | 5.0 | -3.1 | -13.1 |
| Jan-05 | | | | | -12.0 | -84.0 | | | -4.8 | -19.3 | *-1.7* | -7.2 | -9.8 | -66.5 |
| Feb-05 | | | | | -12.0 | -84.0 | | | -4.9 | -18.1 | *-9.8* | -68.0 | -6.8 | -42.6 |
| Mar-05 | | | | | -2.5 | -8.3 | | | -2.5 | -0.9 | -6.6 | -26.3 | -4.0 | -20.3 |
| Apr-05 | | | | | -1.0 | 3.6 | | | -4.1 | -17.3 | | | -4.0 | -20.3 |
| May-05 | -6.4 | -31.6 | | | -2.0 | -4.4 | | | -1.4 | 14.1 | | | -1.0 | 3.6 |
| Jun-05 | -7.6 | -40.6 | -1.8 | 4.9 | -4.9 | -27.5 | | | -2.4 | -0.3 | *-2.3* | -9.5 | -1.0 | 3.6 |
| Jul-05 | -17.2 | -124.7 | -17.6 | -124.3 | -16.6 | -120.3 | | | -5.2 | -24.4 | -10.6 | -78.0 | -12.3 | -86.4 |
| Aug-05 | -11.8 | -81.2 | -9.3 | -68.9 | -10.2 | -69.7 | | | -6.6 | -46.9 | -4.9 | -26.0 | -9.6 | -64.9 |
| Sep-05 | -30.3 | -228.3 | -28.0 | -214.3 | -29.2 | -221.0 | | | -20.8 | -157.0 | -22.0 | -169.0 | -25.5 | -191.5 |
| Oct-05 | | | | | | | | | -0.8 | | | | -5.1 | -30.0 |
| Nov-05 | | | | | -9.5 | -53.2 | | | -12.5 | -90.0 | | | | |
| Dec-05 | | | | | -8.9 | -45.4 | -4.4 | -23.5 | -5.2 | -23.7 | | | | |
| Jan-06 | | | | | -6.8 | -35.3 | -4.4 | -20.3 | -4.8 | -16.9 | | | | |
| Feb-06 | | | | | -3.9 | -14.2 | -3.1 | -13.4 | 1.9 | 30.5 | | | | |
| Mar-06 | | | | | -12.9 | -90.0 | -7.4 | -44.8 | -4.2 | -19.1 | | | | |
| Apr-06 | | | | | | | -2.5 | -19.3 | 0.0 | 7.6 | | | | |
| May-06 | | | -3.1 | -13.2 | 2.5 | 26.0 | 2.0 | 9.0 | 0.1 | 14.6 | -2.4 | -27.0 | -0.9 | -4.8 |
| Jun-06 | -8.4 | -53.7 | -4.8 | -30.2 | -10.2 | -71.6 | -2.6 | -18.4 | -1.7 | -5.3 | -8.2 | -60.8 | -7.7 | -61.1 |
| Jul-06 | -13.4 | -91.1 | -9.9 | -72.4 | -13.3 | -99.3 | -11.0 | -76.3 | -9.7 | -62.2 | -9.4 | -61.6 | -10.9 | -66.4 |
| Aug-06 | -15.3 | -107.1 | -16.3 | -116.2 | -6.3 | -34.6 | -11.1 | -85.5 | -11.9 | -81.3 | -11.4 | -79.4 | -11.4 | -84.7 |
| Sep-06 | -17.6 | -128.4 | -12.4 | -96.6 | -2.3 | -11.4 | -5.8 | -34.2 | -4.0 | -20.5 | -14.0 | -102.6 | -5.1 | -23.0 |
| Oct-06 | | | | | | | -2.4 | -14.1 | -1.2 | -10.2 | -2.4 | -3.3 | | |

The isotope data of precipitation shows seasonal variation in $\delta^{18}O$ and $\delta D$, which indicates the change in source of moisture. The $\delta^{18}O$ and $\delta D$ values in winter precipitation are relatively enriched in comparison to summer monsoon precipitation. The most depleted $\delta^{18}O$ are found in summer monsoon precipitation during 2004, 2005 and 2006 (Table 3.2). The different isotopic signature of rainfall falling during summer monsoon reveals that source of moisture for precipitation in the months of July, August and September is different than in May and June. The depleted value in July, August and September confirms that the precipitation occur in these months due to the continental and altitude effects of SW Monsoon vapour. The source of moisture during the summer months seems to be local evapotranspiration. The isotopic enrichment during premonsoon may be due to the secondary evaporation of rain during the fallout.

Table 3.2: Seasonal aveighted $\delta^{18}O$ in precipitation of Bhagirathi River basin

| Season | $\delta^{18}O$(‰) | | |
|---|---|---|---|
| | 2004 | 2005 | 2006 |
| April-June | -4.8 | -3.1 | -3.2 |
| July-September | -9.9 | -16.0 | -11.3 |
| October-November | -9.4 | -6.9 | -2.6 |
| December-March | - | -5.7 | -5.0 |

In all the seasons, $\delta^{18}O$ is found to be depleting with respect to the altitude (altitude effect). Also at the same station, the depletion of $\delta^{18}O$ has been noticed from July to September as the amount of precipitation increases (amount effect). Continuous depletion of $\delta^{18}O$ values in precipitation from the month of July (onset of monsoon) to the end of monsoon (September and October) occur if good amount of precipitation is occurring in all these months (Fig 3.2). For example in year 2005, the maximum amount of rainfall was recorded in July, while the $\delta^{18}O$ continue to deplete till September even though the amount of rain reduces considerably. This probably reveals that once the monsoon cloud reaches the hilly terrain, fall out process starts; the isotopic signature become depleted and depletion continues for the remaining monsoon period as the clouds remain there. The monthly variation of isotopic signature is very much useful in hydrological studies. The event based variation has also been noticed which is useful in separating the runoff components generated during various storm events.

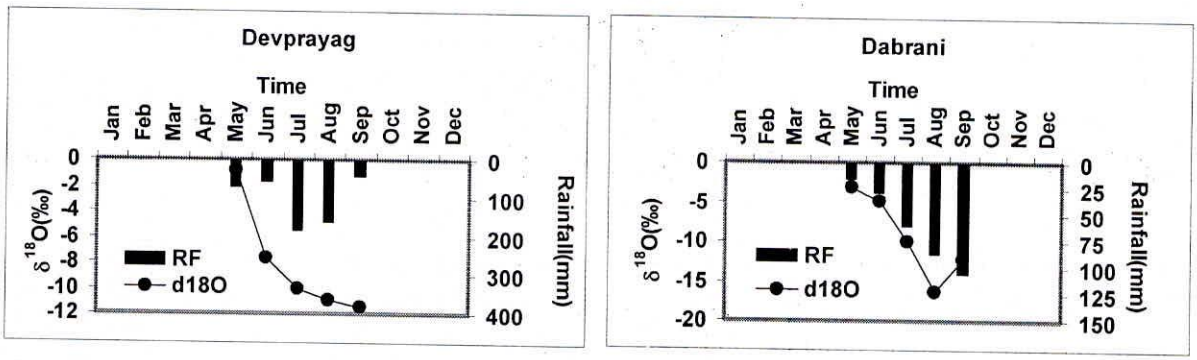


Fig. 3.2: $\delta^{18}O$ with rainfall at Devprayag and Dabrani Station (year 2005).

Meteoric water line is the best fit line of the $\delta^{18}O$ and $\delta D$ content of the precipitation. The LMWL is controlled by the local climatic conditions and the source of the vapour mass, particularly the slope of the line is influenced by the secondary evaporation. The best fit line developed using monthly data of all stations collected during 2004-2006 are given below.

The statistical analyses using the monthly isotopic data of precipitation in the Bhagirathi basin (Table 3.3) yielded the following equations for the study area:

$$\delta D=(8.17\pm0.1)\delta^{18}O + (11.27\pm0.6) \text{ GMWL} \quad (3.1)$$

$$\delta D=(8.0 \pm 0.1)*\delta^{18}O + (11.5 \pm 1.1),\ R^2 = 0.98,\ n = 129 \text{ (LMWL)} \quad (3.2)$$

$$\delta D=(7.4 \pm 0.5)*\delta^{18}O + (8.3 \pm 2.6),\ R^2 = 0.90,\ n = 34 \text{ (Pre-monsoon)} \quad (3.3)$$

$$\delta D=(8.0 \pm 0.1)*\delta^{18}O + (11.3 \pm 1.7),\ R^2 = 0.99,\ n = 52 \text{ (Monsoon)} \quad (3.4)$$

$$\delta D=(7.4 \pm 0.3)*\delta^{18}O + (7.5 \pm 2.7),\ R^2 = 0.98,\ n = 15 \text{ (Post monsoon)} \quad (3.5)$$

$$\delta D=(8.0 \pm 0.3)*\delta^{18}O + (15.4 \pm 1.9),\ R^2 = 0.96,\ n = 28 \text{ (Winter)} \quad (3.6)$$

The slope and the y-intercept of the best fit line of Bhagirathi River basin (Eq. 3.2) are close to those of precipitation defining the global meteoric water line (GMWL) reported by Yurtsever and Gat (1981). The similarity in slope and the y-intercept between LMWL and GMWL indicates that the

precipitation at Bhagirathi basin did not suffer any kinetic effect during the rainfall. The similarity in d-excess for the three consecutive years (Table 3.3) indicates that origin of vapour sources and other climatic parameters (temperature, humidity etc) did not significantly vary. Otherwise also, monthly weighted values can be considered as the representative values as they are collected from the Bhagirathi basin.

Table 3.3 : Annual averaged isotopic composition of precipitation based on samples collected at different altitudes in the Bhagirathi basin for 2004-2006.

| Location | Elevation (m) | Year | □'□O‰ | □D‰ | d-excess |
|---|---|---|---|---|---|
| Gaumukh | 3800 | 2004 | -15.0 | -106.7 | 14 |
| | | 2005 | -19.7 | -144.7 | 13 |
| | | 2006 | -15.4 | -108.8 | 15 |
| Gangotri | 3053 | 2004 | -13.7 | -97.5 | 12 |
| | | 2005 | -18.3 | -135.8 | 11 |
| | | 2006 | -12.9 | -95.1 | 8 |
| Dabrani | 2050 | 2004 | -11.2 | -79.6 | 10 |
| | | 2005 | -18.7 | -137.0 | 13 |
| | | 2006 | -9.8 | -66.9 | 11 |
| Maneri | 1250 | 2004 | | | |
| | | 2005 | | | |
| | | 2006 | -9.3 | -65.3 | 9 |
| Uttarkashi | 1140 | 2004 | -5.0 | -29.1 | 11 |
| | | 2005 | -10.8 | -76.1 | 11 |
| | | 2006 | -8.5 | -54.7 | 14 |
| Tehri | 1050 | 2004 | -7.9 | -51.0 | 12 |
| | | 2005 | -12.5 | -87.8 | 12 |
| | | 2006 | -11.6 | -81.1 | 12 |
| Devprayag | 465 | 2004 | -6.7 | -45.1 | 9 |
| | | 2005 | -15.8 | -114.3 | 12 |
| | | 2006 | -9.1 | -58.0 | 15 |

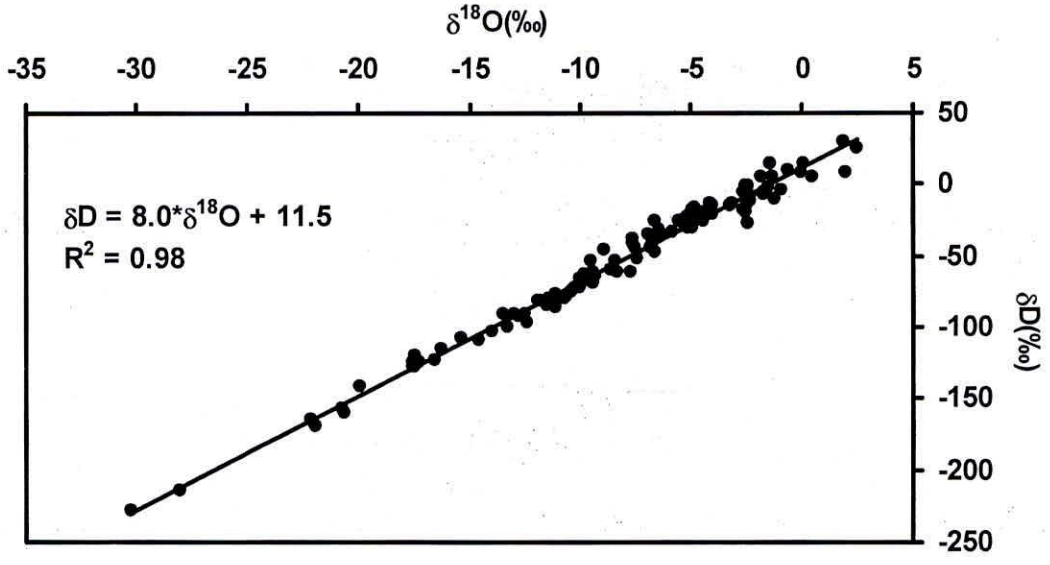


Fig. 3.3: Meteoric water Line for Bhagirathi River basin based on monthly data.

Equation 3.2 represents the LMWL of precipitation during the monsoon period i.e. months of July, August and September. The equation compares very well with that proposed by other investigators (Bhattacharya et al., 1985; Seigel and Jenkins 1987; Krishnamurthy and Bhattacharya, 1991; and Bartarya et al. 1995). The slope of the MWL for Indian monsoon, proposed by Bhattacharya et al. (1985) as 7.2 on the basis of extensive groundwater samples collected in the northern India, is distinctly different from 8.4 proposed by Datta et al (1991) on the basis of long-term annual weighted mean values of isotope ratios in the precipitation samples collected at New Delhi and the finding of the present study. Since 7.2 slope is based on groundwater samples it could be due to evaporation of groundwater. But we have not found any evaporation effect in groundwater. The variation in the slope of the MWL indicates that the relation between $\delta^{18}O$ and $\delta D$ is more complex in case of Indian monsoon precipitation. The difference in the slope could be due to some evaporation effect on precipitation which recharges the groundwater in Bhattacharya et al. (1991). Bartarya et al. (1995) proposed an equation with a slope of ~7.1 and intercept of ~15 for Gaula basin of the Kumaun Himalayas. However, the equation by Bartarya et al. (1995) is not based on isotopic composition of monthly-integrated precipitation samples, but it is based on randomly selected individual storm events.

The lower value of slope and intercept have been found for premonsoon and postmonsoon season in comparison to monsoon and winter (Eqs. 3.3 to 3.6). When equations for various seasons are compared with LMWL, the change in slope as well as intercept can be explained, only if the effect of secondary evaporation during rainfall is considered. Bhattacharya et al. (1985), Krishnamurthy and Bhattacharya (1991) and Datta et al. (1991) have also reported the effect of secondary evaporation in the Indian precipitation. Ehhalt et al. (1963) reported that under dry conditions the re-evaporation of falling rain drops has an effect of obscuring the seasonal variations. Secondary evaporation effect on falling raindrops are visible in the Bhagirathi basin during the pre and post monsoon season. The partially evaporated rain is characterised by relatively higher $\delta^{18}O$ values and small to negative d excess.

The best fit line for the winter season is having a slope of 8 and y-intercept of 15.5. The y-intercept varies between 11 to 25, which is higher in comparison to the monsoon season precipitation value. As 38% of the annual precipitation in this region is derived from the westerlies (Western Disturbance) whose source is the Mediterranean Sea (Raina, 1977) with a characteristically higher d-excess (Gat and Carmi 1970). All along the path of the Western Disturbance (Iran, Afghanistan, Pakistan and Kashmir) the precipitation is characterised by high d-excess (Yurtsever and Gat 1981). Rozanski et al (1993) found that between $30^0$ and $40^0$ N, most of the precipitation show high deuterium excess (in the range 15 to 25‰). Thus the high values of deuterium excess in winter samples in Bhagirathi basin confirm that the vapour source is coming from the western disturbances. The lower d- excess values at Gaumukh, Gangotri and Uttarkashi during premonsoon season may be due to the contribution of moisture from the evaporation with in the Bhagirathi basin. The evaporation from the Maneri dam is the main source of moisture for Uttarkashi rainfall likewise high rate of evaporation from glacier due to the infrared radiation at high altitude are the probably main cause for higher d-excess values during pre monsoon period.

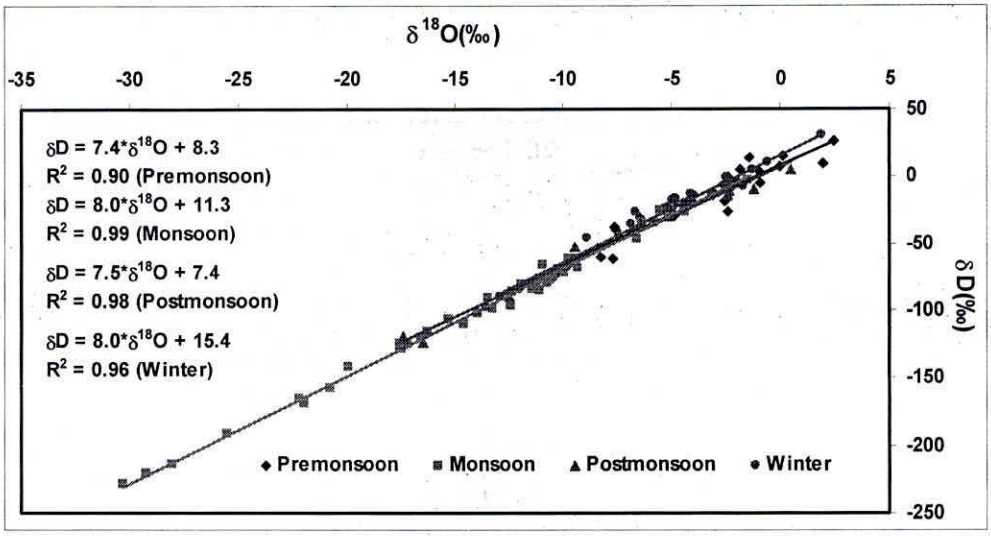


Fig. 3.4 : Seasonal variation of $\delta^{18}O$ and $\delta D$ for Bhagirathi River basin based on monthly data

The best fit line developed for all the stations (Eq. 3.7 to 3.13 ) reveals a slope of 8 and intercept of ~10 to 12 except at Maneri and Gaumukh. At Maneri, the slope is lower than the 8 and at Gaumukh it is higher than 8. A slope higher than 8 at Gaumukh appears to be mainly caused by the low air temperature and snow precipitation. Rozanski et al (1993) noted that for stations with substantial contribution of snow precipitation, higher deuterium excess values during winter may result from additional kinetic fractionation during snow formation (Jouzel and Merlivat, 1984). This could also lead to a slope greater than 8.

| | | |
|---|---|---|
| $\delta D=(8.2 \pm 0.1)*\delta^{18}O + (17.1 \pm 2.5)$, $R^2 = 0.99$, n = 15 | (Gaumukh) | 3.7 |
| $\delta D=(8.0 \pm 0.2)*\delta^{18}O + (12.7 \pm 3.6)$, $R^2 = 0.99$, n = 15 | (Gangotri) | 3.8 |
| $\delta D=(7.9 \pm 0.4)*\delta^{18}O + (12.5 \pm 3.4)$, $R^2 = 0.99$, n = 21 | (Dabrani) | 3.9 |
| $\delta D=(7.0 \pm 0.5)*\delta^{18}O + (2.8 \pm 3.0)$, $R^2 = 0.95$, n = 11 | (Maneri) | 3.10 |
| $\delta D=(8.1 \pm 0.2)*\delta^{18}O + (14.8 \pm 1.7)$, $R^2 = 0.98$, n = 28 | (Uttarkashi) | 3.11 |
| $\delta D=(7.9 \pm 0.4)*\delta^{18}O + (9.4 \pm 3.6)$, $R^2 = 0.97$, n = 17 | (Tehri) | 3.12 |
| $\delta D=(7.9 \pm 0.3)*\delta^{18}O + (10.0 \pm 3.4)$, $R^2 = 0.99$, n = 21 | (Devprayag) | 3.13 |

### 3.1 'd' excess Parameter

In $\delta^{18}O$-$\delta D$ plot, when a line with a slope equal to 8 is drawn through the data points, the intercept 'd' (also called d-excess parameter) on the $\delta D$ axis indicates the secondary processes. The 'd' values at different altitudes for precipitation during any given month should be comparable, if secondary evaporation is not significant. In other words the 'd' values should have poor correlation with the altitude. This is true for the study area for the month of July and August precipitation, and a significant correlation is observed for the month of September. This secondary evaporation gives rise to 'secondary-altitude effect' in mountainous regions (Coplen, 1993). This 'secondary-altitude effect' is different from the 'altitude effect' which is a direct resultant of the adiabatic cooling related rain-out process as originally perceived by Dansgaard (1964).

### 3.2 Altitude Effect

The isotopic composition of precipitation changes with the altitude of the terrain and becomes more and more depleted in $\delta^{18}O$ and $\delta D$ of precipitation occurring at higher elevations. This enables the identification of elevation at which groundwater recharge takes place, one of the most useful applications in isotope hydrology, namely identification of recharge zone of springs in mountainous

region. Literatures available on isotope characteristics of precipitation cite altitude effect mainly as a resultant of adiabatic cooling and related rain-out process.

The precipitation data of Bhagirathi basin during the monsoon period (2005, 2006) have been used for the estimation of mean altitude effect. The elevation versus δ values of precipitation are plotted and are given in Figure 3.3 a, b and c. It is seen from these figures that the $\delta^{18}O$ data have a higher slope for September than for July or August. As discussed in the preceding section, this higher slope is due to the effect of secondary evaporation of falling raindrops and the evaporation effect appears to be linearly related to the distance travelled by the droplets through the air. The weighted mean altitude effect in $\delta^{18}O$ and δD is estimated using the yearly isotopic data for the year 2004, 2005 and 2006. The estimated altitude effects in $\delta^{18}O$ found between 0.24 to 0.29‰ /100m and in δD between 1.8 to 2.3‰ /100 m for Bhagirathi basin on the basis of data collected during the study period.

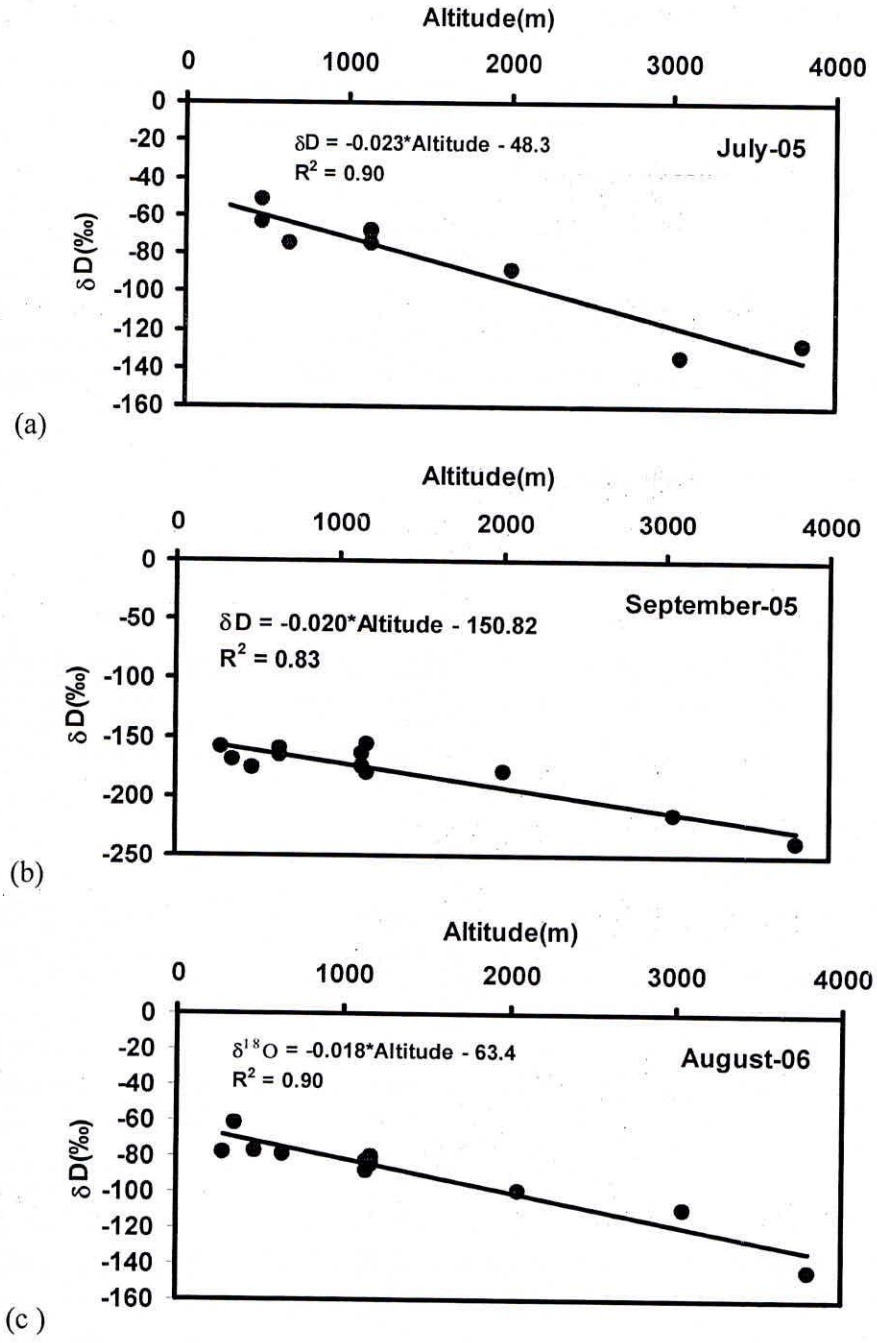


Fig. 3.5: Estimated altitude effect for Bhagirathi basin using $\delta^{18}O$ and δD data of precipitation.

The mean altitude effects presented above are within the range of values reported from other parts of the world (Yurtsever and Gat, 1981; Clark and Fritz, 1997). However, the values are higher than -0.19‰ for $\delta^{18}O$ and -1.6‰ for $\delta D$ derived by Ramesh and Sarin (1992) through isotopic compositions of headwaters of river Ganges from the Himalayas. The lower values of Ramesh and Sarin (1992) can be ascribed to the fact that the river at different points of its reach, represents the integrated run-off up to the respective points. In addition, the contribution from groundwater that is recharged at different altitudes will also have significant dampening effect on the isotopic signatures of the river waters.

The mean altitude effect observed in the present study are also significantly higher than the altitude effect reported for $\delta^{18}O$ (0.14‰ per 100 m) by Bartarya et al. (1995) who used the spring water isotopic compositions. This low value is due to the difference in altitude of recharge areas of springs and their outlets. This fact clearly brings out the risks in using surface expressions of subterranean waters as proxy for precipitation to study the altitude effect.

### 3.3 Spatial Variability

Figure 3.4 shows the spatial variability in $\delta^{18}O$ of precipitation in the study area. The $\delta^{18}O$ values range from -5‰ (Maneri) to -15‰ (Gaumukh). At a glance the figure reveals the depletion of $\delta^{18}O$ from Devprayag to Gaumukh with exception at Maneri. The enriched value at Maneri may be due to impact of evaporation from Maneri Bhali dam. The continuous depletion in $\delta^{18}O$ of precipitation reveals it due to altitude effect.

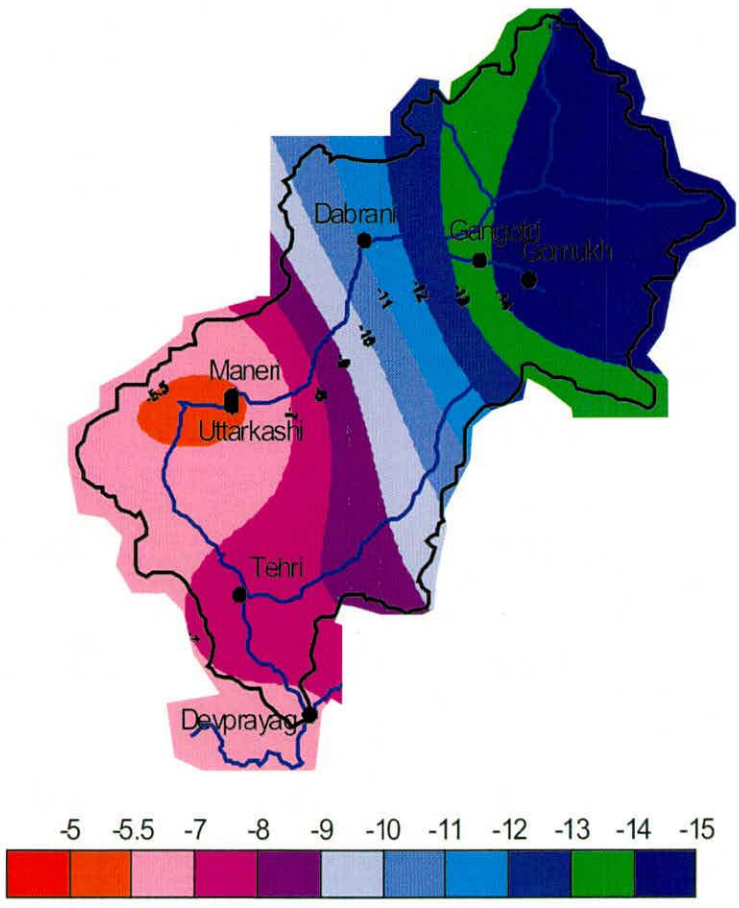


Fig. 3.6 Spatial variation of $\delta^{18}O$ along Bhagirathi River basin

# CHAPTER 4

## ISOTOPIC CHARACTERISATION OF GROUNDWATER

### 4.0 Introduction

During summer season the rivers of the Himalayas receive water either from snow and glacial melt water or from seepages and springs. Majority of the head water rivers are fed by snow and glacial melt water. However, rivers originating from the southern slopes of Middle Himalayas and either slope of the Siwalik range are spring and seepage fed. Generally, the groundwater emerge out in the form of natural springs is the only source of drinking water to the mountainous regions of Himalayas. The hydrogeological studies of springs in Western Himalayan region have been carried out by Valdiya and Bartarya (1989, 1991) in Gaula catchment and Rai (1993) in Khulgad watershed of Kumaun Lesser Himalayas. Valdiya and Bartarya (1989, 1991) and Valdiya (1985, 1987) in the Gaula Catchment in the south central Kumaun showed alarming rate of reduction in spring discharges and flow in the Gaula River. The decrease of discharge in them ranges from 25% to 75% during the past 5 to 50 years. These studies reveal that the origin of springs are mainly controlled by the geological structures in the study area.

Studies conducted worldwide during the last few decades have established that the stable oxygen and hydrogen isotope ratios act as useful tools for hydrological investigations (Clark and Fritz, 1997; Mazor, 1991; Fontes, 1980). In the case of groundwater, stable isotopes have been used to estimate recharge and identify the recharge zones, to determine the effects of evaporation on groundwater systems, to estimate diffusion rates in unsaturated zones, to study the groundwater surface water interaction and to identify source of salinity (Bhattacharya et al., 1985, Navada et al., 1986; Deshpande et al., 2003) etc. However, groundwater occurring in Himalayas have not received due attention in spite of their importance in providing drinking water and also feeding the stream originating from non glacier area. In order to understand the contribution of groundwater in the Bhagirathi river stream, an attempt has been made to characterize the groundwaters in Bhagirathi basin from Devprayag (467 m a.m.s.l.) to Gangotri (3050 m a.m.s.l.) using stable isotopes of oxygen and hydrogen ($\delta^{18}O$ and $\delta D$). The tritium analysis has been carried out for the dating of the groundwater. The study area is shown in figure 4.1

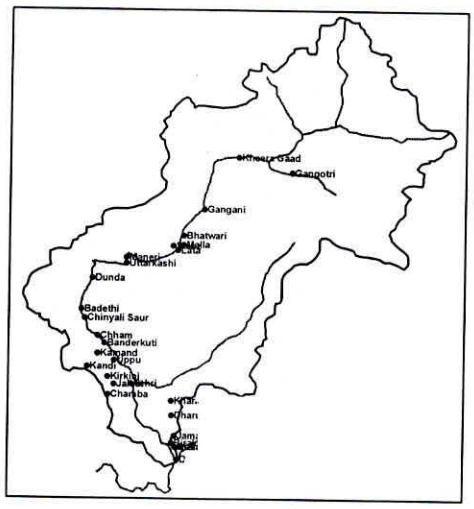


Fig. 4.1: Location of springs and handpumps in Bhagirathi River basin.

### 4.1 Results and Discussion

The groundwater samples from seepages, springs and handpumps were collected all along the Bhagirathi river from Devprayag to Gangotri (Plate-4.1). The oxygen isotopic composition of groundwater ($\delta^{18}O$) varies from -4.2‰ (maximum) to -13.2‰ (minimum) and hydrogen isotopic values ($\delta D$) varies from -21.9‰ (maximum) to -92.9‰ (minimum). In general the tritium values varies between 7 TU to 13 TU but a minimum value of 0.62 TU is found for Devprayag hand pump.


Plate 4.1: Groundwater sampling from Hand Pump and Spring (Dhara)

In situ measurement of physico-chemical parameters in the field show a wide range of variations. All the groundwater samples in the study area were cold water (temperature below 22°C) except a hot spring (temperature 63°C) in Gangnani at an altitude of 1950 m, which emanates through highly deformed, contorted and sheared phyllonite and mylonitized schist near the Vaikrita Thrust. pH values of groundwater samples were found to vary between 6.5 (Gangotri) to 8.5 (Devprayag). Electrical conductivity (EC) of these samples ranges between 180 µs/cm to 1375 µs/cm.

### 4.1.1 The $\delta^{18}O$-$\delta D$ relationship

A regression line drawn in $\delta^{18}O$-$\delta D$ plot for the global precipitation defines the Global Meteoric Water Line (GMWL) and that for the precipitation in a region and at a location are named as the Regional Meteoric Water Line (RMWL) and Local Meteoric Water Line (LMWL), respectively. The $\delta^{18}O$-$\delta D$ relationship of groundwater when compared with LMWL provides information on the preservation/alteration of stable isotopic composition of precipitation in groundwater. Figures 4.2a and 4.2b show the $\delta^{18}O$-$\delta D$ plot for groundwater samples collected from handpumps (Table 4.1) and springs (Table 4.2). The regression analysis of the data gives the best fit line (BFL) as follows:

$\delta D = (8.1 \pm 0.1) * \delta^{18}O + (11.3 \pm 0.1)$ $(n = 162, r^2 = 0.96)$ (for handpump)

$\delta D = (7.2 \pm 0.3) * \delta^{18}O + (3.4 \pm 2.5)$ $(n = 37, r^2 = 0.94)$ (spring)

where, n is the number of samples, r is the correlation coefficient. The slope of this BFL is similar to that of GMWL, $\delta D = (8.17)*\delta^{18}O + 10.35$ (Rozanski et al., 1993) and Local Meteoric Water Line of Bhagirathi Basin $\delta D = (8.0)*\delta^{18}O + 11.5$.

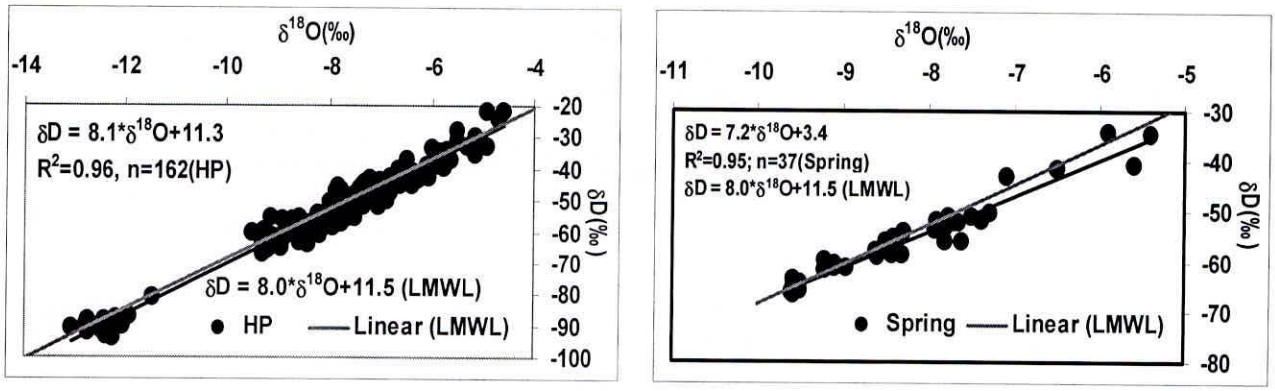


(a) Handpump

(b) Spring

Fig. 4.2 a & b: The $\delta^{18}O$-$\delta D$ regression line for groundwater representing handpumps and springs of Bhagirathi River basin.

Table 4.1 Variation of isotopic value in Handpump at different sites

| Date | Location | Altitude (m) | $\delta^{18}O$ | $\delta D$ |
|---|---|---|---|---|
| 27-Nov-05 | Haridwar | 284 | -9.1 | -61.9 |
| 28-Nov-05 | Haridwar | 284 | -9.1 | -55.6 |
| 1-Jun-04 | Rishikesh | 347 | -5.8 | -35.5 |
| 1-Jul-04 | Rishikesh | 347 | -6.0 | -33.6 |
| 21-Sep-04 | Rishikesh | 347 | -4.7 | -24.0 |
| 15-Dec-04 | Rishikesh | 347 | -5.5 | -30.7 |
| 26-Apr-05 | Rishikesh | 347 | -5.7 | -34.0 |
| 17-Jun-05 | Rishikesh | 347 | -4.6 | -21.9 |
| 13-Jul-05 | Rishikesh | 347 | -5.7 | -34.5 |
| 1-Nov-05 | Rishikesh | 347 | -6.1 | -38.7 |
| 28-Nov-05 | Rishikesh | 347 | -5.8 | -36.1 |
| 1-Apr-06 | Rishikesh | 347 | -4.9 | -22.0 |
| 1-May-06 | Rishikesh | 347 | -8.4 | -64.1 |
| 3-May-06 | Rishikesh | 347 | -5.2 | -30.0 |
| 1-Jul-06 | Rishikesh | 347 | -5.5 | -27.7 |
| 3-Aug-06 | Rishikesh | 347 | -4.9 | -32.8 |
| 15-Aug-06 | Rishikesh | 347 | -5.3 | -32.7 |
| 1-Sep-06 | Rishikesh | 347 | -5.2 | -35.3 |
| 15-Sep-06 | Rishikesh | 347 | -5.8 | -39.3 |
| 20-Sep-06 | Rishikesh | 347 | -5.8 | -35.4 |
| 15-Nov-06 | Rishikesh | 347 | -5.9 | -39.1 |
| 1-Dec-06 | Rishikesh | 347 | -5.6 | -37.0 |
| 15-Jun-04 | Devaprayag | 465 | -8.1 | -54.2 |
| 1-Jul-04 | Devaprayag | 465 | -8.7 | -57.4 |
| 16-Jul-04 | Devaprayag | 465 | -8.5 | -58.0 |
| 1-Aug-04 | Devaprayag | 465 | -8.3 | -57.1 |
| 16-Aug-04 | Devaprayag | 465 | -7.0 | -46.3 |
| 1-Sep-04 | Devaprayag | 465 | -7.5 | -50.8 |
| 12-Sep-04 | Devaprayag | 465 | -7.6 | -49.1 |
| 16-Sep-04 | Devaprayag | 465 | -7.5 | -48.0 |
| 16-Oct-04 | Devaprayag | 465 | -7.6 | -51.2 |
| 16-Nov-04 | Devaprayag | 465 | -7.4 | -46.2 |
| 15-Dec-04 | Devaprayag | 465 | -7.6 | -49.1 |
| 15-Jan-05 | Devaprayag | 465 | -7.5 | -50.4 |
| 15-Feb-05 | Devaprayag | 465 | -7.4 | -49.0 |
| 16-Mar-05 | Devaprayag | 465 | -7.3 | -46.4 |
| 26-Apr-05 | Devaprayag | 465 | -6.5 | -40.4 |
| 15-Jun-05 | Devaprayag | 465 | -6.6 | -42.6 |
| 19-Jul-05 | Devaprayag | 465 | -6.2 | -42.6 |
| 16-Aug-05 | Devaprayag | 465 | -7.1 | -48.8 |
| 16-Aug-05 | Devaprayag | 465 | -7.1 | -48.8 |
| 15-Sep-05 | Devaprayag | 465 | -6.8 | -42.9 |
| 15-Oct-05 | Devaprayag | 465 | -6.6 | -42.4 |
| 15-Nov-05 | Devaprayag | 465 | -6.7 | -43.5 |
| 15-Dec-05 | Devaprayag | 465 | -6.6 | -42.5 |
| 2-Jan-06 | Devaprayag | 465 | -5.6 | -33.8 |
| 7-Feb-06 | Devaprayag | 465 | -6.0 | -37.1 |
| 16-Apr-06 | Devaprayag | 465 | -5.8 | -34.6 |
| 15-May-06 | Devprayag | 465 | -5.8 | -34.7 |
| 15-Jun-06 | Devprayag | 465 | -6.5 | -37.2 |
| 8-Aug-06 | Devprayag | 465 | -6.6 | -42.6 |
| 15-Aug-06 | Devprayag | 465 | -6.6 | -42.7 |

| Date | Location | Altitude (m) | $\delta^{18}O$ | $\delta D$ |
|---|---|---|---|---|
| 22-Aug-06 | Devprayag | 465 | -6.7 | -43.2 |
| 1-Sep-06 | Devprayag | 465 | -6.7 | -41.5 |
| 8-Sep-06 | Devprayag | 465 | -6.7 | -40.4 |
| 15-Sep-06 | Devprayag | 465 | -6.4 | -44.6 |
| 22-Sep-06 | Devprayag | 465 | -6.6 | -45.1 |
| 15-Oct-06 | Devprayag | 465 | -6.1 | -42.3 |
| 15-Nov-06 | Devprayag | 465 | -6.1 | -40.1 |
| 15-Dec-06 | Devprayag | 465 | -6.3 | -43.0 |
| 4-Dec-05 | Tehri | 640 | -8.7 | -59.4 |
| 4-Dec-05 | Tehri | 640 | -8.5 | -57.7 |
| 27-Dec-05 | Tehri | 640 | -8.9 | -60.8 |
| 27-Dec-05 | Tehri | 640 | -8.7 | -59.0 |
| 5-Jan-06 | Tehri | 640 | -9.3 | -63.9 |
| 3-Feb-06 | Tehri | 640 | -8.3 | -55.8 |
| 3-Feb-06 | Tehri | 640 | -8.9 | -60.8 |
| 21-Feb-06 | Tehri | 640 | -8.5 | -57.7 |
| 21-Feb-06 | Tehri | 640 | -9.3 | -64.0 |
| 1-Mar-06 | Tehri | 640 | -7.8 | -57.0 |
| 27-Mar-06 | Tehri | 640 | -7.9 | -58.4 |
| 1-Apr-06 | Tehri | 640 | -8.2 | -59.4 |
| 18-Apr-06 | Tehri | 640 | -8.1 | -57.4 |
| 4-Jun-06 | Tehri | 640 | -8.4 | -57.3 |
| 22-Jun-06 | Tehri | 640 | -7.7 | -55.8 |
| 11-Jul-06 | Tehri | 640 | -8.9 | -65.1 |
| 8-Aug-06 | Tehri | 640 | -9.3 | -66.9 |
| 16-Aug-06 | Tehri | 640 | -9.0 | -64.7 |
| 22-Aug-06 | Tehri | 640 | -8.9 | -61.8 |
| 7-Sep-06 | Tehri | 640 | -8.9 | -62.7 |
| 23-Sep-06 | Tehri | 640 | -8.5 | -61.2 |
| 4-Oct-06 | Tehri | 640 | -8.5 | -59.2 |
| 3-Nov-06 | Tehri | 640 | -8.6 | -63.3 |
| 31-Dec-06 | Tehri | 640 | -7.8 | -57.1 |
| 2-Jan-07 | Tehri | 640 | -8.1 | -57.1 |
| 28-Nov-05 | Banderkuti | 801 | -7.9 | -52.9 |
| 12-Aug-04 | Chinyali Saur | 880 | -7.9 | -53.7 |
| 2-Jun-04 | Mathli | 1055 | -7.2 | -47.9 |
| 12-Sep-04 | Manbir | 1073 | -6.6 | -42.6 |
| 2-Jun-04 | Dharuna | 1114 | -8.5 | -58.5 |
| 12-Sep-04 | Badethi | 1130 | -7.0 | -44.7 |
| 3-Jun-04 | Uttarkashi | 1140 | -8.0 | -50.6 |
| 15-Jun-04 | Uttarkashi | 1140 | -7.8 | -51.8 |
| 1-Jul-04 | Uttarkashi | 1140 | -8.0 | -53.1 |
| 12-Aug-04 | Uttarkashi | 1140 | -7.2 | -43.5 |
| 12-Aug-04 | Uttarkashi | 1140 | -7.1 | -44.9 |
| 23-Sep-04 | Uttarkashi | 1140 | -7.1 | -47.6 |
| 1-Oct-04 | Uttarkashi | 1140 | -7.3 | -47.8 |
| 1-Nov-04 | Uttarkashi | 1140 | -7.6 | -50.3 |
| 15-Dec-04 | Uttarkashi | 1140 | -7.3 | -46.3 |
| 3-Jan-05 | Uttarkashi | 1140 | -7.3 | -46.3 |
| 15-Feb-05 | Uttarkashi | 1140 | -6.4 | -40.5 |
| 16-Mar-05 | Uttarkashi | 1140 | -7.3 | -44.3 |
| 26-Apr-05 | Uttarkashi | 1140 | -7.3 | -45.0 |
| 1-May-05 | Uttarkashi | 1140 | -7.0 | -43.8 |
| 1-Jun-05 | Uttarkashi | 1140 | -7.4 | -47.5 |

| Date | Location | Altitude (m) | $\delta^{18}O$ | $\delta D$ |
|---|---|---|---|---|
| 17-Jun-05 | Uttarkashi | 1140 | -8.0 | -55.3 |
| 1-Aug-05 | Uttarkashi | 1140 | -7.2 | -46.0 |
| 16-Aug-05 | Uttarkashi | 1140 | -7.3 | -46.8 |
| 1-Oct-05 | Uttarkashi | 1140 | -7.3 | -46.6 |
| 30-Nov-05 | Uttarkashi | 1140 | -7.8 | -47.1 |
| 1-Dec-05 | Uttarkashi | 1140 | -7.8 | -51.6 |
| 15-Dec-05 | Uttarkashi | 1140 | -7.1 | -46.0 |
| 15-Jan-06 | Uttarkashi | 1140 | -7.9 | -52.8 |
| 15-Feb-06 | Uttarkashi | 1140 | -6.4 | -45.0 |
| 15-Mar-06 | Uttarkashi | 1140 | -6.8 | -47.6 |
| 15-Apr-06 | Uttarkashi | 1140 | -6.9 | -49.8 |
| 5-May-06 | Uttarkashi | 1140 | -7.0 | -51.6 |
| 15-May-06 | Uttarkashi | 1140 | -7.3 | -44.8 |
| 15-Jun-06 | Uttarkashi | 1140 | -7.8 | -45.4 |
| 15-Jul-06 | Uttarkashi | 1140 | -7.9 | -47.2 |
| 15-Aug-06 | Uttarkashi | 1140 | -7.8 | -52.8 |
| 15-Aug-06 | Uttarkashi | 1140 | -7.8 | -52.8 |
| 15-Oct-06 | Uttarkashi | 1140 | -7.3 | -51.5 |
| 16-Oct-05 | Uttarkashi | 1140 | -7.7 | -49.2 |
| 1-Nov-05 | Uttarkashi | 1140 | -7.8 | -49.3 |
| 16-Nov-05 | Uttarkashi | 1140 | -7.7 | -49.8 |
| 9-Nov-06 | Maneri | 1190 | -11.5 | -80.9 |
| 2-Jun-04 | Gosai | 1241 | -9.1 | -61.3 |
| 28-Nov-05 | Facot | 1267 | -6.5 | -39.5 |
| 2-Jun-04 | Gyoli | 1300 | -9.2 | -65.8 |
| 2-Jun-04 | Birakot | 1373 | -9.3 | -63.5 |
| 12-Sep-04 | Birakot | 1373 | -8.9 | -56.2 |
| 2-Jun-04 | Old Hindolakhal | 1472 | -9.3 | -59.7 |
| 1-Jul-04 | Lata Sera | 1472 | -6.8 | -44.9 |
| 12-Sep-04 | Hindolakhal | 1472 | -8.2 | -54.2 |
| 12-Sep-04 | Latasera | 1472 | -6.0 | -38.6 |
| 29-Nov-05 | Lata | 1472 | -6.5 | -41.1 |
| 2-Jun-04 | Jamia Khal | 1552 | -9.5 | -60.6 |
| 12-Sep-04 | Bhatwari | 1610 | -7.3 | -47.7 |
| 16-Jun-05 | Bhatwari | 1610 | -7.2 | -47.7 |
| 29-Nov-05 | Bhatwari | 1610 | -7.9 | -50.0 |
| 2-Jun-04 | Khandogi | 1660 | -8.6 | -57.9 |
| 12-Aug-04 | Khandogi | 1660 | -7.9 | -53.4 |
| 6-Aug-06 | Khandogi | 1660 | -8.8 | -57.7 |
| 22-Sep-06 | Khandogi | 1660 | -8.8 | -58.4 |
| 10-Nov-06 | Anjani Sain | 2000 | -8.2 | -59.5 |
| 29-Nov-05 | Harsil | 2640 | -9.1 | -55.6 |
| 8-Feb-06 | Harsil | 2640 | -12.6 | -91.1 |
| 12-Aug-04 | Gangotri | 3053 | -12.4 | -88.6 |
| 21-Sep-05 | Gangotri | 3053 | -12.3 | -89.1 |
| 29-Nov-05 | Gangotri | 3053 | -12.7 | -88.4 |
| 8-May-06 | Gangotri | 3053 | -11.9 | -87.2 |
| 15-Jun-06 | Gangotri | 3053 | -12.8 | -89.7 |
| 15-Jul-06 | Gangotri | 3053 | -12.6 | -90.2 |
| 1-Sep-06 | Gangotri | 3053 | -12.2 | -87.6 |
| 7-Sep-06 | Gangotri | 3053 | -13.0 | -90.9 |
| 15-Sep-06 | Gangotri | 3053 | -12.5 | -91.2 |
| 24-Sep-06 | Gangotri | 3053 | -12.1 | -90.4 |
| 28-Sep-06 | Gangotri | 3053 | -12.2 | -93.8 |

| Date | Location | Altitude (m) | $\delta^{18}O$ | $\delta D$ |
|---|---|---|---|---|
| 12-Oct-06 | Gangotri | 3053 | -12.4 | -93.6 |
| 21-Oct-06 | Gangotri | 3053 | -12.0 | -90.1 |
| 2-Nov-06 | Gangotri | 3053 | -12.7 | -92.2 |
| 12-Sep-04 | Gabeli | | -8.8 | -59.3 |
| 12-Sep-04 | Uppu | | -8.2 | -55.6 |
| 17-Jun-05 | Tikoli | | -8.0 | -55.3 |
| 30-Nov-05 | Dunda | | -7.8 | -49.4 |
| 30-Nov-05 | Jaledi | | -8.6 | -55.2 |
| 30-Nov-05 | Jardar Gano | | -8.0 | -50.9 |
| 5-Aug-06 | Kandi | | -8.7 | -58.8 |
| 5-Aug-06 | Mahar | | -8.7 | -59.4 |
| 22-Sep-06 | Jantri | | -8.7 | -56.1 |
| 22-Sep-06 | Kandi | | -8.7 | -60.7 |
| 22-Sep-06 | Petab | | -8.2 | -60.7 |
| 8-Nov-06 | Netala | | -6.9 | -48.4 |
| 10-Nov-06 | Chinyali Saur | 880 | -8.5 | -63.7 |
| 10-Nov-06 | Jajhani Dhaar | | -7.6 | -54.5 |
| 10-Nov-06 | Kamand | | -7.5 | -55.7 |

Table 4.2 Variation of isotopic values in Springs at different sites

| Date | Location | Altitude (m) | $\delta^{18}O$ | $\delta D$ |
|---|---|---|---|---|
| 28-Nov-05 | Tehri | 640 | -8.3 | -54.2 |
| 10-Dec-05 | Madh | 640 | -8.2 | -55.6 |
| 23-Dec-05 | Madh | 640 | -8.5 | -57.9 |
| 2-Jan-06 | Madh | 640 | -8.2 | -55.4 |
| 20-Jan-06 | Madh | 640 | -8.0 | -54.4 |
| 2-Feb-06 | Madh | 640 | -8.2 | -55.6 |
| 2-Mar-06 | Tehri | 640 | -7.9 | -53.6 |
| 28-Mar-06 | Tehri | 640 | -7.7 | -52.0 |
| 4-Apr-06 | Tehri | 640 | -7.3 | -50.1 |
| 2-May-06 | Tehri | 640 | -7.6 | -55.9 |
| 5-May-06 | Tehri | 640 | -7.8 | -55.8 |
| 5-Jun-06 | Tehri | 640 | -7.4 | -51.7 |
| 24-Sep-06 | Tehri | 640 | -8.4 | -58.5 |
| 6-Nov-06 | Tehri | 640 | -8.3 | -58.6 |
| 12-Jul-04 | Sirai | 646 | -8.4 | -55.0 |
| 2-Feb-05 | Sirai | 646 | -7.7 | -51.8 |
| 16-Mar-05 | Sirai | 658 | -5.6 | -40.8 |
| 26-Apr-05 | Sirai | 658 | -8.6 | -59.1 |
| 20-Sep-05 | Sirai | 658 | -9.2 | -61.8 |
| 2-Jun-04 | Siyansu | 752 | -7.8 | -51.0 |
| 28-Nov-05 | Siyansu | 752 | -8.4 | -55.5 |
| 2-Jun-04 | Maldewal | 755 | -7.9 | -51.8 |
| 12-Jul-04 | Maldewal | 755 | -7.7 | -52.1 |
| 7-Dec-04 | Maldewal | 755 | -7.8 | -53.2 |
| 15-Jun-05 | Maldewal | 755 | -7.5 | -51.0 |
| 28-Nov-05 | Maldewal | 755 | -8.5 | -56.4 |
| 15-Jun-05 | Bhinu | 1256 | -5.9 | -34.2 |
| 19-Jul-05 | Bhinu | 1256 | -7.1 | -42.9 |
| 2-Jun-04 | Koti | 1450 | -8.6 | -57.8 |
| 2-Jun-04 | Andekhi | 1642 | -9.1 | -60.5 |
| 27-Apr-04 | Gangnani | 1950 | -9.5 | -64.4 |
| 12-Sep-04 | Gangnani | 1950 | -9.5 | -66.0 |

| Date | Location | Altitude (m) | $\delta^{18}O$ | $\delta D$ |
|---|---|---|---|---|
| 16-Jun-05 | Gangnani | 1950 | -9.6 | -66.4 |
| 20-Jul-05 | Gangnani | 1950 | -8.5 | -56.0 |
| 29-Nov-05 | Gangnani | 1950 | -9.6 | -63.5 |
| 4-May-06 | Gangnani | 1950 | -9.1 | -61.3 |
| 21-Sep-06 | Gangnani | 1950 | -9.0 | -61.1 |
| 8-Nov-06 | Gangnani | 1950 | -9.6 | -66.7 |
| 4-May-06 | Limhi Gaad | 2058 | -9.6 | -65.2 |
| 4-May-06 | Harsil | 2640 | -9.2 | -59.8 |
| 17-Jun-05 | Matheli | | -6.5 | -41.4 |
| 17-Jun-05 | Nirguda | | -5.4 | -34.7 |
| 30-Nov-05 | Lata | | -6.7 | -45.1 |

This similarity in the slope of BFL of groundwater samples collected from handpump with LMWL suggests that isotopic composition of precipitation is well preserved in handpump samples while low slope and d intercept are found in the case of springs. This reveals that evaporation during infiltration, if any, is minor in the case of handpump where as in the case of spring water effect of evaporation is visible. Also spring water may get some local recharge which gives it slight evaporated signature. These results show that in the absence of Local Meteoric Line for Himalayan basin, the $\delta^{18}O$-$\delta D$ relationship for handpump represents rainfall $\delta^{18}O$-$\delta D$ relationship and isotopic composition of groundwater (handpump) can be treated as the annually average of the precipitation.

In the $\delta^{18}O$-$\delta D$ plot, the hot springs fall in the same cluster as the cold springs. This suggests that the hot spring is recharged from local precipitation water. Similar results have also been reported by Giggenbach et al (1983) for hot springs emerging out in Parbati Valley of Himachal Pradesh.

### 4.1.2 Seasonal variation

The pre-monsoon and post-monsoon results show no marked variation in isotopic signature of groundwater. The $\delta^{18}O$ in groundwater varies between –12.8‰ to –4.4‰ during pre-monsoon period and -12.7‰ to –4.2‰ during post-monsoon period. The $\delta^{18}O$ - $\delta D$ regression line (Fig. 4.3) representing the groundwater Line in the Bhagirathi basin is established for the pre-monsoon and post-monsoon periods are as following:

$\delta D = (8.4 \pm 0.3)*\delta^{18}O + (13.4 \pm 2.6)$ ($r^2 = 0.94$, n = 43 ) for Pre-monsoon
$\delta D = (7.9 \pm 0.3)*\delta^{18}O + (9.8 \pm 2.1)$ ($r^2 = 0.96$, n = 51) for Post monsoon

As indicated earlier, the large spatial variations in $\delta^{18}O$ and $\delta D$ of groundwater are the result of altitude effect in precipitation which is the only source of recharge to the groundwater in the Bhagirathi basin.

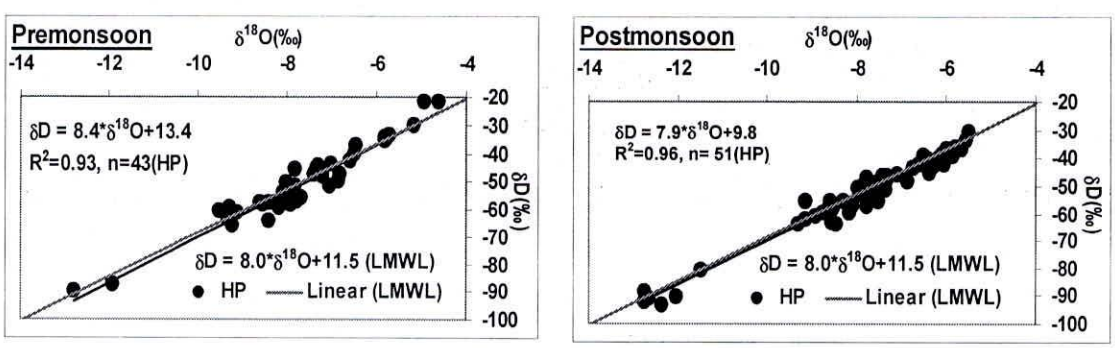


Fig. 4.3: The $\delta^{18}O$ and $\delta D$ regression line plot of groundwater collected during pre and post-monsoon.

### 4.1.3 Temporal variation

To measure the temporal variation of $\delta^{18}O$ and $\delta D$ in groundwater, regular water samples from Gangotri, Uttarkashi, Tehri, Devprayag and Rishikesh (Downstream of Devprayag) sites were collected on monthly and seasonal basis. The temporal variation of $\delta^{18}O$ and $\delta D$ of groundwater are presented in figure 4.4. The oxygen isotopic composition of groundwater at Rishikesh varies between -4.2‰ (maximum) to –8.1‰ (minimum) with an annual average of –5.5‰, at Devprayag –5.6‰ (maximum) to –8.7‰ (minimum) with an annual average of -6.8‰, at Uttarkashi –6.4‰ (maximum) to -8‰ (minimum) with an average value of –7.4‰ and at Mingwali (Tehri) –6.3‰ (maximum) to –9.3‰ (minimum) with an average value of –8.2‰. The $\delta^{18}O$ varied between –3.13‰ to –1.4‰ at all the sites. Although the groundwater at each site shows distinct isotopic characteristics but the temporal variation at Devprayag and Tehri sites are relatively significant.

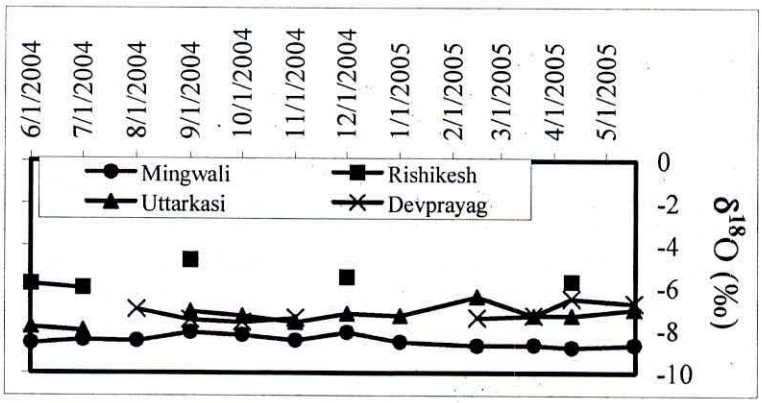


Fig. 4.4: Variation of $\delta^{18}O$ values at selected sites of hand pump and spring.

### 4.1.4 Altitude effect:

As the air masses are lifted orographically, they cool and ensuing precipitation is enriched preferentially in the heavier isotopes. As a result, the next phase of precipitation at still higher altitude condensing from the residual cloud mass is relatively depleted in heavy isotopes; the progressive depletion with height is known as the altitude effect (Yurtsever and Gat, 1981; Clark and Fritz, 1997). The altitude effect depends on factors such as precipitation history, topography and precipitable moisture remaining in the cloud. The altitude effect on $\delta^{18}O$ in mid – latitude precipitation generally ranges between -0.15‰ and -0.30‰ for each 100 m of altitude gained. Both continental effect and altitude effects are manifestations of Rayleigh distillation-one operating on a large spatial scale as a result of cloud migration; the other operating in a given region owing to continuous extraction of water from ascending cloud resulting from the drop in temperature with height. The plot between altitude and $\delta^{18}O$ of groundwater shows that altitude effect for groundwater during pre-monsoon and post monsoon is almost similar (Fig. 4.5).

$\delta^{18}O$ = -0.0023*altitude (m) – 5.0 (r = 0.91) for post monsoon
$\delta^{18}O$ = -0.0024*altitude (m) – 5.1 (r = 0.81) for pre-monsoon

The altitude effect in groundwater of Himalayan catchment would be very useful in identifying the recharge zones of the springs whose discharge is dwindling due to various anthropogenic factors. A recent application of altitude effect derived from stream waters concerned with the determination of paleoelevation in mountain belts (Garzione et al., 2000 a, and b; Poage and Chamberlain, 2001).

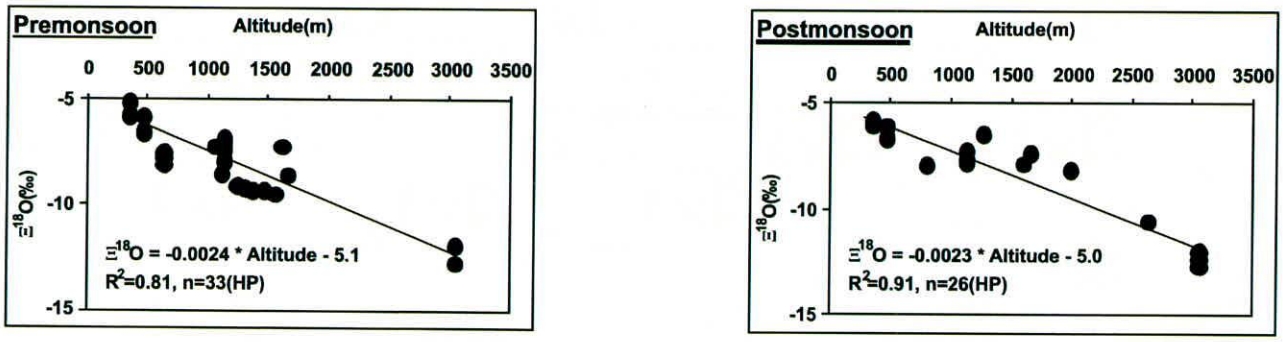


Fig. 4.5: Altitude effect of $\delta^{18}O$ determined in groundwater of Bhagirathi catchment for pre-monsoon and post-monsoon samples.

### 4.1.5 Spatial variation

Figure 4.6 shows the spatial variability of $\delta^{18}O$ in the study area. The $\delta^{18}O$ ranging from -5.5‰ (Sainz) to -12.8‰ (Gangotri). The figure reveals $\delta^{18}O$ depletion from Devprayag to Gaumukh with an exception at Maneri. The enriched value at Maneri may be due to impact of evaporation from Maneri Bhali dam.

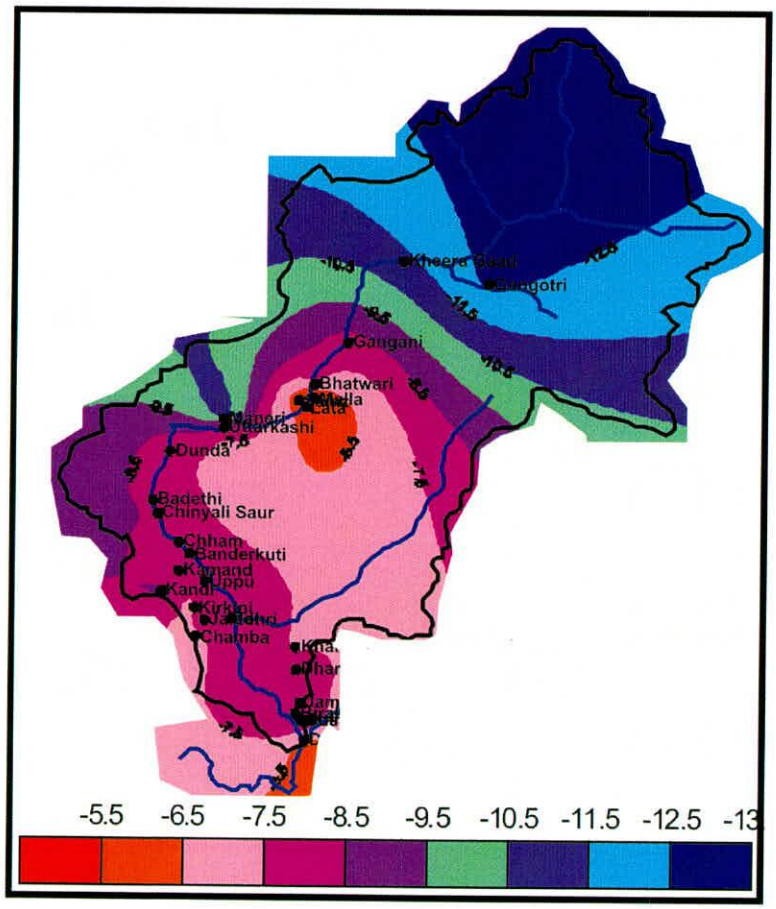


Fig. 4.6 Spatial variation of $\delta^{18}O$ along Bhagirathi River basin.

## 4.2 Isotopic Findings

The groundwaters in Bhagirathi catchment have been analysed for oxygen and hydrogen stable isotopes. The following important conclusions have been drawn from the isotopic data:

1. The $\delta^{18}O$-$\delta D$ relationship for handpump samples yields a slope of 8.0 that is similar to Local Meteoric Water Line of Bhagirathi River basin. It reveals that isotopic composition of precipitation is well preserved in groundwater samples of handpumps collected from the study area and evaporation during infiltration, if any, is minor. The springs samples reveal same evaporation effect.
2. Since groundwater and precipitation samples have the same isotopic composition ($\delta^{18}O$ and $\delta D$) in the Bhagirathi basin, groundwater isotopic values could be used to compute LMWL, in absence of precipitation samples.
3. Similar slope of pre-monsoon and post-monsoon groundwaters in $\delta^{18}O$ - $\delta D$ relationship represents a well-mixed aggregate of waters from different seasons.
4. The distinct $\delta^{18}O$ in groundwater at each sites reveals that groundwater in the area is recharged through local precipitation and has a fairly good storage.
5. The altitude effect in $\delta^{18}O$ in groundwater is found to be -0.24‰ per 100 m, which is more depleted than the altitude effect calculated using $\delta^{18}O$ value of river water in Indian Himalayas a nd slightly enriched than the Nepal Himalayas stream data.

# CHAPTER 5

## ISOTOPIC CHARACTERIZATION OF RIVER WATER

### 5.0 Introduction

The spatial and temporal variations in the isotopic composition of river waters $\delta_R$ are mainly brought about by the number and type of its sources, and to some extent in certain climatic regions by the evaporation from the river surface. The variations in the observed $\delta_R$, reflect the variable contributions from isotopically different sources, which can be evaluated if isotopic indices of the sources are known. Therefore, the river water isotopic characterisation and its utility in determining the contribution from different sources and understanding the river - aquifer interactions are of great importance.

Amplitude of the seasonal variations in $\delta_R$ gives some insight in to the hydrologic regimes that controls the flow in the river. Seasonal variation of the isotopic composition of river water will be more pronounced in case of rivers dominated by surface runoff than that dominated by groundwater inputs. This is due to the fact that groundwater bodies are isotopically constant and closely reflect the average annual isotopic composition of local precipitation ($\delta_P$) (even if seasonal variations in the precipitation isotopic composition are large). The rivers fed by karstic systems with a short residence time ($\tau$) will show a pronounced seasonal variation in $\delta_R$, than the one fed by porous aquifers (where $\tau$ will be longer). On the other hand, in precipitation dominated basins, the seasonality in the isotopic composition of precipitation will be reflected in more enriched $\delta_R$ during summer and more depleted $\delta_R$ during winter. But, snowmelt during summer may reverse the above trend or in some cases shift them. The isotopic characteristics of river waters (both precipitation dominated and groundwater dominated) will also be affected by the altitude effect in precipitation, which is reflected in both surface and sub-surface components of the river flow. It is also noticeable that, the altitude effect $\delta p$ might produce changes in $\delta_R$ which super-impose changes due to the seasonal variation of $\delta p$.

In order to characterise the isotopic composition of river Bhagirathi, over 5000 river samples were collected from the Gaumukh, Gangotri, Dabrani, Uttarkashi, Tehri and Devprayag sites. These river samples were analysed for $\delta^{18}O$, $\delta D$ and tritium. The isotopic composition and its variations found in the river water from Gaumukh to Devprayag are discussed below:

### 5.1 Isotopic Composition of River Bhagirathi

For characterising the isotopic variations in the river discharge of Bhagirathi samples were collected from the Gaumukh, Gangotri, Dabrani, Uttarkasi, Tehri and Devpryag during June 2004 to October 2006. At Gaumukh, the samples were collected on ten daily bases for the ablation period during May to October during 2004 and 2006.

#### Gaumukh

For the measurement of isotopic composition of meltwater, river samples were collected from Bhojwasa which is located about 3 km downstream of the snout. Temporal variation in the isotopic composition of river water is observed at Gaumukh. As the discharge start increasing during the months of May and June (up to second week), enrichment in the isotopic values are observed (Figure 1). The maximum enrichment in $\delta^{18}O$ of the river water in the years 2004, 2005 and 2006 is about -12.4‰ indication the isotopic index of meltwater. The observed minimum depletion in $\delta^{18}O$ of meltwater in the years 4004, 2005 and 2006 are -16.6‰, -21‰ and -16.7‰ respectively. The initial meltwater (April to 15$^{th}$ June) $\delta^{18}O$ values ranges from -12‰ to -13‰, which is very close to the $\delta^{18}O$ value of the snow (-9.7‰ to -14.4‰) (measured for a few samples collected in May and June). This reveals that the melting of snow cover is the main source of river discharge during summer months (May and June) at Gaumukh. However, the variation in isotopic values near Gaumukh in Bhagirathi River clearly indicates

the variation in contribution from different sources in various months of melting. After the third week of June, $\delta^{18}O$ and $\delta D$ values of stream water start depleting, which reveal that the contribution of snow component is decreasing and ice melt component is increasing. Due to the melting of snow, in the glacier becomes exposed and comes in direct contact with the solar radiation, especially at lower altitudes. Depletion in $\delta^{18}O$ and $\delta D$ of stream discharge in July and August reveals that the peak discharge at Gaumukh results from the ice melt. As the precipitation start in the months of July, August and September, the $\delta^{18}O$ and $\delta D$ of stream discharge deplete sharply because the relatively high rainfall occurring in the month of July, August and September are more depleted than snow/ice melt. The sudden depletion in $^{18}O$ and $\delta D$ (Fig 5.1) clearly indicates significant runoff contribution to the river discharge.

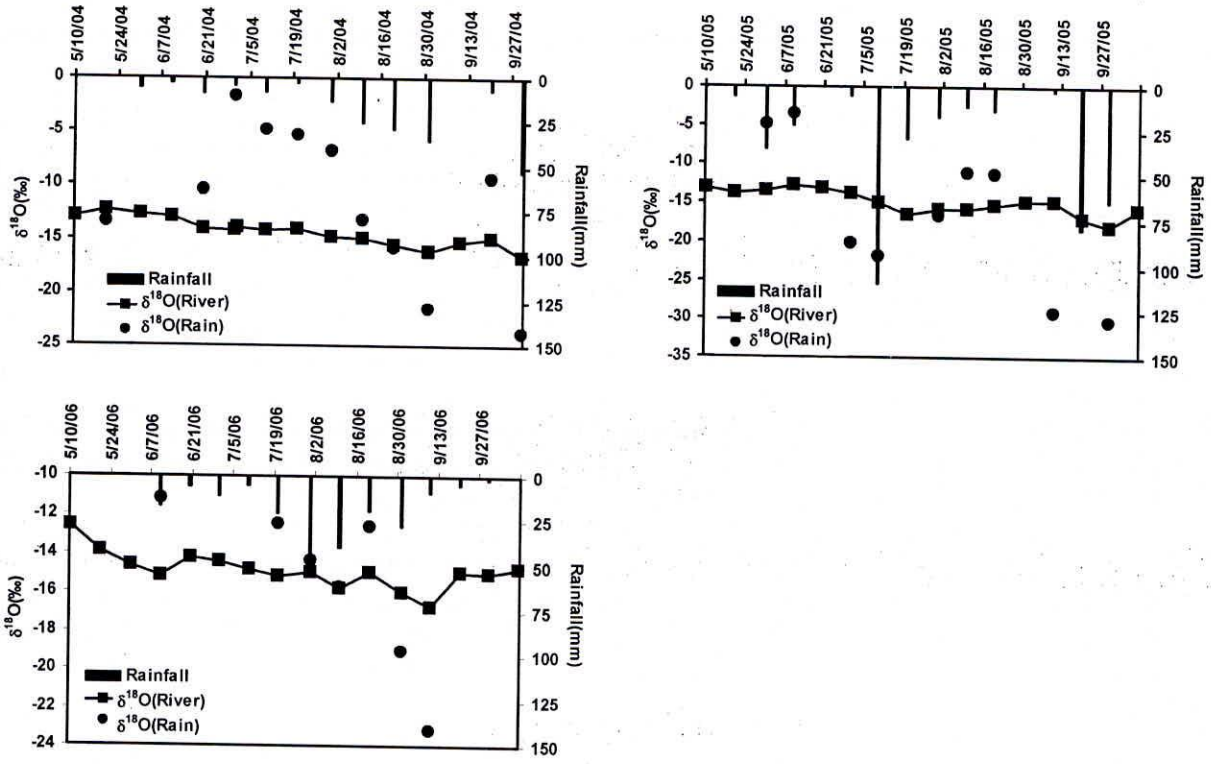


Fig. 5.1: Temporal variation of $\delta^{18}O$ in Bhagirathi River and precipitation at Gaumukh during 2004-2006.

The $\delta D$ vs $\delta^{18}O$ plot of river samples at Gaumukh is shown in figure 5.2. The equation to the best fit line is obtained as $\delta D=(8.4 \pm 0.7)*\delta^{18}O + (21.7 \pm 9.7)$, $R^2 = 0.92$, n = 16 (Fig. 5.3). A large variation in isotopic composition of river water is seen, which ranged between -84‰ and -145‰ in case of the $\delta D$ while for $\delta^{18}O$ it varied from -12.3‰ to -20‰. However, carefully segregation of isotopic data reveals that stream water is enriched in $\delta D$ or $\delta^{18}O$ values during the premonsoon period and comparatively depleted during the monsoon period. However, there is an overlap in isotopic values of river samples belonging to the premonsoon and the monsoon. The comparatively enriched isotopic values during the premonsoon period can be justified as snow melt dominated river water. The isotopic composition of snowmelt is comparatively enriched than ice melt and monsoon rain. The monsoon rains are mostly depleted due to altitude and amount effect.

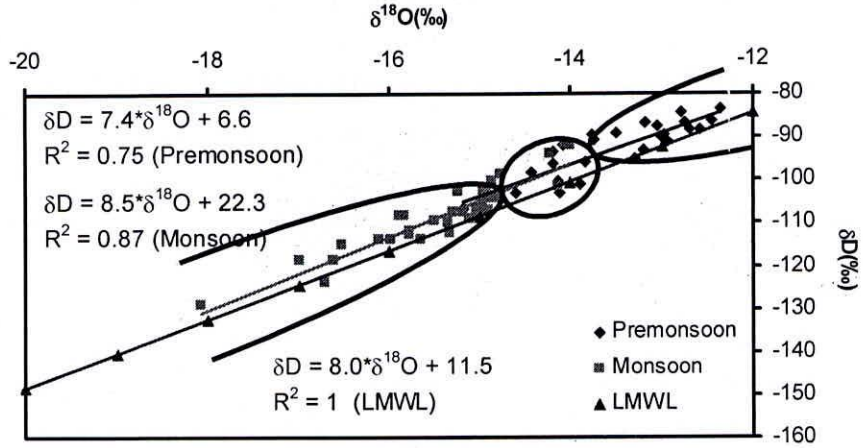


Fig. 5.2 δD vs $\delta^{18}O$ Plot of Bhagirathi River at Gaumukh

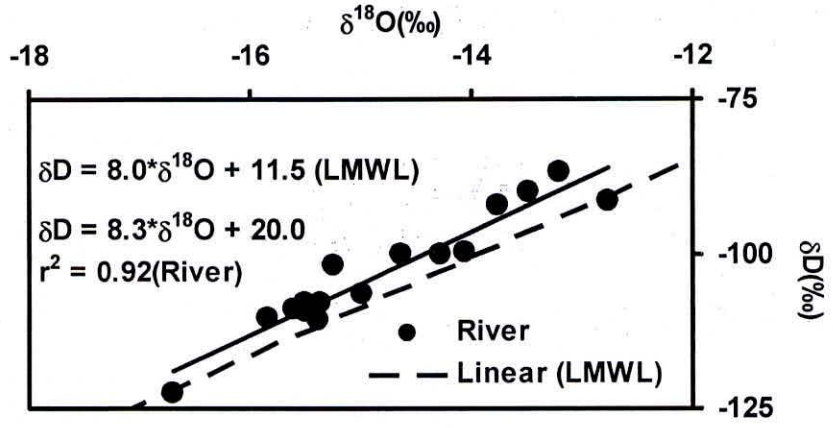


Fig. 5.3 δD and $\delta^{18}O$ of Bhagirathi River at Gaumukh

**Gangotri**

Gangotri is located at about 18 km downstream of Gaumukh at an altitude of 3050 m. At this site the maximum enrichment in $\delta^{18}O$ of the river in the years 2004, 2005 and 2006 varied between -12.0‰ to -13.1‰ while the minimum depletion ranged between -20.2‰ to -16.8‰. The average $\delta^{18}O$ values for the years 2004, 2005 and 2006 are -14.8‰, -15.4‰ and -14.8‰ respectively, Figure 5.4 shows the variation of monthly averaged.

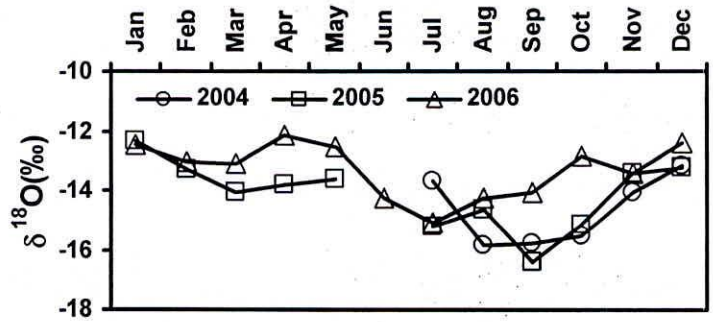


Fig. 5.4: Variation of $\delta^{18}O$ in Bhagirathi River at Gangotri.

The δD vs $\delta^{18}O$ plot for river discharge at Gangotri is shown in figure 5.5. The regression analysis of the data gives the best fit line (BFL) as:

$\delta D = (8.2 \pm 0.4) * \delta^{18}O + (14.9 \pm 6.1)$, $r^2 = 0.93$, n = 29 (2004-2006)

The intercept of this BFL slightly above than that of GMWL $\delta D = (8.17)*\delta^{18}O + 10.35$ (Rozanski et al., 1993) and Local Meteoric Water Line of Bhagirathi Basin $\delta D = (8.0)*\delta^{18}O + 11.5$ and close to the Gaumukh meltwater line. This reveals that at Gangotri, the river discharge is dominated by snow and glacier melt water.

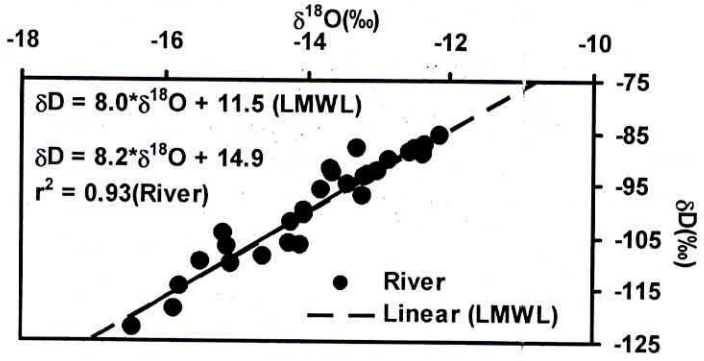


Fig. 5.5 δD vs $\delta^{18}O$ plot of Bhagirathi River at Gangotri

**Dabrani**

Dabrani is located at about 50 km down stream of Gangotri at an altitude of about 2050 m. Discharge data of Dabrani site is available on 10 daily basis for 2004 and on daily basis for 2005 and 2006. The maximum enrichment in $\delta^{18}O$ values of the Bhagirathi river in the years 2004, 2005 and 2006 ranged between -12.4‰ to -11.9‰ while the minimum depletion ranged between -16.5‰ to -15.8‰ and the annual average value ranged between -13.4‰ to -13.7‰. The depleted values in the monsoon period are due to the contribution of runoff to the river discharge. Temporal variation of monthly averaged $\delta^{18}O$ is shown in figure 5.6. The depletion of $\delta^{18}O$ starts in May and reaches a minimum in the rainy months. After the rainy months, the isotopic value gets enriched with time and almost remains constant in the winter. As the monsoon offset in the month of September, the river $\delta^{18}O$ enrich steadily and reach around -11‰ in December. This is due to reduction in the melt water contribution due to the decrease in atmospheric temperature after September. The melt water component becomes almost negligible in December. The enriched $\delta^{18}O$ in December may be due to groundwater component.

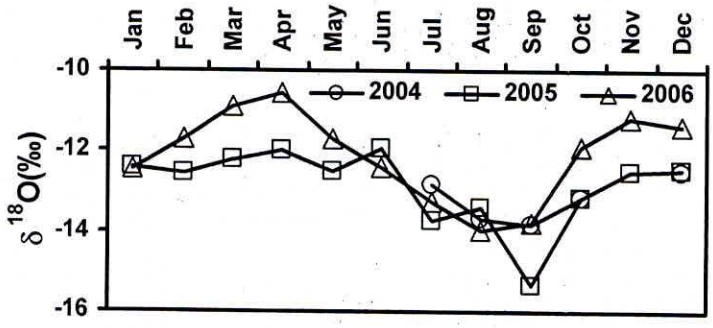


Fig. 5.6: Variation of monthly $\delta^{18}O$ in Bhagirathi River at Dabrani

The best fit line developed using the monthly $\delta^{18}O$ of Bhagirathi river at Dabrani during 2004-2006 (Fig. 5.7) is as:

$\delta D = (8.4 \pm 0.6) * \delta^{18}O + (17.6 \pm 7.3)$, $r^2 = 0.89$, n = 29 (2004-2006)

The slope and intercept values are slightly higher than that of Gangotri. This is probably due to the confluence of Banganga River which brings the smowmelt of higher altitudes. The Banganga River joins the Bhagirathi River at the upstream of Dabrani.

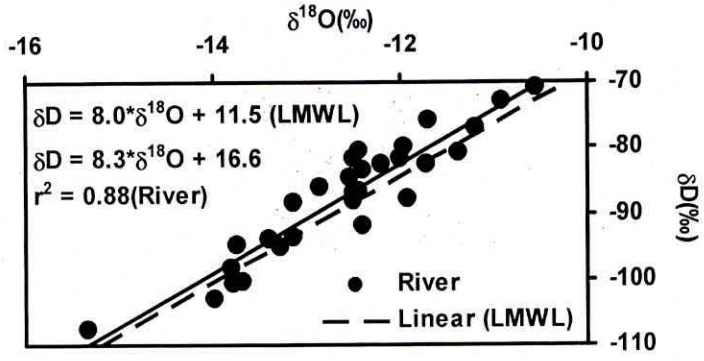


Fig. 5.7: δD Vs $\delta^{18}O$ plot of Bhagirathi River at Dabrani

**Uttarkashi**

Uttarkashi is situated at about 70 km downstream of Dabrani at an altitude of about 1150 m. Discharge data of Bhagirathi River at Uttarkashi is available on a daily basis from 2004 to 2006. A small dam is constructed for hydropower generation at Maneri, upstream of Uttarkashi. Bhagirathi River samples at Uttarkashi were collected from Tiloth bridge during 2004 but 2005 onwards the sampling station was shifted downstream of Uttarkashi. Compared to the upstream sites slight enrichment in $\delta^{18}O$ is observed at Uttarkashi during the nonmonsoon months. This is because of the fact that the Bhagirathi River flows through a tunnel after Maneri and joins the main river downstream of Uttarkashi city. The observed maximum enrichment in $\delta^{18}O$ of Bhagirathi River during the study period (2004, 2005, 2006) are in the range of -8.1‰ to -10.2‰ and the minimum depletion are in the range of -12.9‰ to -13.5‰ with an annual average of -10.9‰ to -12.3‰ (Fig 5.8). The variation in isotopic characteristics of Bhagirathi at Uttarkashi is similar to that of Dabrani. The maximum enrichment and minimum depletion are more in Uttarkashi than Dabrani is due to more groundwater input from lower altitude.

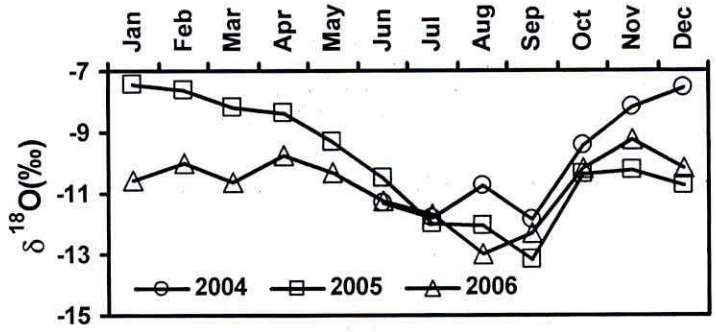


Fig. 5.8: Variation of monthly $\delta^{18}O$ of Bhagirathi River at Uttarkashi

The statistical analyses of monthly isotopic data of the Bhagirathi River at Uttarkashi yielded the following equation (Fig 5.9):

$\delta D = (8.0 \pm 0.3) * \delta^{18}O + (11.1 \pm 3.0)$, $r^2 = 0.96$, $n = 31$ (2004-2006)

The enrichment in isotopic values of the river at Uttarkashi is due to the dominance of local ground water during the non monsoon months.

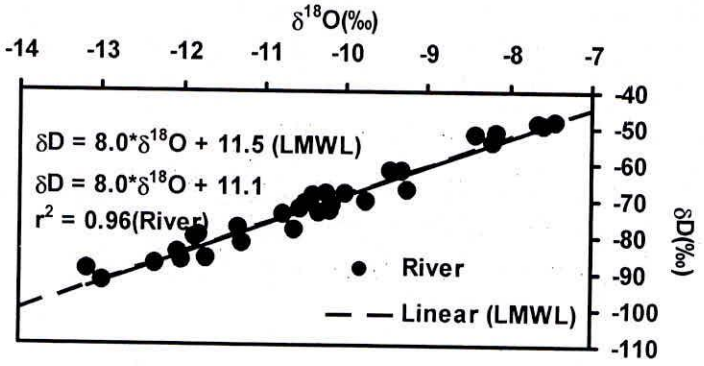


Fig. 5.9 δD Vs $\delta^{18}O$ plot of Bhagirathi River at Uttarkashi

**Tehri**

Tehri is located at about 60 km downstream of Uttarkashi at an altitude of about 640 m. Discharge data of Bhagirathi River at Tehri is available on daily basis from 2004 to 2006. Since Bhilangana River joins the Bhagirathi River at Tehri therefore, the samplings were carried out at three locations in this site i.e., upstream of the confluence of rivers (at Sirayi), downstream of the confluence of the rivers (at zero bridge) and from the Bhilangana River (at Simalasoo). However, the sampling from Siyansu and Simalasoo sites were continued only up to Oct 2005. After that, these sites were submerged due to the storage of water in the Tehri Dam. The maximum $\delta^{18}O$ enrichment observed in the downstream of Bhagirathi River at Tehri during the years 2004, 2005 and 2006 are -8.6 ‰, -8.9 ‰, -9.1‰, respectively, while the minimum depleted values ranged between -11.4 to -12.4‰ (Fig. 5.10 and Table 5.1). The annual average $\delta^{18}O$ values are -10.0‰, -10.4‰ and -10.6‰ for the years of 2004, 2005 and 2006, respectively. In the Bhilangana River, the maximum enrichment in $\delta^{18}O$ varied between -8.1‰ to -8.3‰ and minimum depleted value ranged between -9.3 ‰ to -10.5‰ during 2004 to 2006 respectively.

Table 5.1 Variation in $\delta^{18}O$ and δD of Bhagirathi River at Tehri.

| Year | | Sirayi (u/s of confluence Rivers) | | Simlasoo (Bhilangana River) | | Tehri (d/s of confluence River) | |
|---|---|---|---|---|---|---|---|
| | | $\delta^{18}O$ | δD | $\delta^{18}O$ | δ D | $\delta^{18}O$ | δ D |
| 2004 | Min. | -11.8 | -76.5 | -9.4 | -61.7 | -11.4 | -77.3 |
| | Max. | -9.1 | -60.4 | -8.1 | -51.6 | -8.6 | -55.5 |
| | Avg. | -10.4 | -70.0 | -8.6 | -56.4 | -10.1 | -68.2 |
| 2005 | Min. | -12.0 | -79.9 | -10.5 | -72.2 | -11.9 | -83.1 |
| | Max. | -9.7 | -52.2 | -8.3 | -52.1 | -8.9 | -57.1 |
| | Avg. | -10.6 | -68.0 | -9.3 | -60.5 | -10.4 | -69.0 |
| 2006 | Min. | | | | | -12.4 | -90.0 |
| | Max. | | | | | -9.1 | -63.0 |
| | Avg. | | | | | -10.6 | -74.4 |

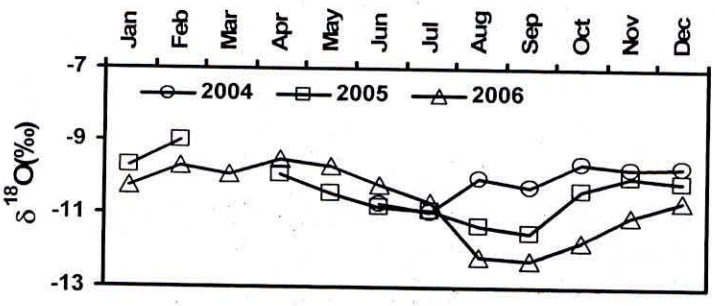


Fig. 5.10: Variation of monthly averaged $\delta^{18}O$ in Bhagirathi River at Zero bridge, Tehri

The statistical analysis of the monthly isotopic data of the Bhagirathi River at Tehri yielded the following equation (fig. 5.11):

$\delta D = (8.1 \pm 0.5) * \delta^{18}O + (13.1 \pm 5.0)$, $r^2 = 0.91$, $n = 30$ (2004-2006)

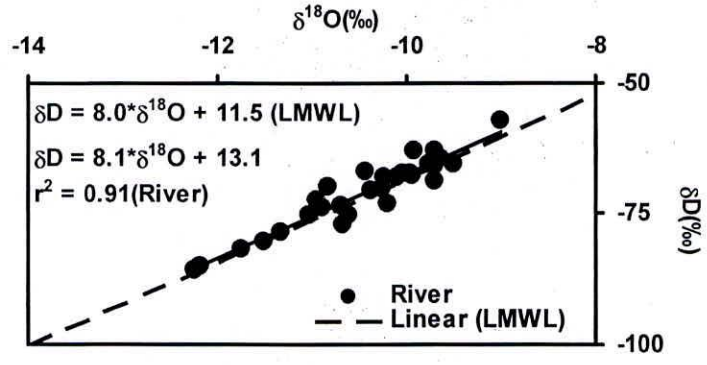


Fig. 5.11 δD Vs $\delta^{18}O$ plot of Bhagirathi River at Zero Bridge, Tehri

**Devprayag**

The Devprayag is the lower most river sampling site of the study area which lie at an altitude of about 465 m and located at about 45 km downstream of Zero bridge, Tehri. At Devprayag, the Alaknanda River joins the Bhagirathi and after the confluence it is known as Ganga River. The maximum and minimum of $\delta^{18}O$ values of the Bhagirathi River at devprayag are presented in the Table 5.2, Fig. 5.12 and Fig. 5.13.

Table 5.2 Variation of stable isotopic values in Bhagirathi River at Devprayag

| Year | Devprayag | | |
|---|---|---|---|
| | | $\delta^{18}O$ | δ D |
| 2004 | Min. | -11.7 | -80.9 |
| | Max. | -9.3 | -62.1 |
| | Avg. | -10.3 | -68.4 |
| 2005 | Min. | -12.4 | -84.7 |
| | Max. | -9.4 | -59.7 |
| | Avg. | -10.2 | -70.2 |
| 2006 | Min. | -12.8 | -91.3 |
| | Max. | -9.2 | -64.8 |
| | Avg. | -10.4 | -70.9 |

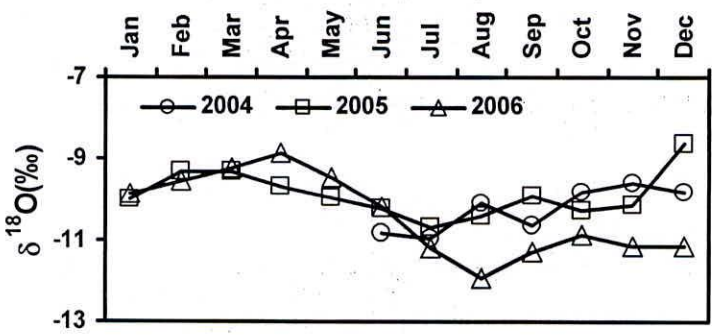


Fig. 5.12: Variation of monthly averaged $\delta^{18}O$ in Bhagirathi River at Devprayag.

The equation to the best fit line of Bhagirathi River samples at Devprayag plotted on a δD Vs $\delta^{18}O$ diagram is given by:

$\delta D = 8.3 \pm 0.5 * \delta^{18}O + 14.7 \pm 4.8$, $R^2 = 0.92$, n = 31 (2004-2006)

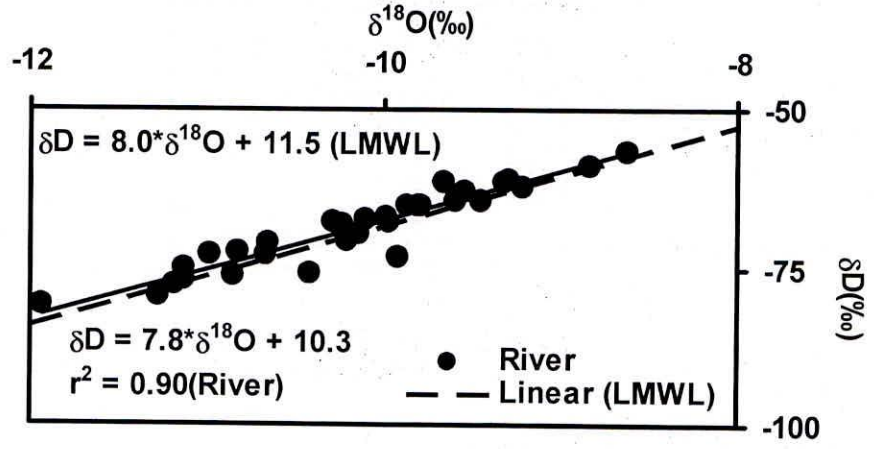


Fig. 5.13: δD Vs $\delta^{18}O$ diagram of Bhagirathi River at Devprayag

## 5.2 Temporal Variation of Stable Isotopes ($\delta^2h$ & $\delta^{18}o$) in Bhagirathi River

Figure 5.14 shows the monthly variation of $\delta^{18}O$ in Bhagirathi River at various sampling stations during 2005 and 2006. The maximum depletion of $\delta^{18}O$ is recorded in the monsoon months (July, August and September). As seen in figures 5.14 and 5.15, the river $\delta^{18}O$ values start depleting from April and continue till September. The monsoon rains occurs in the study area during July to September. The increase in temperature from April to June (pre-monsoon) results in increased melting of snow/glacier at higher reaches. This leads to increased contribution of snow/ice melt and results in depleted isotopic signatures of river water at different sites. The depleted $\delta^{18}O$ of rain occurring during the monsoon period resulted in further depletion in the river waters. The variation of stable isotopic values with time clearly indicates the varying contribution of snow/glacier melt, groundwater runoff.

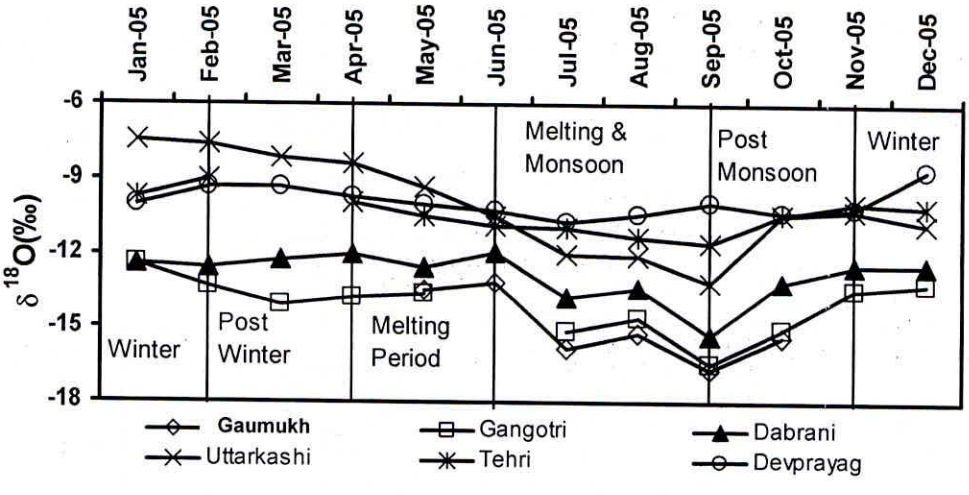


Fig. 5.14: Temporal variation of $\delta^{18}O$ values in Bhagirathi River during the year 2005.

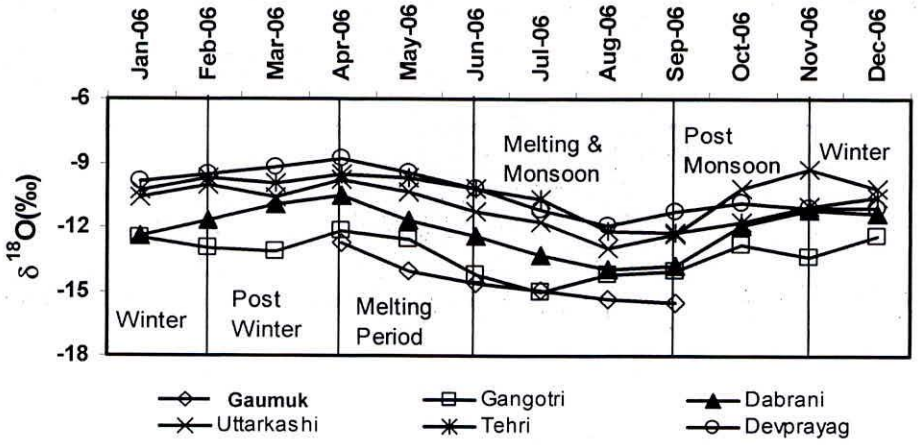


Fig. 5.15: Temporal variation of $\delta^{18}O$ in Bhagirathi River during the year 2006.

The variation in Electrical conductivity (Fig. 5.16) also reveals the varying contribution of groundwater to the river at different months.

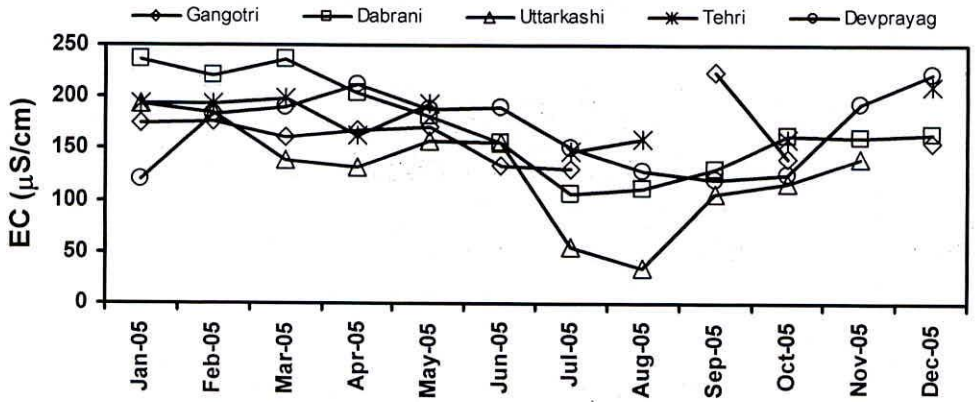


Fig. 5.16: Temporal variation of Electrical Conductivity along the Bhagirathi River.

### 5.3 Spatial Variation of Isotopic Signatures in River

In general, the stable isotopic values gets enriched as the River Bhagirathi flows downwards (Fig. 5.17). In 2004, $\delta^{18}O$ varied from -13.8‰ (Gaumukh) to -10.8‰ (Devprayag) during the pre-monsoon period (June), -15.5‰ (Gaumukh) to -10.1‰ (Devprayag) during monsoon (August) and -13.2‰ (Gangotri) to -9.8‰ (Devprayag) during the winter (December). Similar trend is also found in 2005 and 2006. The degree of enrichment in the river water from Gaumukh to Devprayag in different seasons varied from 3‰ to 5‰. This also clearly indicates the varying contributions of subsurface flow to the stream discharge in different seasons. The varying isotopic composition along the River is due to the altitude effect in surface and subsurface runoffs. As the river flows downwards, more surface and subsurface flows joins the River due to the fact that the larger part of the catchments area is located at lower altitudes which is enriched in stable isotopes.

The figure 5.17 reveals that enrichment of $\delta^{18}O$ in Bhagirathi River between Gaumukh and Gangotri is less, However, at Dabrani, it gets enriched significantly. Further enrichment in $\delta^{18}O$ is observed from Dabrani to Uttarkasi. The variation in $\delta^{18}O$ between Uttarkashi and Tehri is less while between Tehri to Devprayag it is negligible in the year 2004 and 2005. This reveals that the catchment area between Gangotri to Uttarkashi generates more subsurface/groundwater, which sustains the river during the lean flow period. After Tehri, the contribution of groundwater appears to the minimum due to the less catchments area.

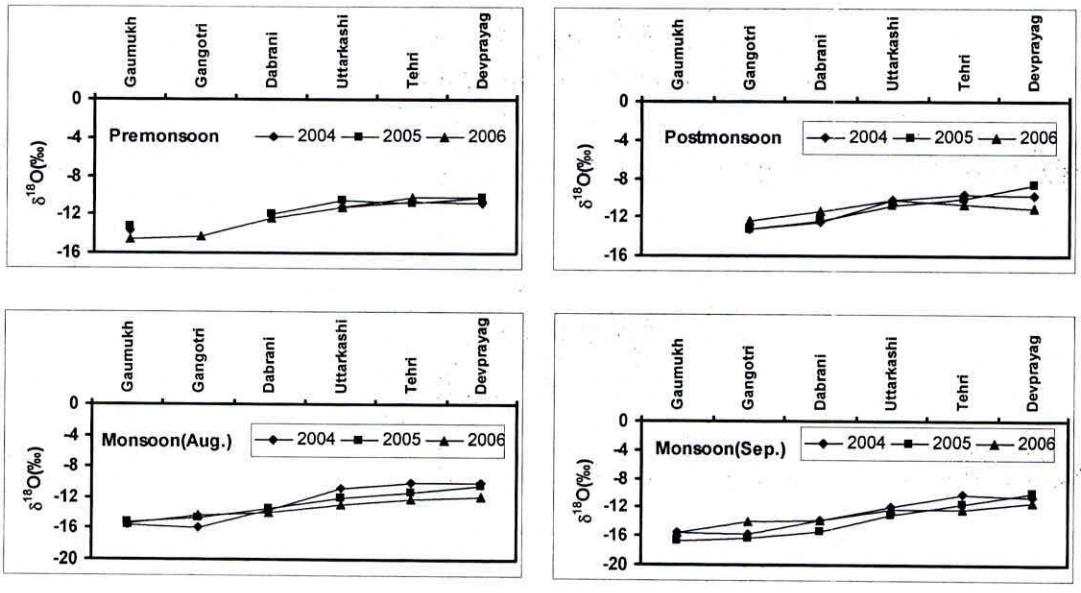


Fig. 5.17. Spatial variation of $\delta^{18}O$ in Bhagirathi River in various seasons.

## 5.4 Isotopic Composition of Bhagirathi River

Figure 5.18 show the $\delta^{18}O$-$\delta D$ plot for all river samples collected at different sites of Bhagirathi River. The monthly weighted average values computed from different sites during study period are presented in Table 5.3. The statistical analyses of monthly isotopic data of the Bhagirathi River yielded the following equation:

$\delta D = (7.9 \pm 0.1) * \delta^{18}O + (11.9 \pm 1.8)$, $R^2 = 0.99$, n = 36 (2004)
$\delta D = (7.8 \pm 0.2) * \delta^{18}O + (10.9 \pm 1.8)$, $R^2 = 0.98$, n = 64 (2005)
$\delta D = (7.6 \pm 0.2) * \delta^{18}O + (7.1 \pm 2.2)$, $R^2 = 0.96$, n =66 (2006)
$\delta D = (7.8 \pm 0.1) * \delta^{18}O + (9.8 \pm 1.2)$, $R^2 = 0.97$, n = 166 (2004-2006)

Slope and the intercept of the best fit line of Bhagitahi River are close to those of local precipitation. It indicates that river water did not suffer any kinetic effect up to Devprayag.

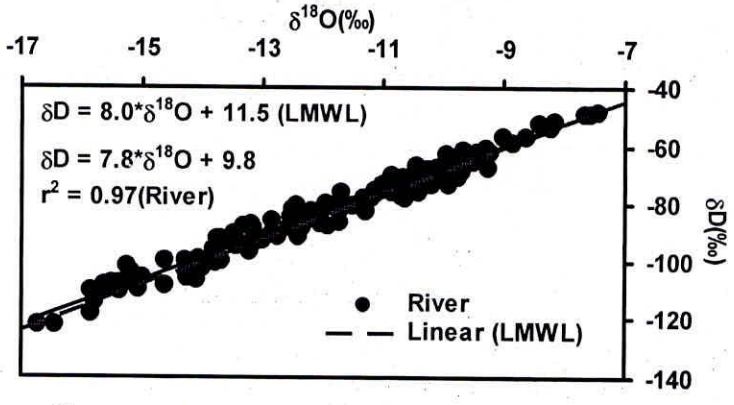


Fig. 5.18 $\delta D$ Vs $\delta^{18}O$ plot of Bhagirathi River during the study period (2004-06)

Table 5.3 Monthly weighted average values computed from different sites.

| Date | Gaumukh | | Gangotri | | Dabrani | | Uttarkashi | | Tehri | | Devprayag | |
|---|---|---|---|---|---|---|---|---|---|---|---|---|
| | $\delta^{18}O$ | $\delta D$ | $\delta^{18}O$ | $\delta D$ | $\delta^{18}O$ | $\delta D$ | $\delta^{18}O$ | $\delta D$ | $\delta^{18}O$ | $\delta D$ | $\delta^{18}O$ | $\delta D$ |
| Jun-04 | -13.8 | -92.2 | | | | | -11.3 | -77.8 | -10.7 | -73.5 | -10.8 | -72.6 |
| Jul-04 | -14.3 | -99.9 | -13.7 | -92.0 | -12.9 | -86.0 | -11.8 | -80.2 | -10.9 | -72.5 | -11.0 | -73.1 |
| Aug-04 | -15.5 | -109.2 | -15.9 | -118.7 | -13.7 | -100.3 | -10.8 | -74.0 | -10.0 | -67.5 | *-10.1* | -67.2 |
| Sep-04 | -15.6 | -108.8 | -15.8 | -114.6 | -13.8 | -98.4 | -11.8 | -80.4 | -10.2 | -68.2 | -10.7 | -71.0 |
| Oct-04 | | | -15.5 | -109.6 | -13.1 | -93.5 | -9.5 | -62.2 | -9.6 | -64.6 | -9.8 | -65.3 |
| Nov-04 | | | -14.1 | -100.0 | | | -8.2 | -54.0 | -9.7 | -65.6 | -9.6 | -64.4 |
| Dec-04 | | | -13.2 | -93.6 | -12.5 | -88.1 | -7.6 | -49.2 | -9.7 | -65.5 | -9.8 | -65.3 |
| Jan-05 | | | -12.4 | -87.4 | -12.4 | -83.6 | -7.4 | -48.5 | -9.7 | -62.9 | -10.0 | -66.9 |
| Feb-05 | | | -13.3 | -88.0 | -12.5 | -84.6 | -7.6 | -49.2 | -9.0 | -57.2 | -9.6 | -64.1 |
| Mar-05 | | | -14.0 | -100.6 | -12.5 | -84.5 | -8.2 | -51.4 | | | -9.6 | -64.1 |
| Apr-05 | | | -13.8 | -96.0 | -12.0 | -81.6 | -8.4 | -52.2 | -9.9 | -62.9 | -9.9 | -67.1 |
| May-05 | -13.5 | -90.0 | -13.7 | -92.7 | -12.5 | -81.8 | -9.3 | -62.2 | -10.4 | -67.0 | -10.2 | -70.1 |
| Jun-05 | -13.2 | -86.8 | | | -12.1 | -83.8 | -10.5 | -71.0 | -10.8 | -69.9 | -10.2 | -70.1 |
| Jul-05 | -15.8 | -110.4 | -15.2 | -104.2 | -13.8 | -97.9 | -12.0 | -86.9 | -10.9 | -73.9 | -12.0 | -88.3 |
| Aug-05 | -15.3 | -101.9 | -14.6 | -108.7 | -13.4 | -93.9 | -12.1 | -84.9 | -11.3 | -78.5 | -11.6 | -84.2 |
| Sep-05 | -16.7 | -122.5 | -16.4 | -122.5 | -15.3 | -107.7 | -13.2 | -89.3 | -11.5 | -80.4 | -9.9 | -73.2 |
| Oct-05 | -15.4 | -110.6 | -15.1 | -106.7 | -13.0 | -91.3 | -10.4 | -69.1 | -10.4 | -70.8 | -10.3 | -67.8 |
| Nov-05 | | | -13.4 | -95.0 | -12.5 | -87.0 | -10.2 | -68.7 | -10.0 | -67.4 | -10.1 | -69.7 |
| Dec-05 | | | -13.2 | -97.1 | -12.4 | -86.6 | -10.8 | -74.3 | -10.1 | -68.3 | -8.6 | -56.8 |
| Jan-06 | | | -12.5 | -88.0 | -12.4 | -80.6 | -10.6 | -72.9 | -10.2 | -70.3 | -9.9 | -65.2 |
| Feb-06 | | | -13.0 | -92.4 | -11.7 | -75.7 | -10.0 | -68.5 | -9.7 | -66.0 | -9.5 | -63.1 |
| Mar-06 | | | -13.1 | -93.3 | -10.9 | -73.0 | -10.6 | -78.2 | -9.9 | -67.7 | -9.2 | -62.1 |
| Apr-06 | -12.8 | -91.4 | -12.1 | -85.3 | -10.6 | -71.0 | -9.8 | -70.6 | -9.5 | -65.7 | -8.8 | -59.0 |
| May-06 | -14.0 | -99.7 | -12.6 | -88.6 | -11.7 | -82.7 | -10.3 | -73.7 | -9.7 | -69.0 | -9.5 | -64.4 |
| Jun-06 | -14.6 | -100.1 | -14.2 | -102.2 | -12.4 | -91.9 | -11.3 | -82.2 | -10.2 | -73.3 | -10.2 | -70.9 |
| Jul-06 | -15.0 | -106.3 | -15.1 | -110.2 | -13.3 | -95.1 | -11.7 | -86.1 | -10.7 | -77.1 | -11.2 | -77.7 |
| Aug-06 | -15.4 | -107.8 | -14.3 | -106.3 | -14.0 | -103.0 | -13.0 | -92.7 | -12.2 | -85.0 | -11.9 | -81.2 |
| Sep-06 | -15.5 | -108.0 | -14.1 | -106.4 | -13.8 | -100.6 | -12.3 | -88.1 | -12.2 | -85.7 | -11.3 | -79.5 |
| Oct-06 | | | -12.8 | -90.3 | -11.9 | -87.9 | -10.2 | -73.0 | -11.8 | -82.0 | -10.9 | -76.2 |
| Nov-06 | | | -13.4 | -95.0 | -11.2 | -77.0 | -9.2 | -67.3 | -11.0 | -75.3 | -11.1 | -76.9 |
| Dec-06 | | | -12.4 | -89.0 | -11.4 | -80.8 | -10.2 | -71.6 | -10.6 | -75.2 | -11.1 | -75.2 |

# CHAPTER 6

## HYDROGRAPH SEPARATION

### 6.1 Introduction

The variation in discharge occurs due to the variations in climatic conditions which affects the contribution of different components to the river discharge. For separating the rainfall contribution to the Bhagirathi River, the isotopic composition of river water and rainfall were studied. The $\delta^{18}O$ of river water was found isotopically different during pre and post events of a rainfall. In order to measure the changes in isotopic composition of river water, the sampling of the river water was carried out during the pre and post rainfall events along with the sampling of the rainfall. The proportion of two components to the total discharge can be separated out using a two components model. The water balance equation can be written as:

$$Q_t = Q_{sm} + Q_r \quad \text{(i)}$$

Where, Q is the discharge component, and subscripts t, sm and r represent total river flow, snow/ice melt and runoff, respectively. Similarly, the isotopic balance equation can be written as

$$\delta_t Q_t = \delta_{sm} Q_{sm} + \delta_r Q_r \quad \text{(ii)}$$

By substituting $Q_r = Q_t - Q_{sm}$ and rearranging the equation (ii), we get

$$Q_{sm} = Q_t(\delta_t - \delta_r)/(\delta_{sm} - \delta_r) \quad \text{(iii)}$$

Using the equation (iii), the runoff component can be separated.

In the case of Bhagirathi River, snow/glacier melt, groundwater (subsurface water) and surface runoff contributes to river discharge in most of the months. Hence, for hydrograph separation, a three components mixing model is derived for the Bhagirathi River basin. The isotopic composition ($\delta^{18}O$) and electrical conductivity of snow/ice melt, rainfall, river and subsurface component were used along with the river discharge for the derivation of the model given below:

$$g_w + g_m + R = Q \quad \text{(i)}$$

$$g_w \delta_{g_w} + g_m \delta_{g_m} + R\delta_R = Q\delta_Q \quad \text{(ii)}$$

$$g_w C_{g_w} + g_m C_{g_m} + RC_R = QC_Q \quad \text{(iii)}$$

Where Q, R, gw and gm are the total river discharge, surface runoff, groundwater and glacier melt contribution in $m^3$/sec and $\delta_Q$, $\delta_R$, $\delta_{g_w}$ and $\delta_{g_m}$ are the corresponding $\delta^{18}O$ values, respectively.

From (i)

$$g_m = Q - R - g_w \quad \text{(iv)}$$

Substituting eq. (iv) in eq. (ii)

$$g_w \delta_{g_w} + (Q - R - g_w)\delta_{g_m} + R\delta_R = Q\delta_Q$$

Rearranging the term, we get:

$$g_w \delta_{g_w} + Q\delta_{g_m} - R\delta_{g_m} - g_w \delta_{g_m} + R\delta_R = Q\delta_Q$$

$$g_w(\delta_{g_w} - \delta_{g_m}) + R(\delta_R - \delta_{g_m}) = Q(\delta_Q - \delta_{g_m}) \quad \text{(v)}$$

Now substituting eq. (iv) in eq. (iii)

$$g_w C_{g_w} + QC_{g_m} - RC_{g_m} - g_w C_{g_m} + RC_R = QC_Q$$

$$g_w(C_{g_w} - C_{g_m}) + R(C_R - C_{g_m}) = Q(C_Q - C_{g_m}) \quad \text{(vi)}$$

From eq. (v)

$$R = \frac{Q(\delta_Q - \delta_{g_m}) - g_w(\delta_{g_w} - \delta_{g_m})}{(\delta_R - \delta_{g_m})} \quad \text{(vii)}$$

Put eq. (vii) in eq. (vi) we get

$$g_w(C_{g_w} - C_{g_m}) + \frac{Q(\delta_Q - \delta_{g_m}) - g_w(\delta_{g_w} - \delta_{g_m})}{(\delta_R - \delta_{g_m})}(C_R - C_{g_m}) = Q(C_Q - C_{g_m})$$

$$g_w\left[(C_{g_w} - C_{g_m}) - (C_R - C_{g_m})\left\{\frac{(\delta_{g_w} - \delta_{g_m})}{(\delta_R - \delta_{g_m})}\right\}\right] + (C_R - C_{g_m})$$

$$= Q\left[(C_Q - C_{g_m}) - (C_R - C_{g_m})\left\{\frac{(\delta_Q - \delta_{g_m})}{(\delta_R - \delta_{g_m})}\right\}\right]$$

$$g_w = Q\left[\frac{(C_Q - C_{g_m}) - (C_R - C_{g_m})\left\{\frac{(\delta_Q - \delta_{g_m})}{(\delta_R - \delta_{g_m})}\right\}}{(C_{g_w} - C_{g_m}) - (C_R - C_{g_m})\left\{\frac{(\delta_{g_w} - \delta_{g_m})}{(\delta_R - \delta_{g_m})}\right\}}\right]$$

### 6.1 Development of Isotopic Indices for Various Component of River Discharge

On the basis of availability of data, the hydrograph separation of Bhagirathi River has been carried out for the period October 2004 to September 2005 at Dabrani and Devprayag station. The different components of river discharge was computed on a fortnightly basis from October 2004 to April 2005, monthly basis during April 2005 and 10 daily basis during the monsoon periods (July-September 2005).

#### 6.1.1 Isotopic indices of snow and ice

At the higher altitudes the melting of snow and ice starts during the ablation period (from May and continues up to October) (Fig 6.1.1). During this period 10 daily basis samples were collected at Gaumukh for isotopic and EC measurements. The river flow is sustained by the melting of snow and glacier during the ablation period provides the isotopic indices of snow and glacier. From October to May, the river discharge become negligible at Gaumukh and the site becomes in accessible due to heavy snowfall. Therefore, the isotopic signature of river at Gangotri during the ablation period along with the snowfall samples collected at Gangotri, Dabrani is taken as the isotopic indices of snow and glacier. The isotopic indices of snow and glacier used for the hydrograph separation are presented in the Table 6.1.1.

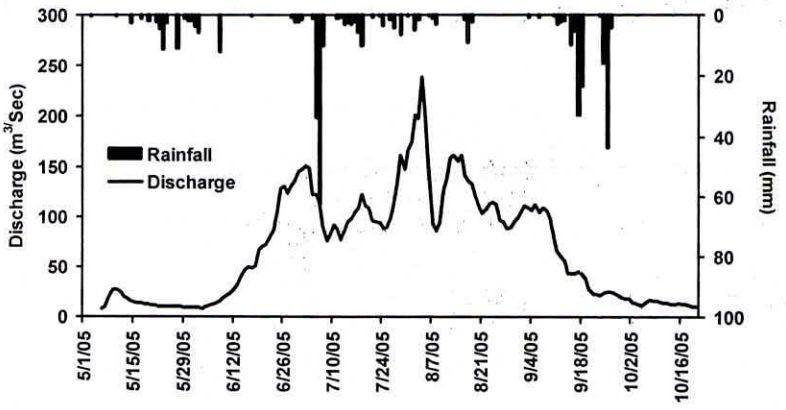


Fig 6.1.1 Rainfall and discharge of Bhagirathi River at Gaumukh

Table 6.1.1: Isotopic indices of snow/glacier, rain, subsurface flow and river at Dabrani

| Date | $\delta^{18}O$ | | | |
|---|---|---|---|---|
| | River | GM | Rain | GW |
| Oct-04 | -13.1 | -14.0 | -13.6 | -12.4 |
| Nov-04 | -12.9 | -14.0 | | -12.4 |
| Dec-04 | -12.5 | -13.2 | | -12.4 |
| Jan-05 | -12.4 | -14.0 | -12.0 | -12.4 |
| Feb-05 | -12.5 | -13.8 | -12.0 | -12.4 |
| Mar-05 | -12.5 | -14.0 | -2.5 | -12.4 |
| Apr-05 | -12.0 | -13.8 | -1.0 | -12.4 |
| May-05 | -12.5 | -14.5 | -2.0 | -12.4 |
| Jun-05 | -12.1 | -13.4 | -4.9 | -12.4 |
| 7/10/2005 | -13.2 | -13.7 | -20.3 | -12.4 |
| 7/20/2005 | -14.2 | -13.7 | -15.6 | -12.4 |
| 7/30/2005 | -14.0 | -15.8 | -13.8 | -12.4 |
| 8/10/2005 | -13.7 | -15.9 | -10.4 | -12.4 |
| 8/20/2005 | -13.1 | -15.2 | -10.2 | -12.4 |
| 8/30/2005 | -13.5 | -14.8 | -10.0 | -12.4 |
| 9/30/2005 | -17.0 | -18.1 | -29.2 | -12 |
| 10/10/2005 | -13.7 | -15.8 | | -12.4 |
| 10/20/2005 | -12.8 | -15.2 | | -12.4 |
| 10/30/2005 | -12.6 | -15.2 | | -12.4 |

### 6.1.2 Isotopic indices of groundwater

In order to develop the isotopic indices of groundwater, samples of springs, spring fed streams and handpumps were analysed and isotopic signatures were estimated. In December and January, the average $\delta^{18}O$ of groundwater was found similar to that of the river at Dabrani. Hence, in these two months, the river flow is sustained only by subsurface flow while other components such as snow/glacier melt and surface runoff are negligible due to the absence of rainfall and low temperature in the winter.

### 6.1.3 Isotopic indices of rain

Rainfall samples at Dabrani (1950 m), Gangotri (3150 m) and Gaumukh (3600 m) were collected for isotopic analysis. The isotopic composition was found to be varying with altitudes and rainfall events (Fig. 6.1.2). The $\delta^{18}O$ of rainfall at the above stations were amont weighted on a ten daily basis, and

these $\delta^{18}O$ were again weighted with respect to the corresponding altitude for obtaining the representative values for the whole catchment (Table 6.1.1). These weighted values of rain were used for the hydrograph separation at Dabrani.

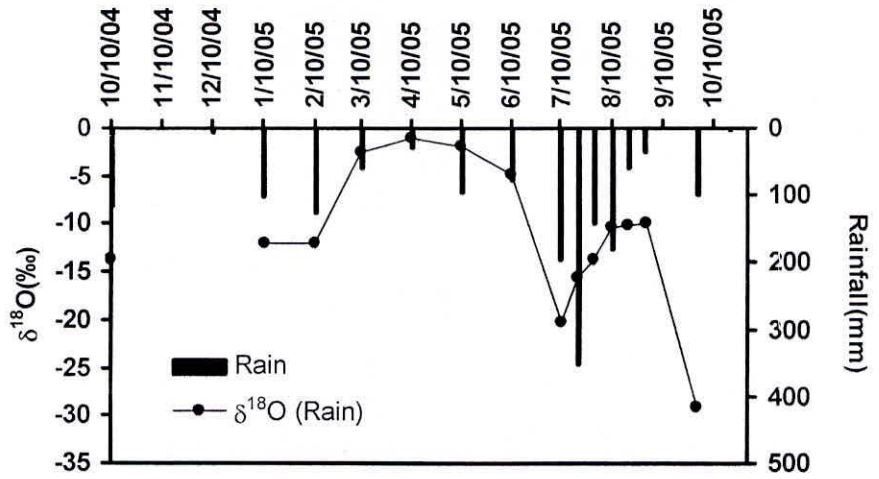


Fig. 6.1.2: Variation of rainfall and $\delta^{18}O$ of river at Dabrani during 2005

### 6.1.4 Isotopic Indices of river

Fortnightly samples during non-rainy months and daily samples during rainy months were collected for isotope analysis from the Bhagirathi River at Dabrani site. The weighted average of river isotopic signature was computed on monthly and 10 daily basis. The discharge data at Dabrani site of river Bhagirathi were collected from CWC, Dehradun office and NTPC, Bhatwari office for the period of 2004 to 2006.

### 6.1.5 Electrical conductivity

The electrical conductivity (EC) of river, snow and glacier melt and groundwater were measured and is given in Table 6.1.2. The EC of Bhagirathi River at Gaumukh during March July is taken as the representative of snow and ice melt runoff. EC of groundwater is derived from the measured EC of various springs, handpump and spring fed streams occurring in the upper reached of Dabrani.

Table 6.1.2: Electrical conductivity of snow/glacier, subsurface flow and river for Dabrani site during Oct.-04 to Oct-05.

| Date | EC(μS/cm) | | |
|---|---|---|---|
| | gm | river | GW |
| Oct-04 | 40 | 121 | 210 |
| Nov-04 | 45 | 142 | |
| Dec-04 | 45 | 163 | |
| Jan-05 | 50 | 230 | 280 |
| Feb-05 | 50 | 221 | 320 |
| Mar-05 | 50 | 180 | 360 |
| Apr-05 | 60 | 150 | 380 |
| May-05 | 60 | 130 | 380 |
| Jun-05 | 50 | 111 | 210 |
| 7/10/2005 | 60 | 100 | 250 |
| 7/20/2005 | 50 | 90 | 250 |
| 7/30/2005 | 50 | 80 | 230 |
| 8/10/2005 | 40 | 70 | 240 |
| 8/20/2005 | 40 | 70 | 240 |
| 8/30/2005 | 40 | 90 | 240 |
| 9/30/2005 | 40 | 140 | 240 |
| 10/10/2005 | 40 | 120 | 200 |
| 10/20/2005 | 50 | 122 | 194 |
| 10/30/2005 | 50 | 121 | 194 |

## 6.2 Hydrograph Separation of Bhagirathi River at Dabrani

In order to separate out the three major components, (i.e., snow/glacier melt, surface runoff and subsurface/groundwater) in the total flow isotopic indices, Ec and discharge data were used in three component model estimation of contribution. The hydrograph of Bhagirathi River at Dabrani site is dominated by multiple peaks of surface runoff occurring during the rainy season (Fig. 6.1.3). The minimum flow is recorded during the winter months of December and January when the other two components mainly runoff and snow/glacier melt are negligible i.e., the river discharge is sustained by the subsurface/groundwater. The river discharge starts increasing from April due to the melting of snow at the lower altitude melt. This increasing trend continues till June when there is very less rainfall. This clearly indicates that the increase in river discharge is due to the contribution of melting of snow and glacier.

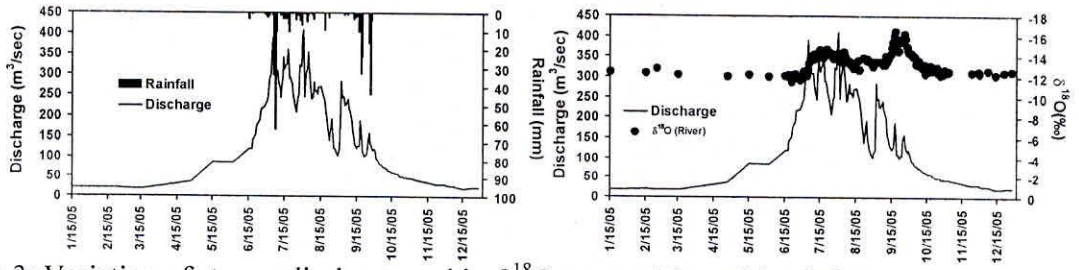


Fig. 6.1.3: Variation of stream discharge and its $\delta^{18}O$ composition with rainfall during in the year 2005.

Maximum river discharge is observed during the rainy season (July, August and September) and the peek flows corresponds to high intensity rain events. A similar trend is seen in the corresponds $\delta^{18}O$ value due to the amount effect (Fig 6.1.3). Using a two components mixing model, the computed maximum runoff contribution to the river discharge is up to 49% on a particular day of rain event.

Similarly, the maximum runoff contribution were computed during three events in 2005. The maximum contribution is found to be varying from 18% to 49% of the total discharge for the rainfall events that occurred during the July to September 2005. This variation is due to variation in amonut and intensity of rainfall.

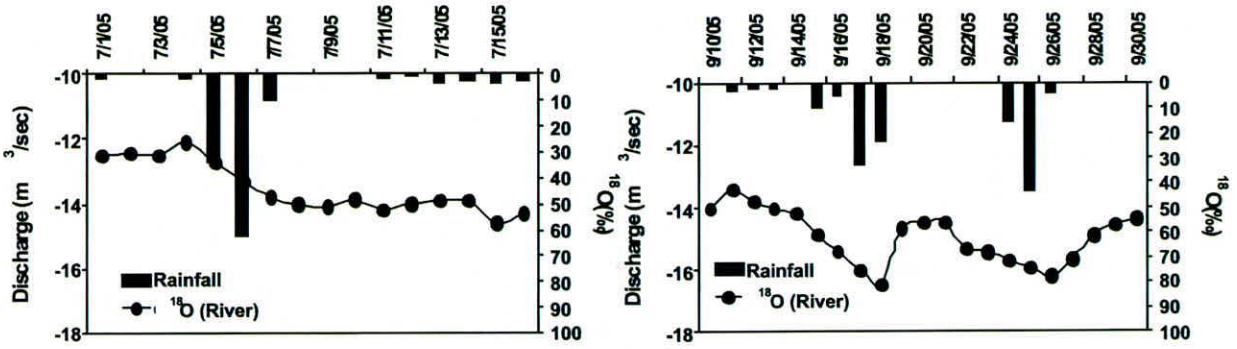


Fig. 6.1.4 Variation of $\delta^{18}O$ values in stream discharge due to rainfall of depleted $\delta^{18}O$ in July and September 2005

Using a three components mixing model on 10 daily basis, the computed surface runoff contribution varied between 7% (April) to 43% (July) with an annual average of 16%. The glacier/snow component was negligible in December/January and a maximum contribution of 64% in May with the an annual average of 35%. The subsurface contribution ranged from 24% in May to 100% in December (Fig 6.1.5). On an average, it comes to 49% of the total annual discharge (Table 6.1.3).

The hydrograph separation clearly indicates that the snow melt started from January and reached a maximum in May. Therefore, if one compares it with the total melt discharge in the ablation period of 2005, it is only about 40% of the total discharge.

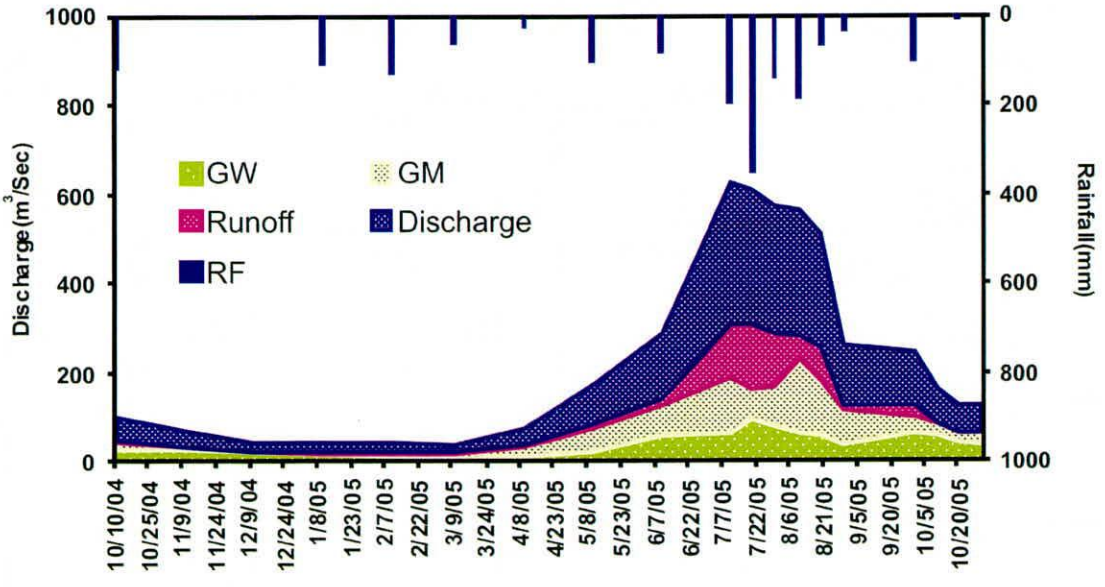


Fig. 6.1.5 Surface runoff, groundwater and glacier melt components separated out using isotopic signatures of stream water, precipitation and geochemical on the basis of daily sampling data during the year 2005 at site Dabrani

Table 6.1.3: Percentage contribution of various components of Bhagirathi River discharge at Dabrani site

| Date | GW(%) | Snow+Glacier Melt(%) | Runoff(%) |
|---|---|---|---|
| Oct-04 | 52 | 30 | 18 |
| Dec-04 | 100 | 0 | 0 |
| Jan-05 | 81 | 4 | 15 |
| Feb-05 | 67 | 15 | 18 |
| Mar-05 | 43 | 50 | 7 |
| Apr-05 | 30 | 59 | 11 |
| May-05 | 24 | 64 | 12 |
| Jun-05 | 41 | 50 | 9 |
| 10-Jul-05 | 22 | 38 | 40 |
| 20-Jul-05 | 32 | 20 | 48 |
| 30-Jul-05 | 28 | 29 | 42 |
| 10-Aug-05 | 22 | 61 | 18 |
| 20-Aug-05 | 22 | 48 | 29 |
| 30-Aug-05 | 27 | 60 | 12 |
| Sep-05 | 53 | 27 | 20 |
| 10-Oct-05 | 71 | 29 | 0 |
| 20-Oct-05 | 67 | 33 | 0 |
| 30-Oct-05 | 57 | 43 | 0 |

## 6.3 Hydrograph Separation at Devprayag

### 6.3.1 Isotopic indices for snow and ice

Discharge data of Bhagirathi river near Gaumukh reveals that melting of snow and ice starts from May and continues up to October i.e., ablation period (Fig 6.1.1). During the ablation period the 10 daily basis samples were collected at Gaumukh for isotopic analysis and EC measurement. The river flows due to melting of snow and glacier during ablation period and it become maximum in July and August. This melt water provides the isotopic composition of snow and glacier join the Bhagirathi river. From October and up to May the discharge become negligible near Gaumukh site due decrease in temperature. Simultaneously, it is not possible to stay during winter period at Gaumukh for collection of the water samples. Therefore, after ablation period, isotopic signatutre of river at Gangotri is used for snow/glacier indices. Further, snowfall samples collected at Gangotri, Dabrani and Uttarkashi sites are used to snow melt component. The indices developed for snow and glacier on monthly basis are presented in table 6.1.4.

### 6.3.2 Isotopic indices for river

For the isotopic characterization of Bhagirathi river, the river water samples were collected fortnightly basis during non rainy season months and on daily basis during rainy searson (June to Setember). The weighted average of river isotopic signature was computed on monthly basis (Table 6.1.4). The discharge of river Bhagirathi were collected from CWC, Dehradun office and NTPC, Bhatwari office for sites Devprayag and Dabrani respectively for the period of 2004 to 2006.

Table 6.1.4: Isotopic indices of snow/glacier, rain, subsurface flow and river for Devprayag site

| Date | $\delta^{18}O$(‰) | | | |
|---|---|---|---|---|
| | River | GM | Rain | GW |
| Oct-04 | -9.8 | -14.0 | -3.0 | -9.8 |
| Nov-04 | -9.6 | -14.0 | | -9.8 |
| Dec-04 | -9.8 | -10.0 | -3.1 | -9.8 |
| Jan-05 | -10.0 | -12.0 | -9.8 | -9.8 |
| Feb-05 | -9.6 | -13.8 | -6.8 | -9.8 |
| Mar-05 | -9.6 | -14.0 | -4.0 | -9.8 |
| Apr-05 | -9.9 | -14.0 | -4.0 | -9.8 |
| May-05 | -10.2 | -14.5 | -1.0 | -9.8 |
| Jun-05 | -10.2 | -13.4 | -1.0 | -9.8 |
| Jul-05 | -12.0 | -14.4 | -12.3 | -9.8 |
| Aug-05 | -11.6 | -15.3 | -9.6 | -9.8 |
| Sep-05 | -16.5 | -17.5 | -25.5 | -9.8 |

### 6.3.3 Isotopic indices for precipitation and groundwater

The results reveal that the discharge in river during December month is sustained by subsurface/groundwater. Therefore isotopic signature of river water of December have been used for subsurface/groundwater signature. The isotopic value of $\delta^{18}O$ of Rain is amount weighted average all stations above the Devprayag. The altitude effect has been also eliminating from the data (Table 6.1.4).

### 6.3.4 Electrical conductivity

The electrical conductivity (EC) of river, snow and glacier melt, rainfall and groundwater were measured from the collected samples. The EC values of river at Gaumukh are taken as representative of snow and ice melt runoff. EC values of rainfall is considered for runoff joining the river. The EC values of groundwater are computed from the measured values of EC of various springs, handpump and spring fed streams occurring in upper reaches of Devprayag. The EC of December months are taken as reprentative of groundwater.

The electrical conductivity (EC) of river, snow and glacier melt, rainfall and groundwater were measured Table 6.1.5. The EC values of river at Gaumukh are taken as representative of snow and ice melt runoff. EC value of groundwater is computed from the measured values of EC of various springs, handpump and spring fed streams occurring in upper reaches of Devprayag.

Table 6.1.5: EC concentration of snow/glacier, subsurface flow and river for Devprayag site.

| Date | EC | | |
|---|---|---|---|
| | River | GM | GW |
| Oct-04 | 131 | 40 | 300 |
| Nov-04 | 139 | 40 | 300 |
| Dec-04 | 140 | 40 | 300 |
| Jan-05 | 130 | 30 | 450 |
| Feb-05 | 183 | 40 | 390 |
| Mar-05 | 190 | 50 | 390 |
| Apr-05 | 200 | 60 | 390 |
| May-05 | 190 | 60 | 380 |
| Jun-05 | 190 | 50 | 320 |
| Jul-05 | 110 | 40 | 250 |
| Aug-05 | 110 | 40 | 250 |
| Sep-05 | 130 | 30 | 190 |

At Devprayag site the hydrograph separation has been carried out using three components model except November, December and April months when two component model is used. The hydrograph of Bhagirathi River at Devprayag site comprise of multiple peaks same as above (Fig. 6.1.6). In starting period January to April the ground water is dominated, the isotopic values ranging -9.4 to -10.1. These values are close to calculated value of groundwater after removing the altitude effect. In May and June month, negligible rain is recorded. As air temperature increases results in melting of snow at higher altitude so snowmelt contribution increase and groundwater component decreases in river due less rainfall in these months. Slight depletion in isotopic values of river water (-9.8‰ and -10.4‰) also reveals the snow melt contribution.

In monsoon period the stream discharge consist depleted isotopic values in the range of -10.1‰ to -12.4‰ from July to September month. The glacier contribution has been recirded maximum in the month of July and August. Therefore, river discharge is greater in the in monsoon period, the isotopic value ranges from-10.1‰ to -12.0‰.

It has been observed that whenever precipitation does not occur after 15th October at the Devprayag, the stream discharge is maximum running due to groundwater, the isotopic value ranging -10.1‰ to -10.9‰.

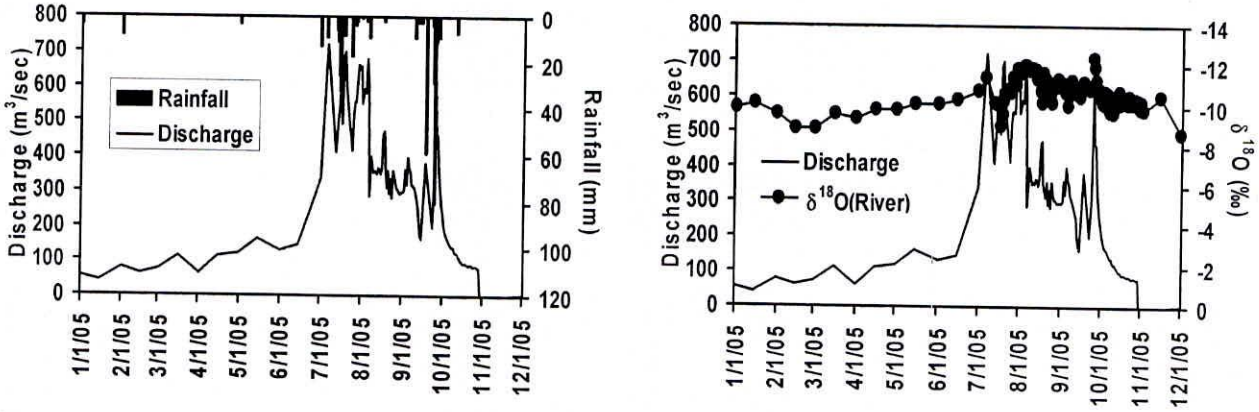


Fig. 6.1.6: Variation of stream discharge and its $\delta^{18}O$ composition with rainfall during ablation period in the year 2005.

The isotopic variations for different events are shown in figure 6.1.7a and 6.1.7b. To separate out the maximum contribution of runoff in river discharge on particular rain events, two components model has been used. The maximum runoff contribution comes out to be 51% of total river discharge. Similarly three more events were used to estimate maximum runoff contribution during year 2005. The maximum contribution has been found 31% to 51% of the total discharge for the rainfall events that occurred during in month July or September in the year 2005. Variation in runoff percentage is due to the amount and intensity variation of rainfall.

Hydrograph seperation is based on monthly weighted average value. In the year 2005, daily isotopic signatures of stream water were measured and the daily based data were converted into monthly. On the monthly basis, contribution of surface runoff varies from 14% to 43% of the total discharge. On average runoff contribution is 19% of the total dischage during the 2005 (Table 6.1.4). The snow and glacier contribution becomes negligible during winter month and maximum snow melt is 60% of the total dischage in April month. The contribution of snow and glacier discharge is estimated 25% of the total discharge during the year 2005.

The groundwater contribution is ranging from 32% to 100%. The maximum contribution of groundwater in December month and minimum in rainy period. If one compares with total discharge in year 2005, it comes about only 56% of the total discharge.

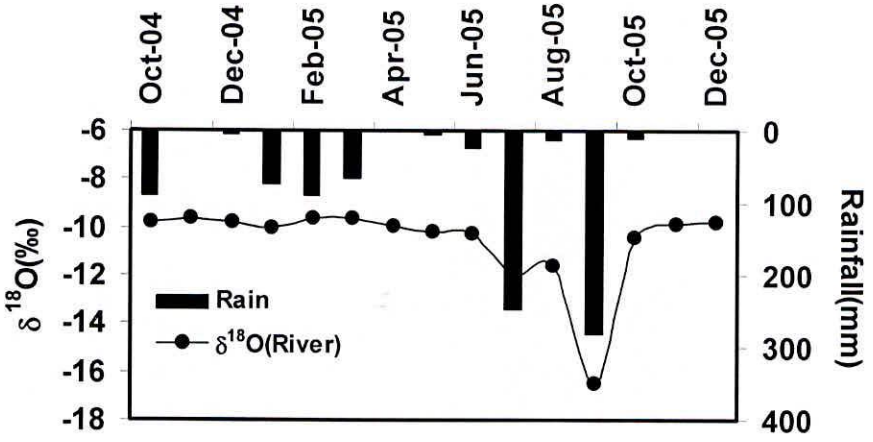


Fig. 6.1.7a Rainfall events and variation of $\delta^{18}O$ composition in precipitation at site Davepryag during the year 2005

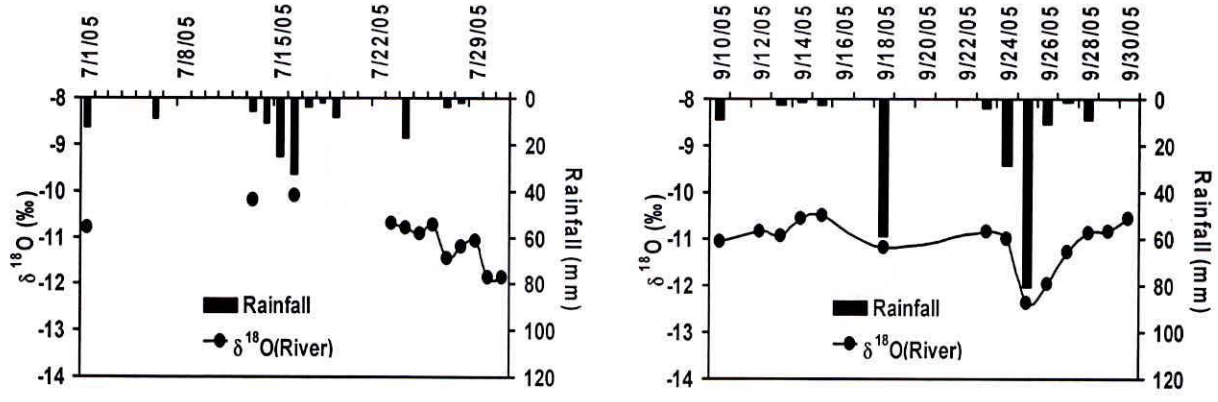


Fig. 6.1.7b Variation of $\delta^{18}O$ values in stream discharge due to rainfall of depleted $\delta^{18}O$ in year 2005

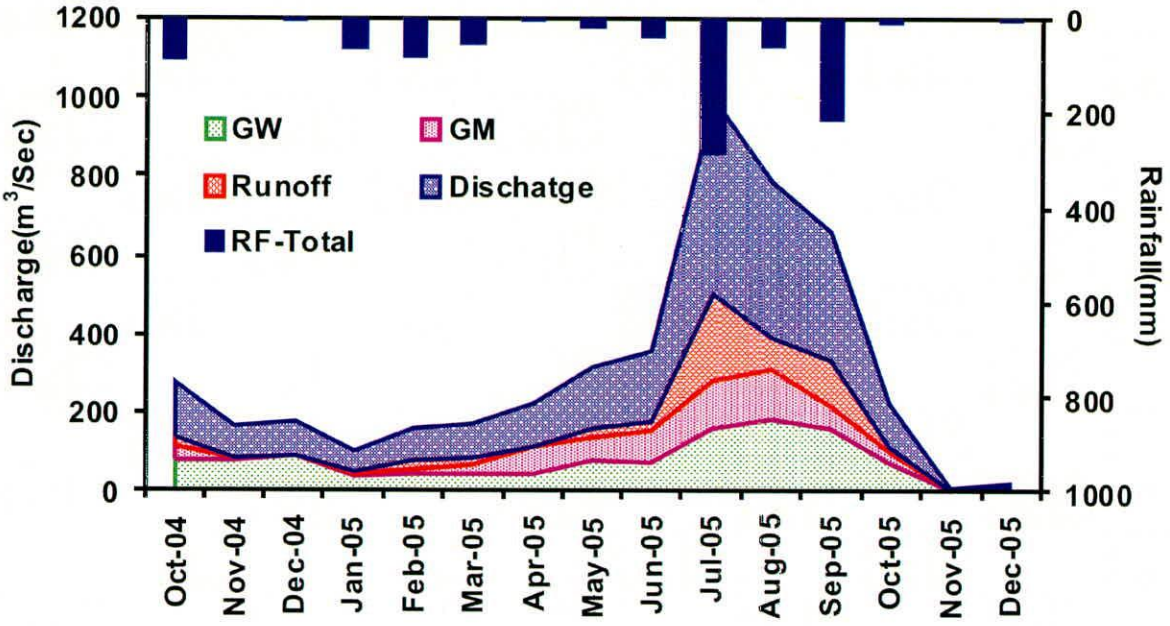


Fig. 6.1.8 Rainfall Runoff, Groundwater and Glacier melt components separated out using isotopic signatures of stream water, precipitation and geochemical on the basis of daily sampling data during the year 2005 at site Devprayag

Table 6.1.6 Different component of hydrograph at Devprayag site

| Date | GW(%) | Snow + Glacier Melt(%) | Runoff (%) |
|---|---|---|---|
| Oct-04 | 56 | 27 | 17 |
| Nov-04 | 95 | 5 | 0 |
| Dec-04 | 100 | 0 | 0 |
| Jan-05 | 65 | 9 | 26 |
| Feb-05 | 49 | 19 | 32 |
| Mar-05 | 50 | 27 | 23 |
| Apr-05 | 40 | 60 | 0 |
| May-05 | 50 | 35 | 14 |
| Jun-05 | 41 | 45 | 14 |
| Jul-05 | 32 | 24 | 43 |
| Aug-05 | 46 | 33 | 21 |
| Sep-05 | 48 | 18 | 34 |

# CHAPTER 7

## STREAM FLOW MODELING USING SNOWMOD AND ANN

### 7.0 Introduction

Modeling of streamflow from a basin is based on transformation of incoming precipitation to outgoing streamflow by considering losses to the atmosphere, temporary storage, lag and attenuation. In most part of the world the seasonal short-term variation in streamflow reflects the variation in rainfall. But in higher latitude and altitudes where snowfall is predominant, runoff depends on heat supplied for snowmelt rather than the timing of precipitation. Hence, to understand the hydrological behavior and to simulate the streamflow it is very important to model the snowmelt runoff. One of the objectives of this study is to simulate the snowmelt runoff in Bhagirathi basin up to Devprayag.

In the last few decades a wide range of hydrological models were proposed for different application from purely statistical methods which neglects the physics of snowmelt process to the complicated energy budget equations. But the most popular among them are the conceptual models, which represent a compromise between scientifically realistic complexity and practically realistic simplicity because of the difficulties in obtaining input data varying in time and space (Sorman, 2005).

The conversion of snow and ice into water is called snowmelt, which needs input of energy (heat). Hence the process of snowmelt is linked to the flow and storage of energy into and through the snowpack (USACE, 1998). The data required to run an energy balance model for snowmelt runoff estimation needs information on air temperature, albedo, solar insolation, wind speed and vapour pressure. The main difficulties faced are to obtain such data in basin scale and extrapolate the point data in areal values. Another difficulty is to obtain such data for highly rugged terrain like Himalaya. Hence application of energy balance equation is limited to small and well-networked watersheds.

The conceptual model fully employs the concept of an "index," where a known variable is used to explain a phenomenon in a statistical rather than in a physical sense. The most commonly available data for any basin is air temperature and it is considered the best index of heat transfer processes associated with snowmelt. This is why temperature indices are most widely used in snowmelt estimation. There are several temperature index based snowmelt models like SNOWMOD, the SSARR Model, the HEC-1 and HEC-1F Models, the NWSRFS Model, the PRMS Model, the SRM, the GAWSER Model. The SRM model is widely used for snowmelt modeling in Himalayan basin. The snowmelt runoff model uses snow-covered area as input instead of snowfall data, but it does not simulate the baseflow component of runoff. In other words, SRM does not consider the contribution to the groundwater reservoir from snowmelt or rainfall, nor its delayed contribution to the streamflow in the form of baseflow, which can be an important component of runoff in the Himalayan rivers, and plays an important role in making these rivers perennial. Almost all the streamflow during winter, when no rainfall or snowmelt occurs, is generated from the baseflow (Singh and Jain, 2003). The SNOWMOD model (Jain, 2001) is unique in this aspect as it simulates all components of runoff, i.e. snowmelt runoff, rainfall-induced runoff and baseflow, using limited data.

### 7.1 Snow melt model (SNOWMOD)

The snowmelt model (SNOWMOD) is a temperature index model, which is designed to simulate daily streamflow for mountainous basins having contribution from both snowmelt and rainfall. The generation of streamflow from such basins involves with the determination of the input derived from snowmelt and rain, and its transformation into runoff. It is a distributed model and for simulating the streamflow, the basin is divided into a number of elevation zones and various hydrological processes relevant to snowmelt and rainfall runoff are evaluated for each zone. The model achieves three operations at each time steps. At first the available meteorological data are extrapolated at different altitude zones. Than the rates of snowmelt is calculated at each time steps. Finally, the snowmelt runoff

from SCA and rainfall runoff from SFA (snow-free area) are integrated, and these components are routed separately with proper accounting of baseflow to the outlet of the basin. The model optimizes the parameters used in routing of the snowmelt runoff and rainfall runoff. Figure 7.1.1 schematically shows the different steps involved with in the model. Details of computation of melt runoff and generation of streamflow from the basin are discussed below.

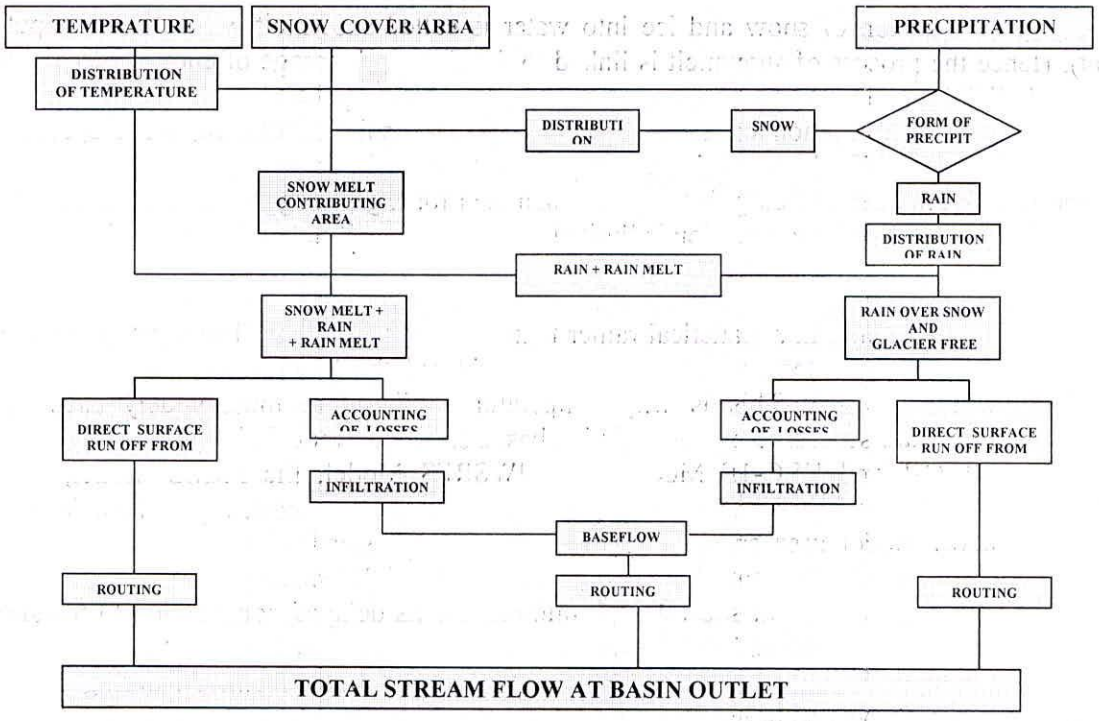


Fig. 7.1.1 Structure of the snowmelt model (SNOWMOD)

### 7.1.1 Input data

In order to execute this SNOWMOD model, the following input data are required:

- Physical features of the basin, which include snow covered area, elevation bands and their areas, altitude of meteorological stations, and other watershed characteristics affecting runoff.
- Time variable data include precipitation, air temperatures, snow-covered area, streamflow data, and other parameters determining the distribution of temperature and precipitation.
- Information on the initial soil moisture status of the basin
- Miscellaneous job control and time control data, which specify such items as total computation period, routing intervals etc.

### 7.1.2 Model variables and parameters

Division of catchment into elevation bands

There are two approaches for defining a computer model of a watershed; a lumped model, which does not take into account spatial variability of processes, and a distributed model, which consider these. Lumped model is a simple approach and can be applied for basins that have a wide variety of physical features. However, the major limitation with this model is that it does not run beyond a single event (USACE, 1998). Distributed model on the other hand can be run for continuous simulation. In such models, the watershed is divided into subunits with variables being computed separately for each. This

method of subdividing the basin is logical one, since in mountainous areas hydrological and meteorological conditions are typically related to elevation.

SNOWMOD is a distributed hydrological model, which allows the basin to be divided into number of bands. The number depends upon the topographic relief of the basin. There is no specified range of altitude for slicing the basin in the bands, but an altitude difference of about 500 to 600 m is considered appropriate for dividing the basin into elevation bands. Moisture input for each band is the sum of snowmelt and rainfall. Runoff for each band is computed from watershed runoff characteristics developed for that particular band. Streamflow for the whole basin is obtained by summing the runoff synthesized for all elevation bands. The program stores a value for each component of flow and each routing increment for every elevation band. It maintains an inventory of snow cover area, soil moisture, snow accumulation, and all other values required for making the computation for the next period.

In the present study, the basin is divided into 9 elevation bands with an altitude difference of 600 m for convenience (Figure 7.1.2). Digital Elevation Model of the study area is used for the preparation of the area-elevation curve, shown in figure 7.1.3. The area covered in each elevation zone of the basin is given in table 7.1.1.

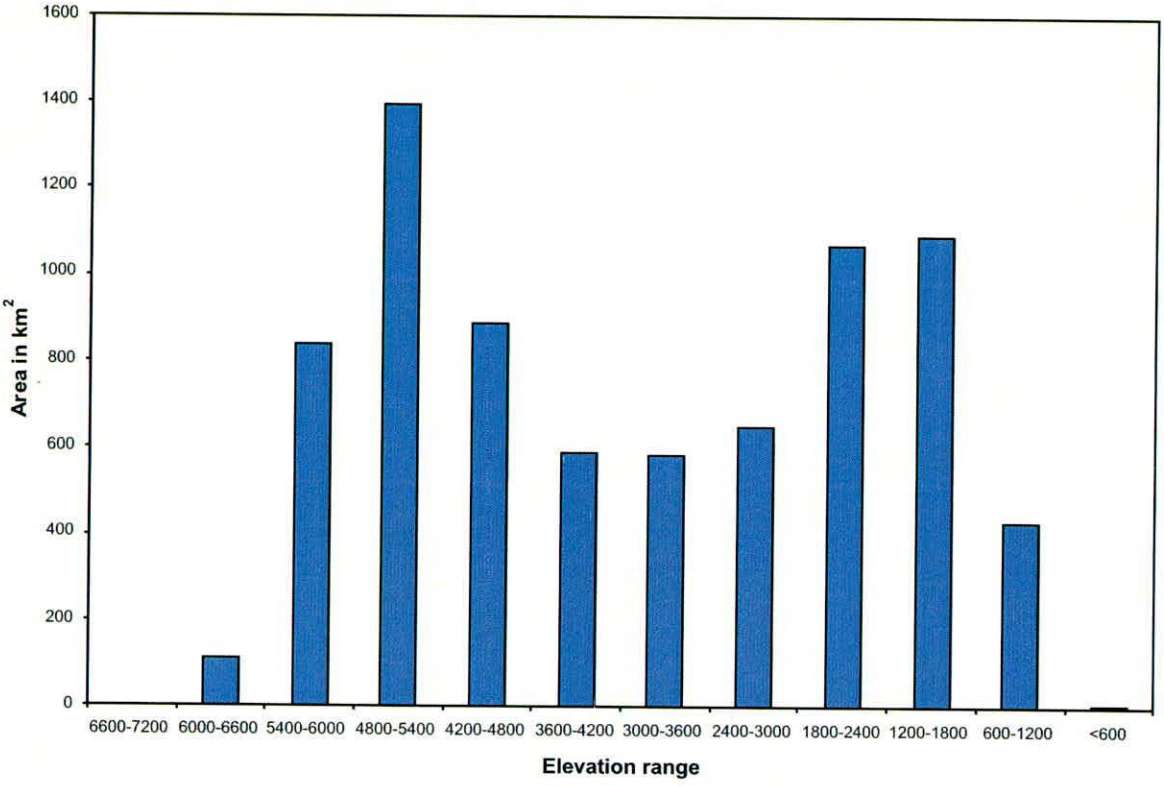


Fig. 7.1.2 The study area divided in 9 elevation band.

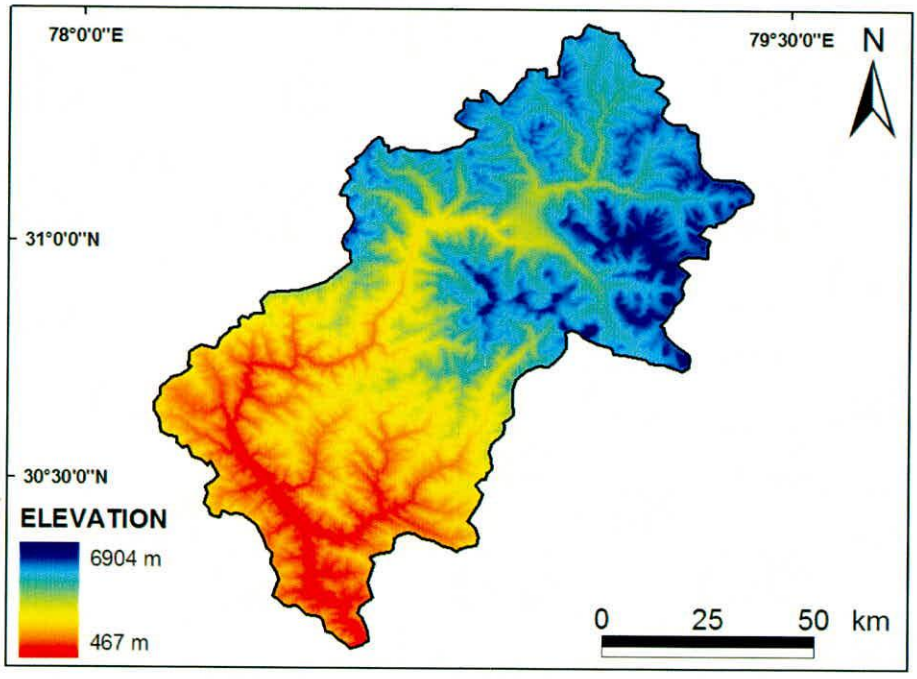


Fig. 7.1.3 Digital Elevation Model of the study area

Table 7.1.1: Bhagirathi basin area covered in different elevation band

| Band | Elevation range(m) | Area Sq. km. |
|---|---|---|
| 1 | <600 | 4.11 |
| 2 | 600-1200 | 429.14 |
| 3 | 1200-1800 | 1091.11 |
| 4 | 1800-2400 | 1070.55 |
| 5 | 2400-3000 | 653.29 |
| 6 | 3000-3600 | 584.49 |
| 7 | 3600-4200 | 590.75 |
| 8 | 4200-4800 | 890.22 |
| 9 | 4800-5400 | 1397.21 |
| 10 | 5400-6000 | 840.89 |
| 11 | 6000-6600 | 108.42 |
| 12 | 6600-7200 | 3.39 |

Precipitation data and distribution

The most challenging object of hydrological simulation of a mountain basin is the measurement of meteorological variables. The major problems posed in high mountain areas are the accessibility to the mountains on a continuous basis, the accuracy of measured meteorological variables, and the areal representativeness of measurements (Panagoulia, 1992). It has been observed that the most important factor in accurate estimation of snowmelt runoff is the assumptions of the spatial distribution and form of precipitation. In a distributed model, it is very essential to distinguish between rain and snow in each elevation band because these two form of precipitation behaves very differently in terms of contribution to the streamflow. Rainfall is contributed faster to the streamflow whereas snowfall is stored in the basin until it melts. The form of precipitation is influenced by two factors; meteorological and topographical. Meteorological factor includes air temperature, lapse rate, wind etc and topographical factors include elevation, slope, aspect, vegetation cover etc. Snow falling through warmer atmosphere or melting level air temperature melts and falls as rain. Similarly, snow falls at elevation above melting level and rain falls at elevation below melting level.

For the present study, the daily precipitation data were available for four stations within the study area namely, Devprayag, Tehri, Uttarkashi and Gangotri (Table 7.1.2). The rain gauge has been assigned to the different bands based on its proximity to the respective band according to altitude of the station. A critical temperature, $T_c$, is specified in the model to determine whether the measured precipitation is rain or snow. In the present study, $T_c$ is considered to be 2°C as suggested by Singh and Jain, 2003. The algorithm used in the model to determine the form of precipitation is as follows:

Table 7.1.2: Raingauge stations used for different elevation band

| Band | Elevation range(m) | Location of Raingange |
|---|---|---|
| 1 | <600 | Devprayag |
| 2 | 600-1200 | Tehri |
| 3 | 1200-1800 | Uttarkashi |
| 4 | 1800-2400 | Uttarkashi |
| 5 | 2400-3000 | Uttarkashi |
| 6 | 3000-3600 | Uttarkashi |
| 7 | 3600-4200 | Gangotri |
| 8 | 4200-4800 | Gangotri |
| 9 | 4800-5400 | Gangotri |
| 10 | 5400-6000 | Gangotri |
| 11 | 6000-6600 | Gangotri |
| 12 | 6600-7200 | Gangotri |

If $T_m \geq T_c$, all precipitation is considered as rain

If $T_m \leq 0°C$, all precipitation is considered as snow

where $T_m$ is mean air temperature. In the cases $T_m \geq 0°C$ and $T_m \leq T_c$, the precipitation is considered as a mixture of rain and snow and their proportion is determined as follows:

$$\text{Rain} = \frac{T_m}{T_c} \times P \quad (1)$$

$$\text{Snow} = P - \text{Rain} \quad (2)$$

where P is the total observed precipitation.

Temperature data – Space and time distribution and Lapse Rate

Air temperature has a logical connection with many of the energy exchanges involved in snowmelt. Also it is the meteorological variable which is readily available to hydrologists in historical and near real time. Hence air temperature is the most widely used index in snowmelt (Sorman, 2005). Daily mean temperature is the most commonly used parameter in snowmelt computation. For the present study daily mean air temperature was calculated by using the equation given below

$$T_{air} = T_{mean} = \frac{(T_{max} + T_{min})}{2} \quad (3)$$

For the study area the daily maximum and minimum air temperature data were available for one meteorological station namely Devprayag. Daily mean air temperature was calculated using equation 3. As mentioned earlier the basin is divided into twelve elevation bands. For corresponding band, the temperature data was interpolated using the air temperature data of Devprayag station and lapse rate data.

The rate with which the temperature changes with increase in elevation is called as lapse rate. Lapse rate is not a constant value but changes with season and region. Lapse rates are known to be quite variable, ranging from high values of about the dry adiabatic lapse rate to low values representing inversion conditions. For example, during continuous rainstorm conditions the lapse rate will approximate the saturated adiabatic rate, whereas under clear sky, dry weather conditions, the lapse rate during the warm part of the day will tend to the dry adiabatic rate. During the night, under clear sky conditions, radiation cooling will cause the temperature to fall to the dew point temperature, and this is

particularly true for a moist air mass. As a result, night-time lapse rates under clear skies will tend to be quite low, and at times even zero lapse rates will occur (Jain, 2001).

The daily temperature in the various elevation bands have been calculated by using the temperature lapse rate approach, by extending data from the base station by the following equation,

$$T_{i,j} = T_{i,base} - \delta(h_j - h_{base}) \quad (4)$$

Where,

$T_{i,j}$ = daily mean temperature on $i^{th}$ day in $j^{th}$ zone (°C)
$T_{i,base}$ = daily mean temperature (°C) on $i^{th}$ day at the base station
$h_j$ = zonal hypsometric mean elevation (m)
$h_{base}$ = elevation of base station (m)
$\delta$ = Temperature lapse rate in °C per 100 m

Degree days

Degree-days are the departures of temperature above or below a particular threshold value. Generally a threshold temperature of 0°C is used, with snowmelt considered to have occurred if the daily mean temperature is above 0°C. This follows from the idea that most snowmelt results directly from the transfer of heat from the air in excess of 0°C. The difference between the daily mean temperature and this threshold value is calculated as the degree-day. Snowmelt-runoff models, which incorporate a degree-day or temperature index, routine are the most commonly used in operational hydrology and have been successfully, verified world-wide over a range of catchment sizes, physical characteristics and climates (WMO, 1986; Bergstrom, 1992; Rango, 1992, Davies, 1997). An early application of a degree-day approach was made by Finsterwalder and Schunk (1887) in the Alps and since then this approach has been used widely all over the world for the estimation of snowmelt (Martinec et al., 1994; Quick and Pipes, 1995). The basic form of the degree-day approach is:

$$M = D(T_{air} - T_{melt}) \quad (5)$$

Where, M = daily snowmelt (mm/day)
D = degree-day factor (mm ° $C^{-1}$ $day^{-1}$)
$T_{air}$ = index air temperature (°C)
$T_{melt}$ = threshold melt temperature (usually, 0°C)

Although air temperature and other hydrological variables vary continuously throughout the day, the daily mean air temperature is the most commonly used index temperature. When daily maximum ($T_{max}$) and minimum ($T_{min}$) air temperature is available, daily mean air temperature is calculated as:

$$T_{air} = T_{mean} = \frac{(T_{max} + T_{min})}{2} \quad (6)$$

Degree Day Factor

The degree-day method is popular because temperature is a reasonably good measure of energy flux, and, at the same time, it is a reasonably easy variable to measure, extrapolate, and forecast (Martinec and Rango, 1986). The degree-day factor, D, is an important parameter for snowmelt computation and converts the degree-days to snow melt expressed in depth of water. D is influenced by the physical properties of snowpack and because these properties change with time, therefore, this factor also changes with time. The seasonal variation in melt factor is well illustrated by the results obtained from the study reported by Anderson (1973); the lower value being in the beginning of melt season and higher towards the end melt season. A wide range of a values has been reported in the literature with a generally increase as the snowpack ripens. For example, Garstaka (1964) reported extreme values of Df as low as 0.7 mm °C-1 d-1 and as high as 9.2 mm °C-1 d-1. Yoshida (1962) reported the values of D to be between 4.0-8.0 mm °C-1 day-1, depending on the location, time of year and meteorological conditions. Singh and Kumar (1996) determined the D factor by monitoring a known snow surface area

of the snow block within the snowpack at an altitude of about 4000m in the western Himalayan region in the summer. The mean daily value of the D was computed to be 5.94 mm °C-1 day-1, while for a dusted block it increased to 6.62 mm °C-1 day-1. In glacierized basins, the degree-day factor usually exceeds 6 mm °C-1 d-1 towards the end of summer when ice becomes exposed (Kotlyakov and Krenke, 1982). As discussed above that D changes with season, therefore, when using degree-day approach, changes in D with season should be taken into account. In the present study in the starting of melt season for every month low value of degree-day factor has been taken and it go on increasing till the end of melt season i.e. the month of September. The range of the values of degree-day factors used in this study is given Table 7.1.3.

Table 7.1.3: Parameter values used in calibration of model

| S. No. | Parameter | Symbol | Value |
|---|---|---|---|
| 1. | Degree-day factor | D | 1.0 – 4.0 mm.$^{o}C^{-1}$.$day^{-1}$ |
| 2. | Runoff coefficient for rain | $C_r$ | 0.40 - 0.70 |
| 3. | Runoff coefficient for snow | $C_S$ | 0.50 – 0.80 |
| 4. | Temperature lapse rate | $\delta$ | Seasonally varying |
| 5. | Critical temperature | $T_c$ | 2° C |
| 6. | Number of linear reservoirs for snow free area | $N_r$ | 2 |
| 7. | Number of linear reservoirs for snow covered area | $N_S$ | 1 |
| 8. | Number of linear reservoirs for subsurface flow | $N_b$ | 1 |

### 7.1.3 SCA Estimation using satellite data

Snow maps derived from satellite data are a pixel-based representation of a snow-covered area. With spatial resolution of a few hundred meters up to one kilometer, a pixel, either classified as 'snow' or 'no-snow', often consists of snow-covered and snow-free parts. In theory, the snow line defines the line separating snow-covered from snow-free areas. However, because of the patchiness of the edge of the snow cover, no distinct line can be drawn. Instead, a more or less narrow belt has to be defined as the snow line, which represents a zone of approximately 50% snow coverage.

The Normalized Difference Snow Index (NDSI) uses the above spectral characteristics of snow and is based on the concept of Normalized Difference Vegetation Index (NDVI) used in vegetation mapping from remote sensing data (Dozier, 1989: Hall et al., 1995, Gupta et al., 2005). The NDVI is defined as the difference of reflectance observed in a visible band and the short-wave infrared band divided by the sum of the two reflectance (Gupta et al., 2005). The equation is given below:

$$NDSI = \frac{\text{Visible Band} - \text{SWIR Band}}{\text{Visible Band} + \text{SWIR Band}}$$

NDSI maps were prepared from NOAA-AVHRR images. The NDSI map was further classified into two classes: (a) snow and (b) snow-free area based on threshold value of 0.4 (Dozier, 1989). This type of classification provided an advantage of SCA estimation under mountain shadow condition and discrimination between snow and cloud.

The MODIS snowcover product is a classified image. The images were further classified by clubbing snow and lake ice into snow category and rest of the classes into non-snow category. The cloud pixels were clubbed into non-snow category. Thus all the images were classified into snow and non-snow category. Using the classified snow maps, the total percentage of snowcover in the study area was estimated for the year 2004-2005 and shown in Figure 7.1.4 (a & b).

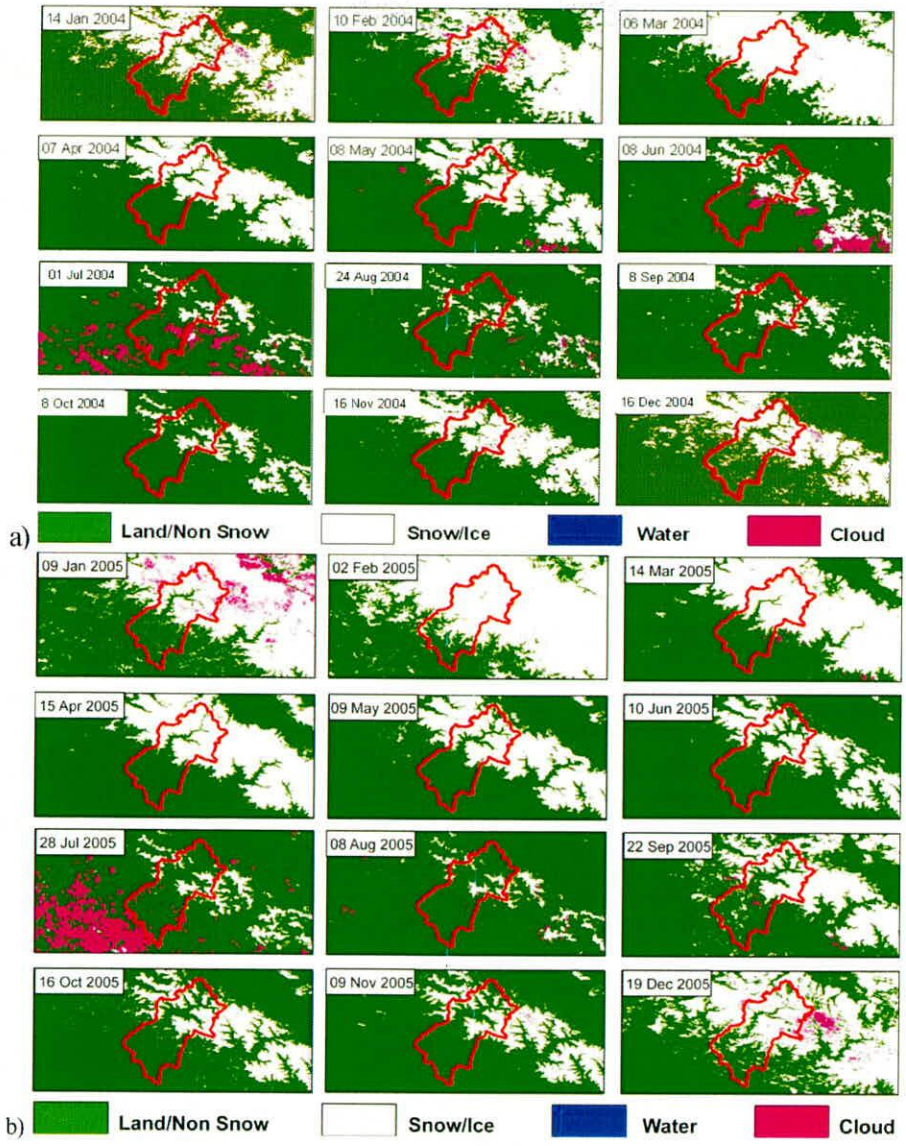


Fig. 7.1.4 (a & b): Variation of snow in different month during year 2004-2005.

One set of SRTM-DEM was resampled to 500 m pixel size to match it with the spatial resolution of the MODIS (MOD11A1) data. In the present study, the SCA has been used for different elevation zones. For this purpose, DEM and SCA maps have been processed for all the dates. As discussed earlier the basin is divided into ten elevation zones. The SCA in each elevation bands were plotted against the elapsed time to construct the depletion curves for the various elevation bands in the basin for all the years. The snow cover depletion curves vary significantly from year to year and hence it has been made separately for each year under consideration. In order to simulate runoff on daily scale from the basin, daily SCA for each band was used as input to the model.

Rain on snow

Rain-on-snow event is hydrologically an important phenomenon as most of the floods in British Columbia, Washington, Oregon and California were reported to have occurred due to this event (Colbeck, 1975; Kattelmann 1987; Brunengo, 1990; Berg et al., 1991; Archer et al., 1994). Further, this event is one of the prime causes of avalanches as rain falling over snow weakens the bond between the snowpacks thereby reducing the mechanical strength of the snowpack (Conway et. al, 1988; Heywood, 1988; Conway and Raymond, 1993).

snowpacks thereby reducing the mechanical strength of the snowpack (Conway et. al, 1988; Heywood, 1988; Conway and Raymond, 1993).

When rain falls on snowpack it is cooled to the temperature of snow. The heat transferred to the snow by rainwater is the difference between its energy content before falling on the snow and its energy content on reaching thermal equilibrium within the snowpack. For snowpacks isothermal at 0°C, the release of heat results in snowmelt, while for the colder snowpack this heat tends to raise the snowpack temperature to 0°C. In case the snowpack is isothermal at 0°C, the melt occurring due to rain is computed by (Jain, 2001)

$$M_r = \frac{4.2\,T_r P_r}{325} \tag{7}$$

where

$M_r$ = melt caused by the energy supplied by rain (mm/day)
$T_r$ = temperature of the rain (°C)
$P_r$ = depth of rain (mm $day^{-1}$)

Only high rainfall events occurring at higher temperatures would cause the melting due to rain, otherwise this component would not be significant (Singh et al., 1997).

### 7.1.4 Computation of different runoff components

The streamflow from a snowfed river has three components namely,

- runoff from the snow-covered area,
- runoff from snow free-area and
- baseflow

The runoff contributed from all the three components are computed separately for each elevation band and the output from all the bands are integrated to provide the total runoff from the basin.

Surface runoff from snow covered area

Runoff contributed from snow-covered area consists of

- Snowmelt triggered by the increase in air temperature above melting temperature
- Under rainy conditions, melt caused by the heat transferred to the snow surface by the rain
- Runoff from the rain itself falling over snow covered area

(a) Snowmelt caused by the increase in air temperature has been estimated by degree-day approach. In this approach degree-day factor is used to convert degree-day into snow expressed in depth of water.

- $$M_{s,i,j} = C_{s,i,j} D_{i,j} T_{i,j} S_{c,i,j} \tag{8}$$

Where,

$M_{s,i,j}$ = snowmelt on $i^{th}$ day for $j^{th}$ band (mm)
$C_{s,i,j}$ = coefficient of runoff for snow on $i^{th}$ day for $j^{th}$ band
$D_{f,i,j}$ = degree-day factor on $i^{th}$ day for $j^{th}$ band ($mm.^{o}C^{-1}d^{-1}$)
$T_{i,j}$ = temperature on $i^{th}$ day for $j^{th}$ band (°C)
$S_{c,i,j}$ = Ratio of snow covered area to the total area of $j^{th}$ band on $i^{th}$ day

(b) Runoff depth from the snowmelt contributed by the heat transferred from rain falling over a snowpack is given by the equation described in section 6.5.7

$$M_{r,i,j} = \frac{4.2\,T_{i,j} P_{i,j} S_{c,i,j}}{325} \tag{9}$$

where, $M_{r,i,j}$ = snowmelt due to rain on snow on $i^{th}$ day for $j^{th}$ band (mm)

(c) Runoff depth from rain itself falling over the snow-covered area, $R_s$, is given by

$$R_{s,i,j} = C_{s,i,j} P_{i,j} S_{i,j} \quad (10)$$

For the computation of runoff from rain, the coefficient $C_s$ is used (not the rainfall runoff coefficient, $C_r$), because the runoff from the rain falling on the SCA behaves like the runoff from the melting of snow.

The daily total discharge from the SCA is computed by adding the contribution from each elevation zone. Thus, discharge from the SCA, $Q_{SCA}$, for all the zones are given by:

$$Q_{SCA} = \alpha \sum_{j=1}^{n} (M_{s,i,j} + M_{r,i,j} + R_{s,i,j}) A_{SCA,i,j} \quad (11)$$

Where, n = total number of zones
$A_{SCA}$ = snow-covered area ($km^2$) in the $j^{th}$ zone on the $i^{th}$ day
$\alpha$ = factor (1000/86400 or 0.0116) used to convert the runoff depth (mm $day^{-1}$) into discharge ($m^3$ $s^{-1}$).

This discharge is routed to the outlet of the basin following the procedure described in the next section.

Surface runoff from snow-free area

The only source of surface runoff from snow-free area (SFA) is rainfall. Like snowmelt runoff computations, runoff from the SFA was computed for each zone using the following expression:

$$R_{f,i,j} = C_{r,i,j} P_{i,j} S_{f,i,j} \quad (12)$$

where, $C_{r,i,j}$ = coefficient of runoff for rain on $i^{th}$ day for $j^{th}$ band
$P_{i,j}$ = rainfall on snow on $i^{th}$ day for $j^{th}$ band (mm)
$S_{f,i,j}$ = Ratio of snow free area to the total area of $j^{th}$ band on $i^{th}$ day.

Because SCA and SFA are complimentary to each other, $S_{f,i,j}$ can be directly calculated as $1 - S_{c,i,j}$. The total runoff from SFA, $Q_{SFA}$ for all the zones is thus given by:

$$Q_{SFA} = \alpha \sum_{j=1}^{n} R_{f,i,j} A_{SFA,i,j} \quad (13)$$

Where, $A_{SFA,j,j}$ = snow-free area in the $j^{th}$ zone on the $i^{th}$ day

The discharge from the SFA was also routed to the outlet of the basin before adding it to the other components of discharge.

Estimation of subsurface runoff

The subsurface flow or baseflow represents the runoff from the unsaturated zone of the basin to the streamflow. After accounting for the direct surface runoff from snowmelt and rainfall, the remaining water contributes to the groundwater storage through infiltration and appears at the outlet of the basin with much delay as subsurface flow or baseflow. Depletion of this groundwater storage also results from evapo-transpiration and percolation of water to the deep groundwater zone. It is assumed that half of the water percolates down to shallow groundwater and contributes to baseflow, while the rest is accounted for by the loss from the basin in the from of evapo-transpiration and percolation to the deep groundwater aquifer, which may appear further downstream or become part of deep inactive groundwater storage. The depth of runoff contributing to baseflow from each zone is given by:

$$R_{b,i,j} = \beta[(1 - C_{r,i,j})R_{f,i,j} + (1 - C_{s,i,j})M_{t,i,j}] \quad (14)$$

where $M_{t,i,j} = M_{s,i,j} + M_{r,i,j} + R_{s,i,j}$ and $\beta$ is 0.50. The baseflow, $Q_b$, is computed by multiplying the depth of runoff by the conversion factor $\alpha$ and area, and is given as:

$$Q_b = \alpha \sum_{j=1}^{n} R_{b,i,j} A_{i,j} \quad (15)$$

where A is the total area ($km^2$) and represents the sum of $A_{SCA}$ and $A_{SFA}$. This component is also routed separately.

Total runoff

The daily total streamflow from the basin is calculated by adding the three different routed components of discharge for each day.

$$Q = Q_{sca} + Q_{sfa} + Q_b \quad (16)$$

As discussed above, the direct runoff results from overland or near surface flow, while baseflow is regarded as being a result of groundwater contribution into the stream. Infact, the contribution to baseflow starts only after the topsoil is saturated. In order to consider the soil moisture deficit, soil moisture index (SMI) has been considered in the present study. The routing of surface and subsurface runoff has been carried out separately and described in the following sections.

### 7.1.5 Efficiency criteria of the model

Numerous statistical criteria are available for numerical evaluations of model accuracy in each single year, in a particular season of the year, or a sequence of years or seasons. In a study of snowmelt models, the World Meteorological Organization (WMO, 1986) suggests several efficiency criteria that are particularly useful for snowmelt modeling. The most important criteria for model evaluation identified in the WMO study are the visual inspection of linear scale plots of simulated and observed hydrographs. Several numerical criteria are also identified as useful for model evaluation.

The model performance on a daily basis is commonly evaluated using the non-dimensional Nash-Sutcliffe '$R^2$' value (Nash and Sutcliffe, 1970) as given by the equation,

$$R^2 = 1 - \frac{\left\{\sum_{t=1}^{n} (Q_0 - Q_e)^2\right\}}{\left\{\sum_{t=1}^{n} (Q_0 - \bar{Q}_0)^2\right\}} \quad (17)$$

Where, $R^2$ = Nash-Sutcliffe coefficient of goodness of fit

$Q_0$ = daily observed discharge from the basin

$Q_e$ = daily estimated discharge from the basin

$\bar{Q}_0$ = mean of observed discharge

n = number of days of discharge simulation

The value of Nash-Sutcliffe coefficient is analogous to the coefficient of determination and is a direct measure of the proportion of the variance of the recorded flows explained by the model.

The model performance on a seasonal basis can also be determined by computing the percentage volume difference between the measured and computed seasonal runoff as,

$$D_v = \frac{\left\{\sum_{t=1}^{n} Q_0 - \sum_{t=1}^{n} Q_e\right\} 100}{\left\{\sum_{t=1}^{n} Q_0\right\}} \qquad 18$$

Where, $D_v$ is the percentage volume difference between the measured and computed seasonal runoff.

### 7.1.6 Simulation of streamflow

The model was simulated for one year 2004-2005. The results of simulation are shown in Figure 7.1.5. In this figure stream flow from snowmelt, rainfall and base flow have been shown separately. The estimated and observed hydrograph shows good matching for the year 2004-2005. The efficiency (R2) of the model for this year is 0.86, while difference in volume is 1.16% and RMSE is 0.38. The results indicate good performance of the model. A close observation of rainfall and stream flow data indicates that most of the peaks in the stream flow were because of rainfall.

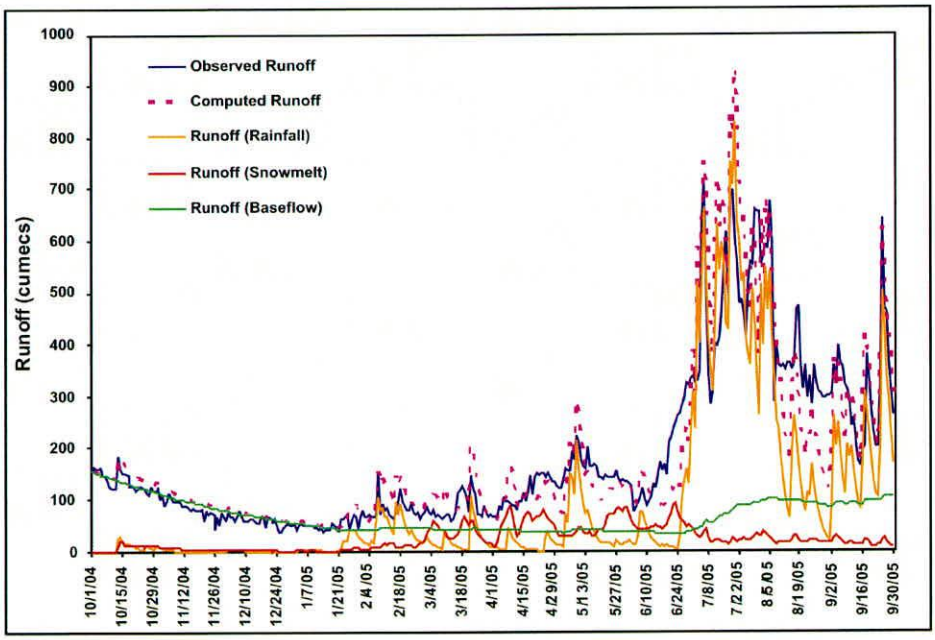


Fig. 7.1.5 Computed discharge using SNOWMOD model with observed discharge of Bhagirathi River at Devprayag

## 7.2 Snow Melt Runoff Modelling Using Artificial Neural Networks

Snowmelt runoff estimates are of high interest for flood warning and management of reservoirs for hydropower generation in drainage basins with significant snowmelt contribution. The rivers originate from Himalayas receive a significant flow from snow melt. The estimation of snow melt runoff in Bhagirathi River helps in operating the Tehri reservoir, useful in planning the hydropower power projects upstream of Tehri reservoir and regulating the flow in the Ganga Canal (Arora, 2008). Conceptual models such as Snowmelt Runoff Model (SRM) (Martinec et al, 2007) and SNOWMOD (Arora, 2008) have been developed to simulate the snow melt runoff using elevation, rainfall, aspect, temperature and snow cover area as input. Development and application of conceptual models for the simulation of snow melt runoff require physical understanding of the process and generation of large quantity of data. Recently, neural networks approach has been applied in many areas of water resources due to its capability in representing any nonlinear processes by given sufficient complexity of the trained networks (Maier and Dandy, 2000). ANNs are proven to produce improved performance over other

traditional models such as conceptual models and black box models, in numerous hydrological studies (Hsu et al., 1995). The main advantage of the ANN models over traditional models is that it does not require information about the complex nature of the underlying process under consideration to be explicitly described in mathematical form. ANNs have found applications in various fields such as pattern recognition, non-linear modelling, classification, association, control. Some of the applications in hydrological studies are rainfall-runoff modeling, rainfall prediction, flood forecasting, water quality modeling, ground water modeling, development of water management policy, suspended sediment concentration, snow melt runoff modelling and reservoir operation studies. (Jain et al, 1999; Kisi,2004 and Kisi, 2005; Maier and Dandy, 2000; Nagy et al., 2002; Parent et al, 2008; Raman et al, 1996; Tayfur et al., 2003; Tokar and Johnson, 1999; ). Tokar and Johnson (1999) developed ANN model for simulating the snowmelt runoff with observed temperature, precipitation (rain plus snow), snowmelt runoff as inputs. They compared the results of ANN with conceptual and regression model and found the ANN performed better than both the traditional models. Parent et al (2008) simulated the snow melt runoff using ANN model with the inputs as considered by Tokar and Johnson (1999) in addition to the snow covered area and they also found that ANN model performed better than other models considered in the study. This chapter discusses the development of ANN models for the prediction of snow melt runoff at Gaumukh and Devprayaag located along the course of Bhagirathi River.

### 7.2.1 ANN – An overview

ANNs are a form of computing inspired by the functioning of the brain and nervous system and are discussed in detail in a number of hydrologic papers, for example, Portugal, 1995; Minns and Hall, 1996; See et al, 1997; Danh et al, 1998; Zealand et al, 1999; ASCE, 2000a,b; Maier and Dandy, 2000; Elshorbagy, 2000. The architecture of a feed forward ANN can have many layers where a layer represents a set of parallel neurons. The basic structure of ANN usually consists of three layers: the input layer, where the data are introduced to the network; the hidden layer or layers, where data are processed; and the output layer, where the results of given outputs are produced. The neurons in the layers are interconnected by strength called weights. A typical three-layered feed forward ANN is shown in Fig. 7.2.1.

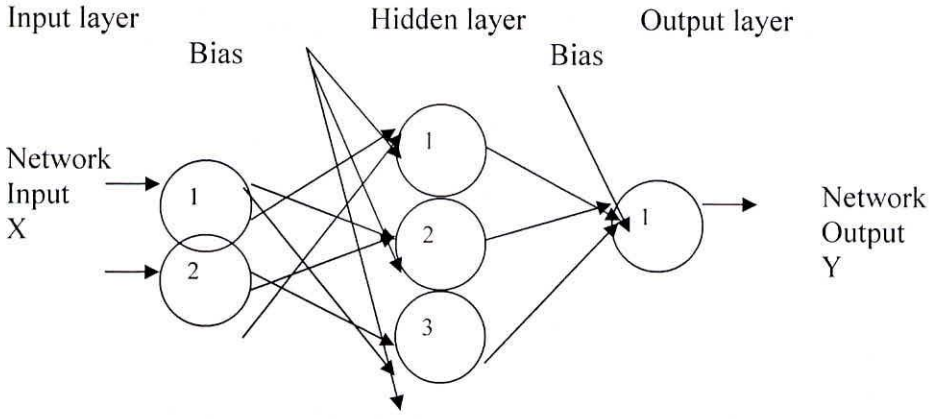


Fig. 7.2.1 A Typical Three-Layer Feed Forward ANN (ASCE, 2000a)

In general, a neuron can have n inputs, labeled from 1 through $n$. For example neuron 3 in the hidden layer shown in Fig. 1, n= 2. In addition, each neuron has an input that is equal to 1.0, called *bias*. Each neuron $j$ receives information from every node $i$ in the pervious layer. A weight ($w_{ji}$) is associated with each input ($x_i$) to node $j$. The effective incoming information ($NET_j$) to node $j$ is the weighted sum of all incoming information, otherwise known as the net input, and is computed as:

$$NET_j = \sum_{i=0}^{n} w_{ji} x_i \qquad (1)$$

where $x_0$ and $w_{j0}$ are called as the bias term ($x_0 = 1.0$) and the bias respectively. Equation 1 applies to the nodes in the output layer and hidden layer(s). The weighted sum of input information is passed through an activation function, called transfer function, to produce the output from the neuron. The transfer function introduces some nonlinearity in the network, which helps in capturing the nonlinearity present in the function being mapped. The commonly employed transfer function is the sigmoid function (ASCE, 2000a) and is given as follows:

$$OUT_j = \frac{1}{1+e^{-NET_j}} \tag{2}$$

The interconnected weights are adjusted using a learning algorithm such that the output from the ANN model is very close to the observed values by minimizing the error through a mathematically formulated procedure. This procedure is called training of network.

Using a set of examples from a given problem domain, comprising inputs and their corresponding outputs, an ANN model can be trained to learn the relationship between the input-output pairs. The feed forward ANN is generally adapted in all studies because of its applicability to a variety of different problems (Hsu et al., 1995). However, there are no guidelines in developing an effective ANN architecture, though some researchers have reported suggestions that can be implemented while developing an ANN model. For instance, Maier and Dandy (2000) report that not more than one hidden layer is required in feed forward networks because a three-layer network can generate arbitrarily complex decision regions. Also, the appropriate input vector to the ANN model can be identified according to the procedure of Sudheer et al. (2000).

The input values should be normalised to the range between 0 and 1 before passing into a neural network since the output of sigmoidal function is bound between 0 and 1. Minns and Hall, 1996, Dawson and Wilby (1998), Sajikumar and Thandaveswara (1999), and Burian et al (2001) emphasised the importance of the normalisation of data and gave the procedure to normalise. The output from the ANN should be denormalised to provide meaningful results. In this study, following equation is used to normalize the data set:

$$N_i = \frac{R_i - Min_i}{Max_i - Min_i} \tag{3}$$

where $R_i$ is the real value applied to neuron $i$; $N_i$ is the subsequent normalized value calculated for neuron $i$; $Min_i$ is the minimum value of all values applied to neuron $i$; $Max_i$ is the maximum value of all values applied to neuron $i$.

Training a network is a procedure during which an ANN processes training set (input-output data pairs) repeatedly, changing the values of its weights, according to a predetermined algorithm and the environment in which the network is embedded. The main objective of training (calibrating) a neural network is to produce an output vector $Y = (y_1, y_2, ...., y_p)$ that is as close as possible to the target vector (variable of interest or forecast variable) $T = (t_1, t_2, ...., t_p)$ when an input vector $X = (x_1, x_2, ...., x_p)$ is fed to the ANN. In this process, weight matrices W and bias vectors V are determined by minimizing a predetermined error function as explained as follows:

$$E = \sum_P \sum_p (y_i - t_i)^2 \tag{4}$$

where $t_i$ is a component of the desired output T; $y_i$ is the corresponding ANN output; $p$ is the number of output nodes; and $P$ is the number of training patterns.

Back propagation is the most popular algorithm used for the training of the feed forward ANNs (Hsu et al, 1995; Dawson and Wilby, 1998; Thirumalaiah and Deo, 1998; Sajikumar and Thandaveswara, 1999; Tokar and Jhonson, 1999; Zealand et al, 1999; Thirumalaiah and Deo, 2000; ASCE, 2000a; Elshorbagy et al, 2000; Maier and Dandy, 2000; Burian et al, 2001). Each input pattern of the training data set is passed through the network from the input layer to output layer. The network output is compared with the desired target output, and an error is computed based the equation 4. This error is propagated backward through the network to each neuron, and the connection weights are adjusted based on the equation

$$\Delta w_{ij}(n) = -\varepsilon * \frac{\partial E}{\partial w_{ij}} + \alpha * \Delta w_{ij}(n-1) \tag{5}$$

where $\Delta w_{ij}(n)$ and $\Delta w_{ij}(n-1)$ are weight increments between node *i* and *j* during *n*th and *(n-1)*th pass, or epoch (ASCE, 2000a). A similar equation is written for correction of bias values. In the equation 5, $\varepsilon$ and $\alpha$ are called learning rate and momentum respectively. The momentum factor can speed up training in very flat regions of the error surface and help prevent oscillations in the weights. A learning rate is used to increase the chance of avoiding the training process being trapped in a local minima instead of global minima. The literature by Rumelhart et al, 1986 can be referred for the details of the algorithm.

### 7.2.2 Performance evaluation of ANN model

The whole data length is divided into two, one for calibration (training) and another for validation of artificial neural network model. The performance during calibration and validation is evaluated by performance indices such as root mean square error (RMSE), model efficiency (Nash and Sutcliffe, 1970) and coefficient of correlation (R). They are defined as follows:

$$\text{RMSE} = \sqrt{\frac{\sum_{k=1}^{K} (t-y)^2}{K}} \tag{6}$$

$$\text{Efficiency} = 1 - \frac{\sum (t-y)^2}{\sum (t-\bar{t})^2} \tag{7}$$

$$\text{Coefficient of Correlation} = \frac{\sum TY}{\sqrt{\sum T^2 \sum Y^2}} \tag{8}$$

where K is the number of observations; t is the observed data; y is computed data; $T = t - \bar{t}$ in which $\bar{t}$ is the mean of the observed data; and $Y = y - \bar{y}$ in which $\bar{y}$ is the mean of the computed data.

### 7.2.3 Model development

For the development of the model, the daily rainfall values for Gaumukh and Devaprayag were available from 2004 to 2006. The discharge and temperature values at Gaumukh and Devaprayag for the same period were also available. The ANN models had been developed for predicting the snow melt runoff in Bhagirathi at Gaumukh and Devaprayag using the available data. The details of the model development are described in the following sections.

Selection of input

The ANN model for the prediction of snow melt runoff is generally using the antecedent rainfall, temperature and discharge values as input vector. Determining the number of antecedent rainfall,

temperature and discharge values involves finding the lags of rainfall, temperature and discharge values that have significant influence on the predicted snow melt runoff. These influencing values corresponding to different lags can be very well established through statistical analysis of the data series. The input vector is selected generally by trial and error method; however, Sudheer et al. (2002) have presented a statistical procedure that avoids the trial and error procedure. They reported that the statistical parameters such as auto correlation function (ACF), partial auto correlation function (PACF) and cross correlation function (CCF) can be used for this purpose. The PACF of the discharge series for Bhagirathi at Gaumukh and Devaprayag with 95 % confidence levels and CCF of discharge series at Gaumukh and Devaprayag between rainfall and temperature of the same stations suggest the input vector to the ANN model. The ACF and PACF of discharge series at Gaumukh and CCF of snow melt runoff series with temperature are represented in figure 7.2.2, 7.2.3, 7.2.4 respectively. Based on PACF and CCF of the data series, the following input vector was selected for neural network training.

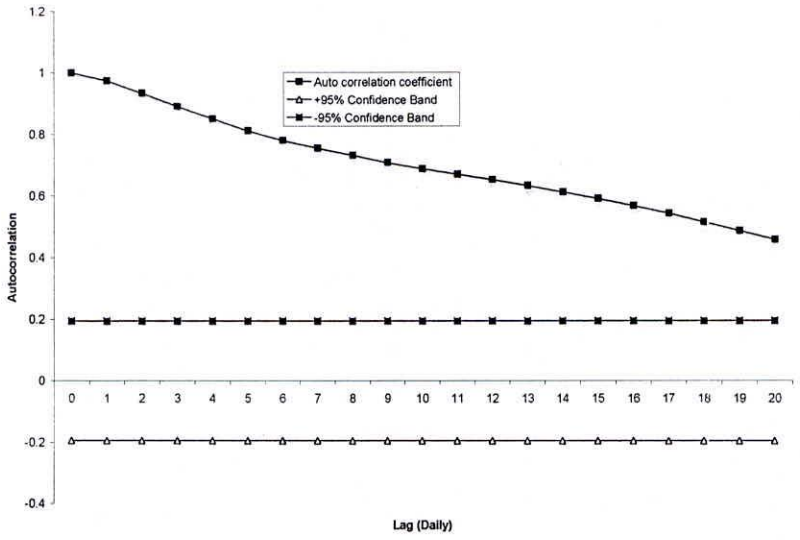


Fig. 7.2.2 The autocorrelation of the discharge series at Gaumukh

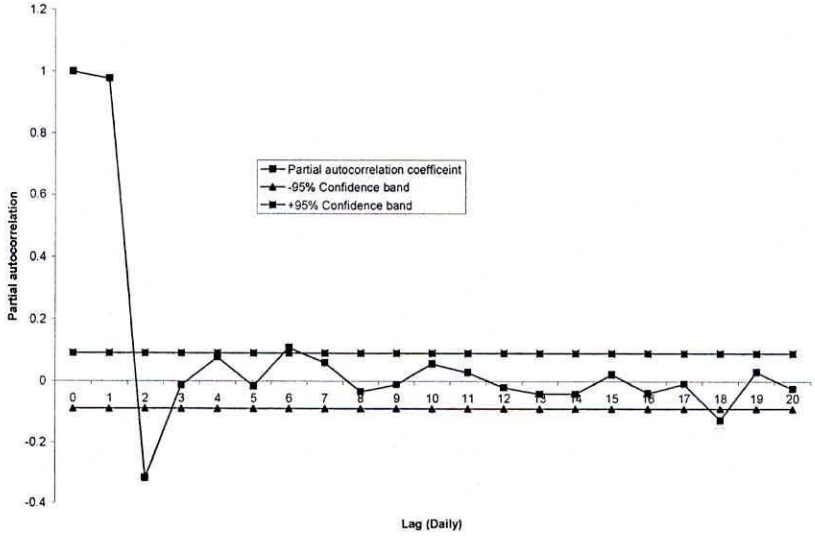


Fig. 7.2.3 The partial autocorrelation of the discharge series at Gaumukh

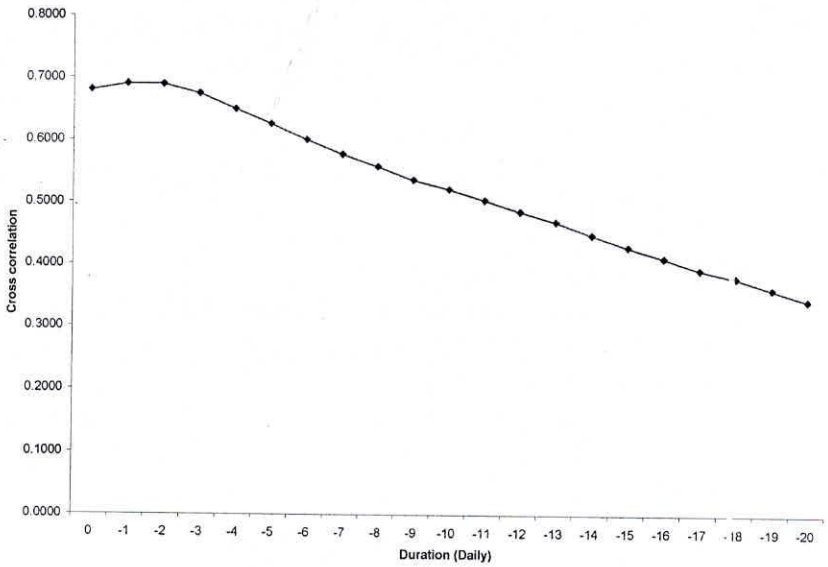


Fig. 7.2.4: The cross correlation between discharge series and temperature series at Gaumukh

For Bhagirathi at Gaumukh, the snow melt runoff is a function of temperature mainly because the snow fall is significantly more compared to rainfall. So the input vector for the ANN model at this site was selected as follows:

$$Q_{,t} = f(Q_{,t-2}, Q_{,t-1}, T_{t-2}, T_{,t-1}) \quad (9)$$

For Bhagirathi at Devaprayag, the snow melt is a function of temperature and rainfall because of the significant rainfall contribution. So the input vector for the ANN model at this site was selected as follows:

$$Q_{,t} = f(Q_{,t-1}, T_{t-1}, T_{,t}, R_{t-1}, R_{,t}) \quad (10)$$

In which Q, R and T are discharge, rainfall and temperature values respectively.

Model Training

The ANN models had been trained using back propagation algorithm. The whole data set were divided into two sets for the training and validation purpose of the ANN model. The data from 2004 to 2005 were considered for the training of the model since it contained the extreme values of sediment concentration. The data of 2006 were considered for the validation of the model. The software used for the training of the model was MATLAB (The Mathworks, Inc., 2001). The number of the hidden neurons in the hidden layer was found by a trail and error procedure, and a number of 6 and 4 neurons were found to be optimum for the ANN model at Gaumukh and Devaprayag respectively. The performance of ANN models were evaluated based on the performance indices.

### 7.2.4 Results and discussion

The performance of best ANN model for the prediction of discharge at Gaumukh during calibration and validation is presented in Figures 7.2.5 and 7.2.6 as scatter plots between observed and computed discharge. The visual inspection of the plots clearly demonstrates the potential of the developed ANN model in prediction of the snow melt runoff at Gaumukh. The results were further analyzed using statistical indices too. The results of the calibration and validation of the ANN models for Gaumukh in terms of various statistical indices are presented in the Table 7.2.1.

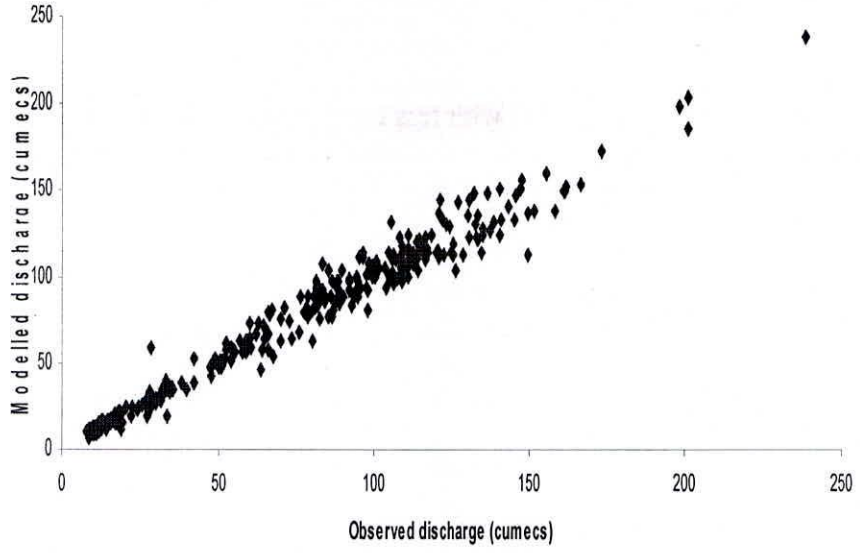


Fig. 7.2.5 Scatter plot of observed Vs modeled discharge for ANN calibration at Gaumukh

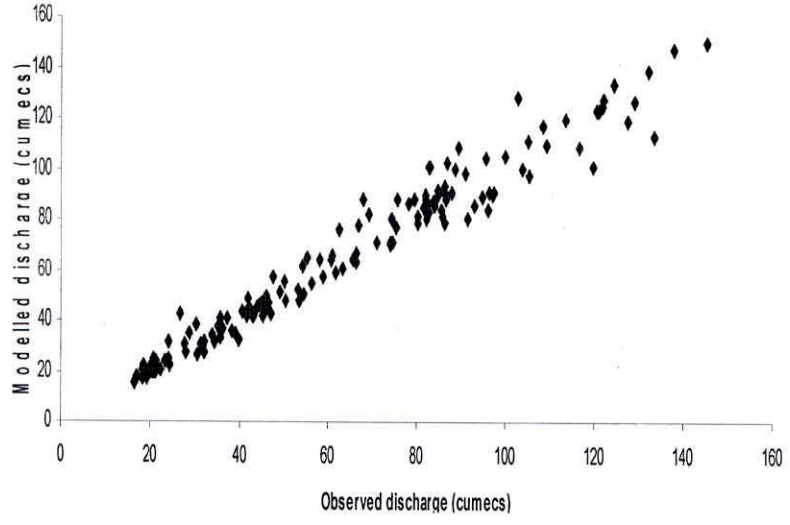


Fig. 7.2.6 Scatter plot of observed Vs modeled discharge for ANN validation at Gaumukh

Table 7.2.1 Calibration and validation Results of ANN models for Gaumukh

| MODEL.No | Input Combinations | ANN Sturcutre | Calibration | | |
|---|---|---|---|---|---|
| | | | CORR | RMSE | EFF |
| ANNFLBD1 | dis(t-1), temp(t-1), temp(t), rain(t-1), rain(t) | 5-2-1 | 0.98 | 36.86 | 96.00 |
| ANNFLBD2 | ,, | 5-3-1 | 0.98 | 33.86 | 96.00 |
| ANNFLBD3 | ,, | 5-4-1 | 0.98 | 33.05 | 96.00 |
| ANNFLBD4 | ,, | 5-5-1 | 0.98 | 33.27 | 96.50 |
| ANNFLBD5 | | 5-6-1 | 0.98 | 31.16 | 96.70 |

In general, the high coefficient of correlation during the calibration and validation for the prediction of snow melt runoff indicates that explained variance was high and the developed ANN model is good to estimate snow melt runoff with less error. The RMSE of ANN, which is a measure of the residual variance, during calibration, was high compared to the value during the validation. But the Nash-Sutcliffe model efficiency was low during the validation. The model performance started deteriorating after increasing the number of hidden layers to 7 during calibration and validation of the model. The best ANN structure for the prediction of snow melt runoff at Gaumukh is 4-6-1. The results were achieved using only three years of recorded data. The performance of the ANN model can be improved by adding more number of data set which is to be observed in future.

The discharge observed at Devaprayag is based on the contribution from snow melt at high altitudes and the rainfall at lower altitudes. Therefore the input variables for the ANN model at Devaprayag is combination of antecedent discharge, rainfall and temperature values as mentioned in the earlier section. The ANN models were trained using different combination of input and hidden layers and the best model was selected on the performance of the ANN model Table 7.2.2. The data available at Devaprayag was only for two years .i.e., from 2004 and 2005 and only the calibration of ANN model could be done using the available data. The performance of model was deteriorated after the introduction of 4 hidden neurons during the training of the model. The best ANN model for the prediction for discharge at Devaprayag is 5-4-1 (Fig. 7.2.7). The calibration performance of the ANN model for Devaprayag was lower than the performance of the model for Gaumukh as it was evidenced from RMSE of the models. The overall performance of the model suggests that these can be used for the prediction of discharge at Gaumukh and Devaprayag along Bhagirathi river.

Table 7.2.2 Calibration Results of ANN models for Devaprayag

| MODEL.No | Input Combinations | ANN Sturcutre | Calibration | | |
|---|---|---|---|---|---|
| | | | CORR | RMSE | EFF |
| ANNFLBD1 | dis(t-1), temp(t-1), temp(t), rain(t-1), rain(t) | 5-2-1 | 0.98 | 36.86 | 96.00 |
| ANNFLBD2 | ,, | 5-3-1 | 0.98 | 33.86 | 96.00 |
| ANNFLBD3 | ,, | 5-4-1 | 0.98 | 33.05 | 96.00 |
| ANNFLBD4 | ,, | 5-5-1 | 0.98 | 33.27 | 96.50 |
| ANNFLBD5 | | 5-6-1 | 0.98 | 31.16 | 96.70 |

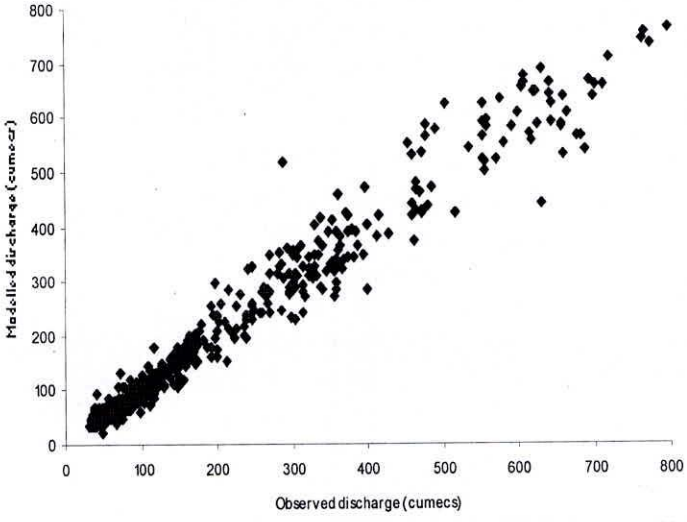


Fig. 7.2.7 Scatter plot of observed Vs modeled discharge for ANN calibration at Devaprayag

### 7.2.5 Summary and conclusion

In this chapter, ANN Models had been developed for predicting the snow melt runoff at Gaumukh and Devaprayag, Bhagirathi River. The ANN models had been developed using daily discharge, rainfall and temperature at Gaumukh and Devaprayag from 2004 to 2006. The statistical parameters ACF, PACF and CCF had been used for selection of Input vector. The model performance evaluation criteria used were coefficient of correlation, RMSE and model efficiency. The calibration performance of the ANN model for Devaprayag was lower than the performance of the model for Gaumukh as it was evidenced from RMSE of the models. The overall performance of the ANN models suggests that these can be used for the prediction of discharge at Gaumukh and Devaprayag along Bhagirathi River.

# CHAPTER 8

## SUMMARY AND CONCLUSIONS

This report presents the details of an isotope hydrological study carried out in the upper Ganga (Bhagirathi) basin during 2004-2006 to understand the stream flow generation processes at various spatial and temporal scales.

River Ganga, having Bhagirathi and Alaknanda as the main tributaries in the upper reaches, continues to play a major role in the socio-economic development of north India and the water demand in the agricultural and hydroelectric power sector is ever growing. Estimation of snow and glacier melt contribution to the River Ganga is important for the water resources development and management in this region as they generally control the flow during the summer season. Despite the importance, only a little hydrological information is avaiable about Bhagirathi and Alaknanda Rivers, due to the inaccessible and difficult terrain. Despite a few studies conducted to understand the rainfall-runoff relationships in this basin using remote sensing and modelling, a number of fundamental issues, such as: (a) role of groundwater in the stream-flow and its temporal variability, (b) role of snowmelt and its temporal variability, (c) rainfall – runoff relationship and (d) relative significance of the tributaries to the streamflow in the main river etc., remain unresolved.

Hence, in the present study, an attempt have been made to understand the spatial and temporal contribution of direct runoff, snow/glacial melt and groundwater (i.e., subsurface flow) to the River Bhagirathi using stable ($^{2}H$ & $^{18}O$) and radioactive ($^{3}H$) isotope techniques. It is accomplished by: (a) isotopic characterization of rainfall, snowmelt, runoff and groundwater (b) hydrograph separation of the river flow using isotopic and hydrochemical techniques (c) development of a stream flow model (using SNOWMOD software). The results of the isotope study are compared with those obtained by conventional and modelling techniques. This study is first of its kind in India.

### 8.1 Isotopic Characteristics of Precipitation

#### 8.1.1 Spatial Variation

Isotopic analysis ($\delta D$ & $\delta^{18}O$) of pecipitation samples collected from Gomukh (altitude: 3800m), Gangotri (3050 m), Dabrani (2050 m), Maneri (1170 m), Uttarkashi (1140 m), Tehri (640 m) and Devprayag (465 m) helped to characterise the isotopic signatures of precipitation in the River Bhagirathi's catchment. The weighted annual average of $\delta^{18}O$ in precipitation varied between -12.9‰ and -18.3‰ at Gangotri, -9.8‰ and -12.9‰ at Dabrani, -5.0‰ and -10.8‰ at Uttarkashi, -7.9‰ and -12.5‰ at Tehri and -15.8‰ and -6.7‰ at Devprayag. It reveals that the isotopic composition decreases with altitude. The depleted values of rain with altitude are due to the continental and altitude effects.

#### 8.1.2 Seasonal Variation

Seasonal isotope data of precipitation reveals that $\delta D$ and $\delta^{18}O$ values are enriched in pre-monsoon (March to June) and post monsoon (October to November) rains while depleted values are observed during the monsoon (July to September) and winter (December to February) periods. The $\delta^{18}O$ and $\delta D$ values in winter precipitation are comparatively enriched than that of monsoon precipitation. This may be because of the change in air moisture source for the summer and winter monsoons. The enriched isotopic values of pre-monsoon rains may be due to the secondary evaporation of falling rain drops.

#### 8.1.3 Establishment of a Local Meteoric Water Line (LMWL) for Bhagirathi Basin

Establishment of a LMWL is essential for any isotope hydrological study in this basin. The best fit line has been developed using monthly precipitation data of all stations during the year 2004-2006. The statistical analysis of monthly isotopic data of precipitation in the Bhagirathi basin yielded the

following equations:

$\delta D=(8.2\pm0.1)\delta^{18}O + (10.6\pm0.6)$ (GMWL) (8.1)

$\delta D=8.0 \pm 0.1*\delta^{18}O + 11.5 \pm 1.1, r^2 = 0.98, n = 129$ (LMWL) (8.2)

$\delta D=7.4 \pm 0.5*\delta^{18}O + 8.3 \pm 2.6, r^2 = 0.90, n = 34$ (Premonsoon) (8.3)

$\delta D=8.0 \pm 0.1*\delta^{18}O + 11.3 \pm 1.7, r^2 = 0.99, n = 52$ (Monsoon) (8.4)

$\delta D=7.4 \pm 0.3*\delta^{18}O + 7.5 \pm 2.7, r^2 = 0.98, n = 15$ (Post monsoon) (8.5)

$\delta D=8.0 \pm 0.3*\delta^{18}O + 15.4 \pm 1.9, r^2 = 0.96, n = 28$ (Winter) (8.6)

The lower slope and y intercept for pre-monsoon and post-monsoon seasons in comparison to monsoon and winter rains are due to local moisture source for precipitation and the effect of secondary evaporation of rain drops. However, the higher y intercept during the winter season is a matter of debate, i.e., may be because of the vapours from the Mediterranean Sea or the evaporation of local water at low temperature.

### 8.1.4 Altitude Effect

The isotopic composition of precipitation changes with the altitude and becomes more and more depleted in $\delta^{18}O$ and $\delta D$ in rains occuring at higher elevations. The estimated altitude effects of $\delta^{18}O$ varied between -0.24‰ to -0.29‰ per 100 m rise while in $\delta D$ it is between -1.8‰ to -2.7‰ per 100 m rise. These values are well within the range reported world over i.e., -0.1‰ to -0.4‰ for $\delta^{18}O$ and -1‰ to -4‰ for $\delta D$. The observed altitude effect would be useful in identifying the recharge zones of the springs in the Himalayan regions whose discharge is dwindling due to various anthropogenic factors.

## 8.2 Isotopic Characteristics of Groundwater

### 8.2.1 $\delta^{18}O$-$\delta D$ relationship in groundwater

Comparison of $\delta^{18}O$-$\delta D$ relationship in groundwater with respect to the LMWL provides information about the hydrological processes prior to the recharge. The regression analysis of stable isotope data of groundwater gives the best fit line (BFL) as:

$\delta D = (8.1 \pm 0.1)* \delta^{18}O + (11.3 \pm 0.1)(n = 162, r^2 = 0.96)$ (samples from hand pumps) (8.7)

$\delta D = (7.2 \pm 0.3)* \delta^{18}O + (3.4 \pm 2.5)$ $(n = 37, r^2 = 0.94)$ (springs) (8.8)

The BFL for hand pump samples is similar to that of LMWL suggesting quick recharge without evaporation. Lesser slope in the case of springs, indicate evaporative enrichment prior to recharge. Hence, $\delta^{18}O$ and $\delta D$ data of hand pumps can be used as a proxy for precipitation for the construction of LMWL in the Himalayan regions, as collection of precipitation samples are difficult in these terrains. From the stable isotope data, two groundwater flowsystems are identified: (i) quick flow through the fractures in the crystaline rocks (non-evaporated) (ii) seepage flow through the thin overburden (evaporated water) which emerge as springs at the contact between the rock and the soil cover.

Similar slope of pre-monsoon and post-monsoon groundwater in the $\delta^{18}O$-$\delta D$ diagram represents a well-mixed aggregate of waters recharged under different seasons. Distinct $\delta^{18}O$ signature of groundwater at various altitudes reveals that the groundwater is recharged locally. The $\delta^{18}O$ and $\delta D$ values of the hot spring (Gangnani) also fall on the same line as that of the cold spring suggesting local recharge.

## 8.3 Isotopic characteristics of River Bhagirathi

The variations in the isotopic composition of river water reflect the variable contributions from isotopically different sources, which can be evaluated if isotopic indices of the sources are known.

Therefore, the river water isotopic characterisation and its utility in determining the contribution from different sources, studying river - aquifer interactions etc. are of great importance.

### 8.3.1 Spatial Variation

As the river flows downwards, it is observed that its isotopic values are getting enriched. The enrichment in $\delta^{18}O$ varies from 3‰ to 5‰ from Gomukh to Devprayag depending on the seasons. This indicate higher contribution of surface / subsurface runoffs generated from the lower subcatchments (having larger catchment areas) to the river (altitude effect).

From Gangotri to Devprayag, the observed enrichment of river water is not uniform. There is less enrichment in $\delta^{18}O$ between Gomukh and Gangotri compared to the enrichment in $\delta^{18}O$ between Gangotri and Dabrani. Further, there is a significant enrichment in $\delta^{18}O$ from Dabrani to Uttarkashi. The $\delta^{18}O$ variation between Uttarkashi and Tehri is comparatively less and it is negligible between Tehri and Devprayag. The difference in isotopic enrichment of river water at various sections shows that the groundwater contribution is more between Gangotri and Uttarkashi, which sustains the river flow during the lean flow period. After Tehri, the contribution of groundwater appears to be less due to smaller catchment area and lower slope.

### 8.3.2 Temporal Variation

Monthly variation in $\delta^{18}O$ of river from 2004 and 2006 shows that the isotopic values start depleting from April and continues till September. The depletion during the premonsoon (April to June) indicate increased contribution from the melting of snow and glacier at higher reaches due to the increase in temperature. Depletion of $\delta^{18}O$ is observed in the rain during the monsoon period (July-September) which resulted in depleted isotopic values of the river. The isotopic variation in river clearly indicates the varying contribution of snow/glacier melt, direct runoff and groundwater to the River Bhagirathi. The variation in electrical conductivity also cofirms the above findings.

### 8.3.3. Isotopic Characteristics of River Bhagirathi

The statistical analyses of the monthly isotopic data of the Bhagirathi River yielded the following river water equation for the period 2004-2006:

$$\delta D = (7.8 \pm 0.1) * \delta^{18}O + (9.7 \pm 1.2),\ R^2 = 0.97,\ n = 166 \qquad (8.12)$$

Slope and the intercept of the best fit line of Bhagitahi River are close to those of local meteoric water line for the Bhagirathi River basin.

### 8.3.4 Hydrograph Separation of Bhagirathi River at Dabrani and Devprayag Sites

Contribution of snow/glacier melt, surface runoff and groundwater in the total flow of Bhagirathi River were estimated using two box and three box models, which are essentially the isotope, solute (EC) and mass balance equations. The isotopic signatures of river water, surface runoff, snow and glacier, precipitation and subsurface/groundwater were developed for Dabrani and Devprayag sites and used for the hydrograph separation.

At Dabrani site, the minimum flow is observed during the winter months of December and January when river discharge is mainly contributed by the groundwater component (subsurface flow) while other two major components i.e., surface runoff and snow and glacier melt have negligible contribution. It can be explained with fact that during post monsoon months, negligible amount of rains are recorded and snow/glacier melt discharge is reduced to minimum due to decrease in atmospheric temperature. Practically, snow accumulation take place during winter months in Bhagirathi River basin. The river discharge starts increasing from April due to the melting of snow at the lower altitudes. The increase in discharge continues till June, however there is scanty rainfall during pre-monsoon period. This clearly indicates that the increase in river discharge is due to the contribution of melting of snow

and glacier.

Maximum river discharge is observed during the rainy season (July, August and September) and the peak flow corresponds to high intensity rain events. Using a two components mixing model, the computed maximum runoff contribution to the river discharge goes up to 49% on a particular day of rain event. The maximum contribution varied between 18% and 49% of the total discharge for the rainfall events occurred during the period from July to September 2005.

Using a three components mixing model on 10 daily basis, the computed surface runoff contribution varied between 7% (April) and 43% (July) with an annual average of 16%. The glacier/snow component was negligible in December/January and a maximum contribution of 64% in May with an annual average of 35%. The subsurface contribution ranged from 24% in May to 100% in December (Fig 8.10). On an average, it comes to 49% of the total annual discharge at Dabrani.

The hydrograph of Bhagirathi River at Devprayag site comprise of multiple peaks which is similar to that of Dabrani. The isotopic signatures of the river varies from month to month. In monsoon period, the stream discharge bears depleted isotopic values in the range of -10.1‰ to -12.4‰ during July, August and September months. It has been observed that during post monsoon months (mainly after 15$^{th}$ October) when precipitation occurs in lesser amount, the stream discharge is sustained mainly by subsurface flow (groundwater) component. At this period river isotopic values are ranging from -10.1‰ to -10.9‰. Depletion in isotopic values of river water during premonsoon reveals the increase of snow melt contribution.

Using the electrical and isotopic signature of rain, river, subsurface flow, snow and glacier melt, hydrograph separation has been carried out through applying the two and three component model at Devprayag. The maximum contribution of rainfall-runoff has been recorded between 31% and 51% of the total discharge for the rainfall events that occurred during in month of July, August and September in the year 2005. At, Devprayag hydrographs have been separated out on monthly basis. On monthly basis, the surface runoff contribution is found maximum up to 44%. Contribution ofsurface runoff is found about 18.6% of the total discharge. The hydrograph clearly indicates the snow melt is started from January and maximum in April and May month of the total discharge. If one compares with total discharge, it comes about only 25% of the total discharge in a year. The subsurface contribution ranged from 32% to 100%. The maximum contribution of groundwater in December month and minimum in rainy period of the total discharge. If one compares with total discharge, it comes about only 56% of the total discharge in a year.

### 8.3.5 Stream flow Modelling Using SNOWMOD

Modeling of streamflow is based on the transformation of incoming precipitation to outgoing streamflow by considering losses to the atmosphere, temporary storage, lag and attenuation. In most part of the world, the seasonal short-term variation in streamflow reflects the variation in rainfall. But at higher latitudes and altitudes where snowfall is predominant, runoff depends on heat supplied for snowmelt rather than the timing of precipitation. Hence, to understand the hydrological behavior and simulate the streamflow it is very important to model the snowmelt runoff. One of the objectives of this study is to simulate the snowmelt runoff in Bhagirathi basin up to Devprayag.

The model was simulated for one year 2004-2005. The estimated and observed hydrographs show good matching for the year 2004-2005. The efficiency ($R^2$) of the model for this year is 0.86, while difference in volume is 1.16% and RMSE is 0.38. The results indicate good performance of the model. A close observation of rainfall and stream flow data indicates that most of the peaks in the stream flow were because of rainfall.

It is clear that the discharge rises from May onwards and reaches its peak by August and September and starts reducing from month of September onwards. The figure also shows that volumes

and peaks of stream flow were reproduced well by model. The results of simulation indicate that high flow occurred in the month of July and August due to higher contribution of rainfall-runoff during this period. The snowmelt contribution computed using isotopic model and SNOWMOD closely match with computed values using isotopic techniques. The study shows that SNOWMOD a temperature index based snowmelt runoff model, predicts different components of the River hydrograph with reasons accuracy where limited data are available.

### 8.3.6 Stream Flow Modelling Using ANN

Development and application of conceptual models for the simulation of snow melt runoff require physical understanding of the process and generation of large quantity of data. Recently, neural networks approach has been applied in many areas of water resources due to its capability in representing any nonlinear processes by given sufficient complexity of the trained networks. ANNs are proven to produce improved performance over other traditional models such as conceptual models and black box models, in numerous hydrological studies. The main advantage of the ANN models over traditional models is that it does not require information about the complex nature of the underlying process under consideration to be explicitly described in mathematical form.

The ANN models had been developed for predicting the snow melt runoff in Bhagirathi at Devaprayag using discharge, temperature and rainfall data from 2004 to 2006. The statistical parameters such as auto correlation function (ACF), partial auto correlation function (PACF) and cross correlation function (CCF) of the time series had been used to select the input vector to the ANN model.

The ANN models had been trained using back propagation algorithm. The whole data set were divided into two sets for the training and validation purpose of the ANN model. The data from 2004 to 2005 were considered for the training of the model since it contained the extreme values of discharge. The data of 2006 were considered for the validation of the model. The software used for the training of the model was MATLAB. The number of the hidden neurons in the hidden layer was found by a trail and error procedure, and a number of 4 neurons were found to be optimum for the ANN model at Devaprayag. The performance of ANN models were evaluated based on the performance indices.

The model could not be validated due to the control flow for the year 2006. However, overall performance of the ANN models suggests that it can be used for the prediction of discharge at Devaprayag of the Bhagirathi River.

## REFERENCE


- ASCE 2000a. Artificial neural networks in hydrology-I: Preliminary concepts, Journal of Hydrologic Engineering, ASCE, 5(2), pp. 115-123.
- ASCE 2000b. Artificial neural networks in hydrology-II: Hydrologic applications, Journal of Hydrologic Engineering, ASCE, 5(2), pp. 124-137.
- Arora, M. 2008. Seasonal characterization of ablation, storage and drainage of melt runoff and simulation of streamflow for the Gangotri glacier, Project report, D.S.T., GOI.
- Atiya, A.F., M.E. Suzan, I.S. Samir. and S.E.Mohamed. 1999. A comparison between neural-network forecasting techniques-case study: river flow forecasting, IEEE Transactions on Neural Networks, 10(2), pp. 402-409.
- Bandopadhyay, J., Rodda, J. C., Kattelmann, R., Kundzewicz, Z. W., and Kraemer, D. (1977) Highland water – a resource of global significance. In mountain of the world – A Global Priority, Messerli B., Ives J. D. (eds). Parthenon Published Group; 131-155.
- Bartarya, S.K., Bhattacharya, S.K., Ramesh, R, Somayajulu B.L.K. (1995) $\delta^{18}O$ and $\delta D$ systematics in the surficial waters of the Gaula catchment area, Kaumaun Himalaya, India. Journal of Hydrology 167:369-379.

- Bhattacharya, S.K., Gupta, S.K., Krishnamurthy, R.V., 1985. Oxygen and hydrogen isotopic ratios in groundwaters from India. Proc. Indian. Acad. Sci. (Earth and Planet. Sci.) 94 (3), 283-295.
- Borowitz, J. L. (1962) The relative volatalities of the system $H_2{}^{17}O$ - $H_2{}^{16}O$. J. Phys. Chem. 66: 1412.
- Bottinga, Y. and Craig, H. (1969) Oxygen isotope fractionation between $CO_2$ and water and the isotopic composition of marine atmosphere. Earth Planet. Sci. Lett. 5: 285-295.
- Burian, S.J., S.R. Durrans, S.J. Nix. and R.E. Pitt. 2001. Training artificial neural networks to perform rainfall disaggregation, Journal of Hydrologic Engineering, ASCE, 6(1), pp. 43-50.
- Central Water Commission. 1989. Manual on Flood Forecasting, River Management Wing, R. K. Puram, New Delhi.
- Chakrapani, G. J. (2005) Major and trace element geochemistry in upper Ganga river in the Himalayas, india, Environ Geol, 48, 189-201.
- Chauhan, D. S. and Hasnain, S. I. (1993) Chemical characteristics, solute and suspended sediment loads in the meltwaters draining from satopanth and Bhagirath Kharak glaciers, Ganga Basin, India. In: Snow and Glacier Hydrology (eds by G. J. Young) Proc. Kathmandu Symp. November 1992, 403-410, IAHS Pub. No. 218.
- Clark, I.D., Fritz, P. (1997) Environmental Isotopes in Hydrogeology, CRC Press, Boca Raton, pp. 328.
- Colman, M.L., Shepherd, T.J., DDurham, J.J, Rouse, J.E. and Moore, G.R. (1982) Reduction of water with zinc for hydrogen isotope analysis. Analytical Chemistry 54, 993-995.
- Coplen, T. B. (1993) Uses of environmental isotopes. In: (Editor W. M. Alley) Regional groundwater quality. Van Nostrand Reinhold, New York. pp 227-254.
- Craig H. and Gordon L. (1965) Deturium and Oxygen-18 variation in the oceanand the marine atmosphere In: E. Tongiorgi (ED), Stable Isotopes in Oceanographic Studies and Paleotemperatures, Spoleto 1965: 9-130.
- Dalai, Tarun, K., Bhattacharya, S.K. and Krishnaswami, S. (2002) Stable isotopes in the source waters of the Yamuna and its tributaries: seasonal and altitudinal variations and relation to major cations, Hydrol. Process, 16, 3345-3364.
- Danh, N.T., H.N. Phien. and A.D. Gupta. 1999. Neural network models for river flow forecasting, Water SA, 25(1), pp. 33-39.
- Dansgaard, W. (1953) The abundance of $O^{18}$ in atmospheric water and vapour. Tellus, 5: 461-468.
- Dansgaard, W. (1964) Stable isotope in precipitation. Tellus, **16**: 436-468.
- Datta, P.S., Tyagi, S.K. and Chandrasekharan, H. (1991) Factors controlling stable isotope composition of rainfall in New Delhi, India, Journal of Hydrology, 128, 223-236.
- Dawson,C.W. and R. Wilby. 1998. An artificial neural network approach to rainfall-runoff modeling, Hydrological Sciences Journal, 43(1), pp. 47-66.
- Deshpande, R.D., Bhattacharya, S,K., Jani, R.A. and Gupta S.K. (2003) Distribution of oxygen and hydrogen isotopes in shallow groundwaters from Southern India: influence of a dual monsoon system, Journal of Hydrology, 271, 226-239.
- De Walle, D. R., Swistock, B. R. and Sharpe, W. E. (1988) Three component tracer model for stormflow on a small Appalachian forested catchment. J. Hydrol. 104: 301-310.

- Ehhalt, D., Knott, K., Nagel, J. F. and vogel, J. C. (1963) Deuterium and oxygen-18 in rain water. J. Geophy. Res. 68: 3775-3780.
- Elshorbagy, A., S.P. Simonovic. and U.S. Panu. 2000. Performance evaluation of artificial neural networks for runoff prediction, Journal of Hydrologic Engineering, 5(4), pp. 424-433.
- Epstein, S. And Mayeda, T. (1953) Variation of $\delta\ ^{18}O$ content in waters from natural sources. Geochim. Cosmochim. Acta 4 213-224.
- Fernando, A.K. and A.W. Jayawardena. 1998. Runoff forecasting using RBF networks with OLS algorithm, Journal of Hydrologic Engineering, ASCE, 3(3), pp. 203-209.
- Fontes, J. –Ch. (1980) Environmental isotopes in isotope hydrology. In: Fritz, P., Fontes, J.-Ch. (Eds.), Handbook of Environmental Isotope Geochemistry, Elsevier, Amsterdam, pp. 411-440.
- Friedman, I. (1953) Deuterium content of natural water and other substances. Geochim. Cosmochim. Acta 4 89-103.
- Garzione, C.N., Dettman, D.L., Quade, J., DeCelles P.G., Butler, R.F. (2000a) High times on the Tibetan Plateau: Palaeoelevation of the Thakkhola graben, Nepal Geology, 28:339-342.
- Garzione, C.N., Quade, J., DeCelles, P.G., English, N.B., (2000b). Predicting palaeoelevation of Tibet and the Himalaya from 18O vs. altitude gradients in meteoric waters across the Nepal Himalaya, Earth and Planetary Science Letters, 183, 215-229.
- Gat, J. R. and Carmi, I. (1970) Evolution of the isotopic composition of atmospheric water in the Mediterranean sea area. J. Geophys Res, 75 3039-3048.
- Gat, J. R. (1981) In stable isotope Hydrology (eds) J R Gat and R Gonfiantini, IAEA Tech. Rep. Series No. 210 7-19.
- Giggenbach, W.F, Gonfiantini, R., Jangi, B.L. and Truesdell A.H. (1983) Isotopic and chemical composition of Parbati Valley geothermal discharges, North-West Himalaya, India, Geothermics, 12 (2/3), 199-222.
- Gonfiantini, R. (1986) Environmental isotope in lake studies. In : Fritz and J. –Ch. Fontes (Eds.) Handbook of Environmental isotope Geochemistry, Vol. 2, The Terrestrial Environment., B. Elsevier, Amsterdam, The Netherlands: 113-168.
- Hasnain, S.I. (1992) Glaciogluvial sediments transfer from Chhota Shigri, Himachal Pradesh In Proc. Int. Symp. On Hydrology of Mountainous Areas (Shimla, India) 273-283, NIH, Roorkee, India.
- Hasnain, S.I.(1996) Factor controlling suspended sediment transport in Himalayan glacier meltwaters, J. of Hydrol., 181., 49-62.
- Hasnain, S.I. Subramanian, V.and Dhanpal K. (1989) Chemical Characteristics of meltwaters from a Himalayan Glacier India I. Hydrol. 106. 98-106.
- Hasnain, S.I. and Renoj (1996) Sediment transport and solute variation in meltwaters of Dokriani glacier (Bamak), Garhwal Himalaya, J. Geol. Soc. India, 47, 731-739.
- Hinton, M. J., Schiff, S. L. and English, M. C. (1994) Examining the contribution of glacial till water to storm runoff using two and three component hydrograph separations. Water Resour. Res., **30**: 983-993.
- Hsu, K-L., H.V. Gupta. and S. Sorooshian. 1995. Artificial neural network modeling of the rainfall-runoff process, Water Resources Research, 31(10), pp. 2517-2530.
- Jain, K. (1971) Stratigraphy and tectonics of Lesser Himalayan region of Uttarkashi,Garhwal Himalaya Himalayan Geology, Volume 1, 25-28, Wadia Institute of Himalayan Geology, Dehradun.

- Jain, S.K., A. Das. and D. K. Srivastava. 1999. Application of ANN for reservoir inflow prediction and operation, Journal of Water Resources Planning and Management, ASCE, 125(5), pp. 263-271.
- Kakiuchi, M. and Matsuo, S. (1979) Direct measurements of D/H and $^{18}O/^{16}O$ fractionation factors between vapour and liquid water in the temperature range from 10° to 40°. Geochemical J., 13: 307-311.
- Kennedy, V. C., Kendall, C., Zellweger, G. W., Wyermann, T. A. and Avazino, R. A. (1986) Determination of the components of stormflow using water chemistry and environmental isotopes, Mattole river basin, California. J. Hydrol. 84: 107-140.
- Kisi, O. 2004. Multi-Layer perceptrons with Levenberg-Marquardt training algorithm for suspended sediment concentration prediction and estimation, Hydrological Sciences Journal, 49(6), pp. 1025-1040.
- Kisi, O. 2005. Suspended sediment estimation using neuro-fuzzy and neural network approaches, Hydrological Sciences Journal, 50(4), pp. 683-696.
- Kumar, Gopendra (2005) Geology of Uttar Pradesh and Uttaranchal, Geological Society of India, Banglore.
- Krishnamurthy, R. V. and Bhattacharya, S. K. (1991) Stable oxygen and hydrogen isotope ratios in shallow groundwaters from India and a study of the role of evapotranspiration in the Indian monsoon. In: H. P. Taylor, Jr., J. R. O'Neil and I. R. Kaplan (Editors), Stable isotope geochemistry: A Tribute to Samuel Epstein, The geochemical society, spl. publ. 3.
- Lambs, L., Balakrishna, K., Brunet, F. and Probst, J. L. (2005) Oxygen and hydrogen isotopic composition of major Indian rivers: a first global assessment. Hydrol. Process. 19, 3345-3355.
- Merlivat, L. (1978) Molecular diffusivities of $H_2{}^{16}O$, $HD^{16}O$ and $H_2{}^{18}O$ in gases. J. Chem. Phys. 69(6): 2864.
- Mazor, E. (1991) Chemical and Isotopic Groundwater Hydrology: The Applied Approach, second ed., Marcel Dekker Inc., New York, pp. 413.
- Mojoube, M. (1971) Fractionnement en oxygen 18 et en deuterium entre l'eau et sa vapeur. J. Chim. Phys. **10** 1423-1436.
- Maier, H.R. and G.C. Dandy. 2000. Neural networks for the prediction and forecasting of water resources variables: A review of modelling Issues and applications, Environmental Modelling & Software, 15, pp. 101-124.
- Martinec, J., A. Rango. and R. Roberts. 2007. Snowmelt Runoff Model (SRM) – User's Manual, USDA, 1400 Independence Ave., S.W. Washington, DC 20250.
- Minns, A.W. and M.J. Hall. 1996. Artificial neural networks as rainfall runoff models, Hydrological Sciences Journal, 41(3), pp. 399-418.
- Mojoube, M. (1971) Fractionnement en oxygen 18 et en deuterium entre l'eau et sa vapeur. J. Chim. Phys. 10 1423-1436.
- Nachiappan, Rm. P., Bhishm Kumar and Rm. Manickavasagam (2002) Estimation of sub-surface components of water balance of lake Nainital (Kumaun Himalayas, India) using environmental isotopes. *Hydrol. Sciences J.* 47SI.
- Nagy, H. M., K. Watanabe. and M. Hirano. 2002. Prediction of sediment load concentration in rivers using artificial neural networks, Journal of Hydraulic Engineering, 128(6), pp. 588-595.
- Navada, S.V., Jain S.K., Shivanna, K and Rao, S.M. (1986) Application of environmental isotopes in groundwater hydrology, Indian Jour. Of Earth Sciences, Vol. 13, No. 3-3, pp 223-234.

- Nash, J.E. and J.V. Sutcliffe. 1970. River flow forecasting through conceptual models:1. A discussion of principles, Journal of Hydrology, 10, pp. 282-290.
- Pandey S. K., Singh A.K. and Hasnain S.I. (1999) Weathering and geochemical processes controlling solute acquisition in Ganga Headwater-Bhagirathi River, Garhwal Himalaya, India, Aqua. Geochem., 5, 357-379.
- Pande, K., Padia, J.T., Ramesh, R. and Sharma, K. K. (2000) Stable isotope systematics of surface water bodies in the Himalayan and Trans-Himalayan (Kashmir) region. Proc. of the Ind. Acad. of Sci. (Earth Planet. Sci.), 109, 109-115.
- Parent, A. C., F. Anctil, V. Cantin. and M. A. Boucher. 2008. Neural network input selection for hydrological forecasting affected by snowmelt, Journal of American Water Resources Association, 44(4), pp. 679-688.
- Portugal, M.S. 1995. Neural networks versus time series methods: a forecasting experience, 14th International Symposium on forecasting, 12-15 June 1995, Stockholm School of Economics, Stockholm, Sweden.
- Rai, S.P., 1993. Hydreogeological and Geomorphological Studies of Syahidevi-Binsar Area, District Almora, Kumaun Himalaya, Unpublished Ph.D. Thesis, Kumaun Univeristy, Nainital, 160pp.
- Raina, A.N. (1977) Geography of Jammu and Kashmir (New Delhi : National Book Trust) 271p.
- Ramesh, R. and Sarin, M.M. (1992) Stable isotope study of the Ganga (Ganges) river system, Jour. of Hydrology, 139, 49-62.
- Raman, H. and V. Chandramauli. 1996. Deriving a general operating policy for reservoirs using Neural Network, Journal of Water Resources Planning and Management, ASCE, 122(5), pp.342-347.
- Rozanski, K., Araguas, L. A. and Gonfiantini, R. (1993) Isotopic patterns in modern global precipitation; In : Climate change in continental isotopic indicators Geophys Monograph 78, Am. Geophys. Union 1-36.
- Rumelhart, D. E., E. Hinton. and J. Williams. 1986. Learning internal representation by error propagation, Parallel Distributed Processing, Vol. 1, MIT Press, Cambridge, Mass., pp. 318-362.
- Sajikumar, S. and B.S. Thandaveswara. 1999. A non-linear rainfall-runoff model using an artificial neural network, Journal of Hydrology, pp. 216, 32-55.
- Saravanakumar, N. Jacob, S. V. Navada, S. M. Rao, Rm. P. Nachiappan, Bhishm Kumar, and J. S. R. Murthy (2001) Study of lake hydrodynamics using environmental isotopes. *Hydrological Processes* 15:425-439.
- Sarin, M.M. Krishnaswamy, S., Dilli, K, Somayajulu, B. L. K. and Moore, W. S. (1989) Major ion chemistry of Ganga-Brahamputra river system: weathering processes and fluxes of the Bay of Bengal, Geochim. Cosmochim Acta., 53, 997-1009.
- Sarin, M.M. Krishnaswamy, S. K., Trivedi, J. R. and Sharma K. K. (1992) Major ion chemistry of the Ganga source waters:weathering in the high altitude Himalaya, In: Proc. Ind. Acad. Sci. (Earth Planet Sci.) 1, 89-98.
- Singh A.K. and Hasnain S.I., (2002) Aspects of weathering and solute acquisition processes controlling chemistry of sub-Alpine proglacial streams of Garhwal Himalaya, India, Hydrological Processes, 16, 835-849.
- See, L., M. Dougherty. and S. Openshaw. 1997. Some initial experiments with neural network models of flood forecasting on the river Ouse, Proceedings of Gecomputation'97 & SIRC'97, University of Otago, New Zealand, pp. 15-22.

- Singh A. K. and Hasnain S. I. (1999) Major ion chemistry and weathering control in a high altitude basin: Alaknanda River, Garhwal Himalaya, India, Hydrol.l Sci. J.,43 (6), 825-843.
- Singh P., Ramasastri K.S. (1994) Study on snow distribution in Chenab basin. Int. Symp. On snow and its Manifestations, 26-28 September 1994. SASE: Manali, India.
- Singh P. and Shastri K. S (1999) Temporal distribution of Dokriani glacier melt runoff and its relationship with meteorological parameters, Project report submitted to DST, National Institute of Hydrology, Roorkee.
- Singh P., Ramasastri K. S., Kumar N. and Bhatnagar N. K. (2003) Suspended sediment transport from the Dokriani glacier in the Garhwal Himalayas, Nord. Hydrol., 34, 221-244.
- Singh P., Haritashya, U. K., Ramasastri, K. S. and Kumar Naresh (2005) Diurnal variations in discharge and suspended sediment concentration, including runoff-delaying characteristics, of the Gangotri Glacier in the Garhwal Himalayas, Hydro. Process. 19, 1445-1457.
- Sklash, M. G. and Farvolden, R. N. (1982) The use of environmental isotopes in the study of high-runoff episodes in streams. In: (Editors E. C. Perry, Jr. and C. M. Montgomery) Isotope studies of hydrological processes. John Wiley, Chichester.
- Subramanian, V. (1979) Chemical and suspended sediment characteristics of rivers of India. J. of Hydrol., 44, 37-55.
- Sudheer, K. P., A.K. Gosain. and K.S. Ramasastri. 2002. A data-driven algorithm for constructing artificial neural network rainfall-runoff models, Hydrological Processes,16, pp. 1325-1330.
- Sudheer, K. P., P. C. Nayak. and K.S. Ramasastri. 2003. Improving Peak Flow Estimates in Artificial Neural Network River Flow Models, Hydrological Processes, 17(1), pp. 677-686.
- Szapiro, S. and Steckel, F. (1967) Physical properties of heavy oxygen water. 2. Vapour presure. Faraday Soci., 63: 883.
- Tangri, Anhani K. (2000) Integration of remote sensing data with conventional methodologies in snowmelt-runoff modelling in Bhagirathi river basin – U.P. Himalaya. Technical Report, Remote Sensing Applications Centre, U.P.
- Tayfur, G., S. Ozdemir. and V.P. Singh. 2003. Fuzzy logic algorithm for runoff-induced sediment transport from bare soil surfaces, Advances in Water Resources, 26, pp. 1249-1256.
- The MathWorks, Inc. 2001. ANN Toolbox User's Guide, 3 Apple Hill Drive, Natick, MA 01760-2098.
- Thirumalaiah, K. and M.C. Deo. 1998. River stage forecasting using artificial neural networks, Journal of Hydrologic Engineering, ASCE, 3 (1), pp. 26-32.
- Thirumalaiah, K. and M.C. Deo. 2000. Hydrological forecasting using neural networks, Journal of Hydrologic Engineering, ASCE, 5 (2), pp. 180-189.
- Tokar, A.S. and A. Johnson. 1999. Rainfall-runoff modeling using artificial neural networks, Journal of Hydrologic Engineering, ASCE, 4(3), pp. 232-239.
- Valdiya K.S. (1962) An outline of stratigraphy and structure of southern part of Pithoragarh district, U.P. Jour. Geol. Soc. India, v 3, pp 27-28.
- Valdiya, K.S.,1985. Himalayan tregedy : big dams, seismicity, erosion and drying up of springs, Central Himalayan Environment Association Bulletin, 1, 1-24.
- Valdiya, K.S. and Bartarya, S. K. (1989) Diminishing discharges of mountain springs in a part of Kumaun Himalaya, Current Science, 58 (8), 417-426.
- Valdiya K.S. and Bartarya S.K. (1991) Hydrogeological Studies of Springs in the catchment of

the Gaula River, Kumaun Lesser Himalaya, India, Mountain Research and Development,Vol. 11 (3), pp 239-258.

- Vogt, H. J. (1976) Isotopentrennung bei der verdampfung von wasser, Staatsexamensarbeit. Universitat Heidelberg, 78p.
- Yurtsever, Y. and Gat, J. R. (1981) In stable isotope hydrology (eds) J R Gat and R Gonfiantini (IAEA Tech. Rep. Series No.) 210 103-142.
- Zealand, C.M., D.H. Burn. and S.P. Simonovic. 1999. Short term streamflow forecasting using artificial neural networks, Journal of Hydrology, 214, pp. 32-48.
- Zimmermann U. (1979) Determination by stable isotopes of underground inflow and outflow and evaporation of young artificial groundwater lakes. Proc. AGM on Application of nuclear tech. to the study of lake dynamics, IAEA, Vienna, Austria, pp 87-94.
- Zimmermann U. and Ehhalt D. (1970) Stable isotopes in the study of the water balance of lake Neusiedl, Austria. In: Isotope Hydrology. Proc. Symp. Use of Isotopes in Hydrology, Unesco/IAEA, Vienna, Austria, pp 129 –
- Zuber A. (1983) On the environmental isotope method for determining the water balance components of some lakes. J. Hydrol. 61, 409-427.

| | |
|---|---|
| **Dr. R.D. SINGH** | **DIRECTOR** |

**PROJECT TEAM**

**NIH**

| | |
|---|---|
| **Dr. Bhishm Kumar** | **Scientist 'F'/ Project Coordinator** |
| **Dr. S. P. Rai** | **Scientist 'E1'** |
| **Dr. S. K. Jain** | **Scientist 'E1'** |
| **Shri. A.K. Senthil Kumar** | **Scientist 'E1'** |
| **Shri. S.K. Verma** | **Scientist 'C'** |
| **Shri. Pankaj Garg** | **Scientist 'B'** |
| **Shri. Y. S. Rawat** | **Project Officer** |

**BARC**

| | |
|---|---|
| **Dr. Noble Jacob** | **SO/E (Project Coordinator)** |

**FIELD / LABORATORY ASSISTANCE**

| | |
|---|---|
| **Shri. Jamil Ahamad** | **RA** |
| **Shri. Vipin Kumar Aggarwal** | **SRA** |
| **Shri. Vishal Gupta** | **RA** |
| **Shri. Mohar Singh** | **Sr. Tech.** |